8-10-2021

The CD98 is a Potential Target for Non-Alcoholic Fatty Liver Disease Treatments

Heliang Song
Georgia State University

The CD98 is a Potential Target for Non-Alcoholic Fatty Liver Disease Treatments

by

Heliang Song

Under the Direction of Hamed Laroui, PhD

A Dissertation Submitted in Partial Fulfillment of the Requirements for the Degree of

Doctor of Philosophy

in the College of Arts and Sciences

Georgia State University

2021

ABSTRACT

CD98 is a glycoprotein with many important biological functions including amino acid transportation, endocytosis regulation, and activation of the integrin β signal pathway. Studies have shown the expression levels of CD98 are increased in the livers from fatty degeneration, although the role of CD98 in non-alcoholic fatty liver disease (NAFLD) is not clear. The inflammatory stress inside of the liver is considered one of the main driving forces for NAFLD development. It has been well-studied that the inhibition of CD98 protects mice from colitis (inflammation). To understand the role of CD98 in NAFLD, CD98 siRNA was loaded into the poly lactic acids (PLA) nanoparticles (NPs) to directly inhibit the CD98 expression level in the liver of the high-fat diet (HFD) mice. The decreased level of NAFLD-related markers and the improvements on the liver tissue conditions were observed in the HFD mice with the treatment of CD98 siRNA-loaded NPs. This study indicated that CD98 was important in the NAFLD progression, and downregulation of CD98 can be an effective way for NAFLD treatment.

The mechanism of how plant-derived nanovesicles uptaken by cells remains unknown. In this study, garlic-derived nanovesicles (GDVs) were isolated and digested with trypsin to remove all surface proteins. Digested GDVs showed less uptake compared to undigested GDVs, confirming the surface proteins played an important role in endocytosis. On the cell side (Hep G2 cells, HepG2), blocking CD98 receptors significantly reduced the uptake of GDVs. During the cellular internalization of GDVs, microcopy concluded that some surface proteins of GDVs were co-localized with CD98. A total lysate of the GDVs surface showed a high presence of a mannose-specific binding protein: II Lectin. Blocking II Lectin on surface of GDVs using mannose highly reduced the GDVs internalization which supports that direct interaction between II Lectin and CD98 plays an important role in internalization. The GDVs also exhibited *in vitro* anti-

inflammatory effect by downregulating pro-inflammatory cytokines on HepG2 cells. This work contributes to understanding a part of the GDVs internalization process and the cellular anti-inflammatory effects of garlic. Since CD98 expression level is increased in many diseases including the NAFLD, the II Lectin-CD98 interaction can be utilized for the design of NPs for liver delivery.

In conclusion, this study indicates that CD98 can be used as the target for drug delivery, and decrease the expression of CD98 can protect mice from high-fat-diet-induced liver damages.

INDEX WORDS: CD98, Garlic-derived nanovesicle, Anti-inflammatory, Lectin, Endocytosis

The CD98 is a Potential Target for Non-Alcoholic Fatty Liver Disease Treatments

by

Heliang Song

Committee Chair: Hamed Laroui

Committee: Donald Hamelberg

Jun Yin

Ning Fang

Electronic Version Approved:

Office of Graduate Studies

College of Arts and Sciences

Georgia State University

August 2021

DEDICATION

I would like to dedicate this to my parents, Xinrong and Liying, for their support and patience throughout my years of education. To my colleagues and friends who were with me throughout my Ph.D. journey.

ACKNOWLEDGEMENTS

First and foremost, I would like to thank my mentor, Dr. Hamed Laroui, for allowing me to join his laboratory and training me throughout my Ph.D. Dr. Laroui has taught me to observe and reason as a real scientist would. This experience has been rewarding and has laid the ground work to becoming a well-rounded researcher. I would especially like to thank Dr. Hamelberg, Dr. Yin, and Dr. Fang for taking time from their busy schedules to serve on my committee. I would like to thank my lab mates for all of their ideas and suggestions.

TABLE OF CONTENTS

LIST OF TABLES

LIST OF FIGURES

LIST OF SCHEMES

LIST OF ABBREVIATIONS

Nanoparticles (NPs)

Plant-derived nanovesicle (PDN)

Garlic derived nanovesicle (GDV)

Nonalcoholic Fatty Liver Disease (NAFLD)

Nonalcoholic Steatohepatitis (NASH)

Hepatocellular carcinoma (HCC)

Small interfering ribonucleic acids (siRNA)

conventional protein secretion (CPS)

unconventional protein secretion (UPS)

trans-Golgi network (TGN)

endoplasmic reticulum (ER)

ER-Golgi intermediate compartment (ER-GIC)

microRNA (miRNA)

indole-3-carboxaldehyde (I3A)

heparan sulfate proteoglycans (HSPG)

non-alcoholic fatty liver (NAFL)

Food and Drug Administration (FDA)

CD98 heavy chain (CD98hc)

CD98 light chain (CD98lc)

large amino acid transporter 1 (LAT 1)

inflammatory bowel disease (IBD)

dynamic light scattering (DLS)

atomic force microscope (AFM)

transmission electron microscopy (TEM)

formic acid (FA)

collision-induced dissociation (CID)

false discovery rate (FDR)

paraformaldehyde acid (PFA)

blood-brain barriers (BBB)

LIST OF BUFFERS

Tris-glycine electrophoresis running buffer: 25 mM Tris, 192 mM glycine, 0.1% SDS, pH 8.3

Western blot transfer buffer: 25 mM Tris, 192 mM glycine, 10% methanol

10x Native running buffer: (1 L) 25 mM Tris base, 192 mM glycine

Phosphate-buffered saline (PBS): 137 mM NaCl, 2.7 mM KCl, 10 mM Na_2HPO_4, 1.8 mM KH_2PO_4, pH 7.4

1 BACKGROUND

1.1 Plant-derived vesicles

In biology, the vesicle is a term that refers to the lipid-based structure which is generated within both mammalian and plant cells. So far, the biogenesis of plant-derived vesicles is not clear due to its complexity.[1] However, we can have an idea of the biogenesis and function of plant vesicles throughout the examination of mammalian cell-derived vesicles. These vesicles play a key role in cargoes (especially for proteins) storage and transportation. There are two major types of protein sorting mechanisms: Conventional Protein Secretion (CPS) and Unconventional Protein Secretion (UPS).[1, 2] The CPS requires signal peptide modification on the protein's N-terminal site. The protein containing with signal peptide(s) can be transferred into the Trans-Golgi Network (TGN) after synthesizing in the Endoplasmic Reticulum (ER), even with a lack of the ER-Golgi Intermediate Compartment (ERGIC) in plants. The proteins are then packaged into vesicles and merged into membranes. However, CPS theory cannot explain the finding of proteins without signal peptides or even non-protein materials (such as RNA) in apoplast which is located outside of plant cell membranes.[2] These findings confirm the existence of UPS, a signal peptide-independent mechanism, in the plant. In mammalian cells, UPS is also involved in the genesis of exosomes which are a type of extracellular vesicles.[3] These two types of protein-sorting systems help in loading cargo from the cytosol into vesicles. Formation of vesicles are very complex which requires the recruitment of coat proteins (COPI, COPII, and clathrin), GTPases, and the ESCRT complex.[4, 5]

1.1.1 Edible plant-derived nanovesicles

Edible plants in the diet help to reduce the risk of many kinds of diseases.[6] Recently, the edible plant-derived nanovesicles (PDNs) provided a new angle to explain plant health benefits.[7-10] These vesicles contain DNA, RNA, proteins, polysaccharides, and lipids from their parent cells.[7] The first PDNs-mediated interspecies communication was reported by Dr. Huang-Ge Zhang's group in 2013. They found that grape nanovesicles that were taken up by mouse intestinal stem cells after gavage, which leads to upregulate the expression of Lgr5 and the potential mechanism was through the wnt/β-catenin signaling pathway.[11] Several nanovesicles obtained from various edible plants were reported including carrot, lemon, broccoli, ginger, and so on. The nanovesicles derived from the varying edible plants were found to be associated with various biological effects such as anti-inflammation and anti-carcinogenic properties.[9, 12-14] PDNs have shown an excellent ability to be internalized by mammalian cells both *in vitro* and *in vivo*. Moreover, edible PDNs have shown good biocompatibility to healthy tissues/cells. The biocompatible advantage has been utilized for the encapsulatation of different drugs into PDNs, making them become promising drug carriers. These studies suggest that plants can exert their biological functions on an animal by delivering the plant-derived active compounds, and can also be utilized as a drug carrier. Recently, it has been further proved that the microRNA (miRNA) in ginger-derived nanovesicles improves the mice gut health by influencing microbiota compositions.[15] They showed the ginger-derived nanovesicles were taken into the *Lactobacillaceae* where serveral genes expression in *Lactobacillus rhamnosus* are modulated by delivery of the ginger miRNA. For example, mdo-miR7267-3p, one of the ginger-derived miRNAs, could upregulate the indole-3-carboxaldehyde (I3A) expression, which can improve the function of the intestinal barrier by enhancing the expression of IL-22. This report also demonstrated the uptake mechanism of ginger

nanovesicles by *Lactobacillus rhamnosus* via lipid fusion. However, it remains largely unknown how PDNs are taken by mammalian cells.

1.1.2 Possible uptake mechanism for vesicles

Similar to the cell membrane structure, the vesicles are also in a lipid layer structure. This property allows the vesicles to merge with the cell membrane simply by lipid fusion, which has been proven using an abiotic system (e.g. liposomes).[16] Protein-free lipid bilayers can merge spontaneously; however, the cell membrane is much more complex than the protein-free bilayers. The extracellular space outside of cell membranes is enriched with the extracellular domains of the transmembrane proteins, and most of the extracellular domains are glycosylated.[17] This makes the cellular uptake of vesicles very complex.

Understanding the mechanisms of the mammalian cell-derived nanovesicles such as exosomes can elucidate potential internalization mechanisms for PDNs. The main uptake mechanisms for mammalian exosomes include phagocytosis, clathrin-dependent, and clathrin-independent pathways.[18-20] Phagocytosis is a special type of endocytosis that is majorly mediated by the phagocytes. For most types of cells, the endocytosis of exosomes is usually dependent on the interaction between vesicle ligands and the cell receptors. For instance, Heparan Sulfate Proteoglycans (HSPG) on cell surfaces could be a possible receptor for exosome endocytosis. While it has been reported that HSPG on the surface of exosomes is not involved in the internalization of exosomes.[20] Another study revealed that fibronectins on the surface of myeloma cell-derived exosomes have interactions with HSPG on target cells.[21] In addition, proteins on both the surface of ovarian cancer cell-derived exosomes and ovarian cancer cells are important for uptake.[22]

1.2 Liver

The liver is an important organ in vertebrate animals. The liver plays central roles in many biological and physiological procedures including nutrients metabolism, energy storage, processing the toxic compounds to less cytotoxic compounds, maintaining the balance of hormones, and breaking down the blood cells.[23-26] In addition to those important roles, the liver also plays critical roles in other functions by coupling with other organs. For example, the liver is involved in the digestion of lipid by secreting the bile which is an alkaline liquid mixture of cholesterol and bile acids. The bile will be temporally stored in the gallbladder, which is an organ connected to the liver directly.[27] Since the liver is so important in maintaining life functions, the loss of function in the liver will lead to serious health problems to the whole body or even cause death.[28, 29]

Understanding the composition of liver cells is the prerequisite thing for understanding liver diseases. The liver is made up by several kinds of cells including hepatocytes, liver sinusoid endothelial cells (LESCs), Kupffer cells, and stellate cells. Among those cells, hepatocytes are the major cell types in the liver which can take up to 60% of total cell number and 80% of the weights. Hepatocytes play a critical role in maintaining the basic functions of liver, such as metabolism and filtration of poison metabolites, and innate immune regulation by secreting innate immune proteins. An example of these innate immune proteins is the soluble CD14 protein (sCD14) that is mainly secreted by the hepatocytes, and the function of this sCD14 on the lipopolysaccharides (LPS) signaling pathway has been shown in a concentration-dependent manner.[30] Liver sinusoidal endothelial cells (LSECs) form the sinusoid, which is the thinnest blood vessel in the liver.[31] The sinusoid separates the contents (for example, Kupffer cells and blood cells) inside the capillaries and the cells (including hepatocytes and stellate cells) outside. These

unique properties make the LSECs important in maintaining immune homeostasis, providing nutrients, and recycling waste. Kupffer cells are a special type of macrophages that are located inside the liver sinusoid.[32-35] Kupffer cells can cause either liver damage or repair the liver damages depending on the immune environment as well as the ongoing metabolism. This is because the Kupffer cells have at least two types of phenotypes, the proinflammatory M1 phenotype, and the several different M2 phenotypes. The M2-type Kupffer cells can inhibit the inflammation and enhance the wound healing, however, more studies are required before promoting Kupffer cells with a specific M2 conversion for certain liver damages.[34] The hepatic stellate cells (HSCs) are distributed within the spaces between LESCs and the hepatocytes.[36] HSCs are important cells for secreting collagen and excessive collagen will lead to liver fibrosis.[37] The HSCs contain up to 80% of the total vitamin A inside the human body and are usually called vitamin A-storing cells. Vitamin A (majorly retinoid) levels inside the HSCs are highly associated with liver fibrosis. The lower the retinoid in HSCs, the easier it to induce liver fibrosis in the rats.[38] As mentioned before, the HSCs barely interact with the Kupffer cells directly as they are separated by the LESCs. However, the HSCs interact with Kupffer cells during liver inflammation. It is important to know that all the cells in the liver are not isolated, in fact, they work with each other tightly. For example, one important function of LESCs is to recruit lymphocytes which are required by the Kupffer cells, hepatocytes, and stellate cells. The Kupffer cells initiate the signaling to simulate the expression of adhesion protein on LESCs by the release of the proinflammatory signals. Once the lymphocytes bind to the sinuous in a selectin-independent manner, the hepatocytes form the firm adhesion between LESCs and lymphocytes by releasing paracrine factors. The transmigration of lymphocytes then activates the HSCs through the release of chemotactic factors.[31]

1.2.1 Common liver diseases

Table 1.1 summarizes some common factors which lead to liver damages. Many issues including viral infections, immune system dysfunction, and even hazards in our diets can damage the liver directly or indirectly. [39-47] The common viruses that lead to liver damage include hepatitis A virus, hepatitis B virus, and hepatitis C virus. Treatments for those virus infections are varied. For hepatitis A infection, there is no recommended medication since this infection can be cured naturally. For hepatitis B or hepatitis C virus-infected patients, antiviral medication is required to reduce liver damages.[46] No drug can cure the hepatitis B virus infections; however, Hepatitis B virus infection can be effectively prevented by the vaccine.[48] Unlike hepatitis B, no vaccines are available for hepatitis C. However, the hepatitis C virus infection can be cured by the treatment with the proper medications. Contaminated food is a risk for induction of liver damages, too. The aflatoxin is an example of such a toxin. There are four types of aflatoxins, i.e., aflatoxin B1, B2, G1, and G2, which are majorly produced by *Aspergillus flavus* and *Aspergillus parasiticus* (Figure 1.1 A). Among those, the aflatoxin B1 (AFB1) has shown the strongest hepatotoxicity. In the liver, AFB1 will be converted into the intermediate called AFB1-exo-8,9 epoxide (AFBO, Figure 1.1 E), which will insert into the gene, leading to the mutation of the tumor suppression gene (p53), and eventually lead to liver cancer. These aflatoxin-producing fungi exist everywhere, and they could contaminate crops, peanuts, as well as other nuts during the harvest or storage procedures. In addition, aflatoxin can also be found in milk, meat, and eggs due to feeding animals with contaminated food.[39] According to the United States Food and Drug Administration (FDA), aflatoxins contamination in food cannot be eliminated and this contamination threats about 4.5 billion population worldwide.

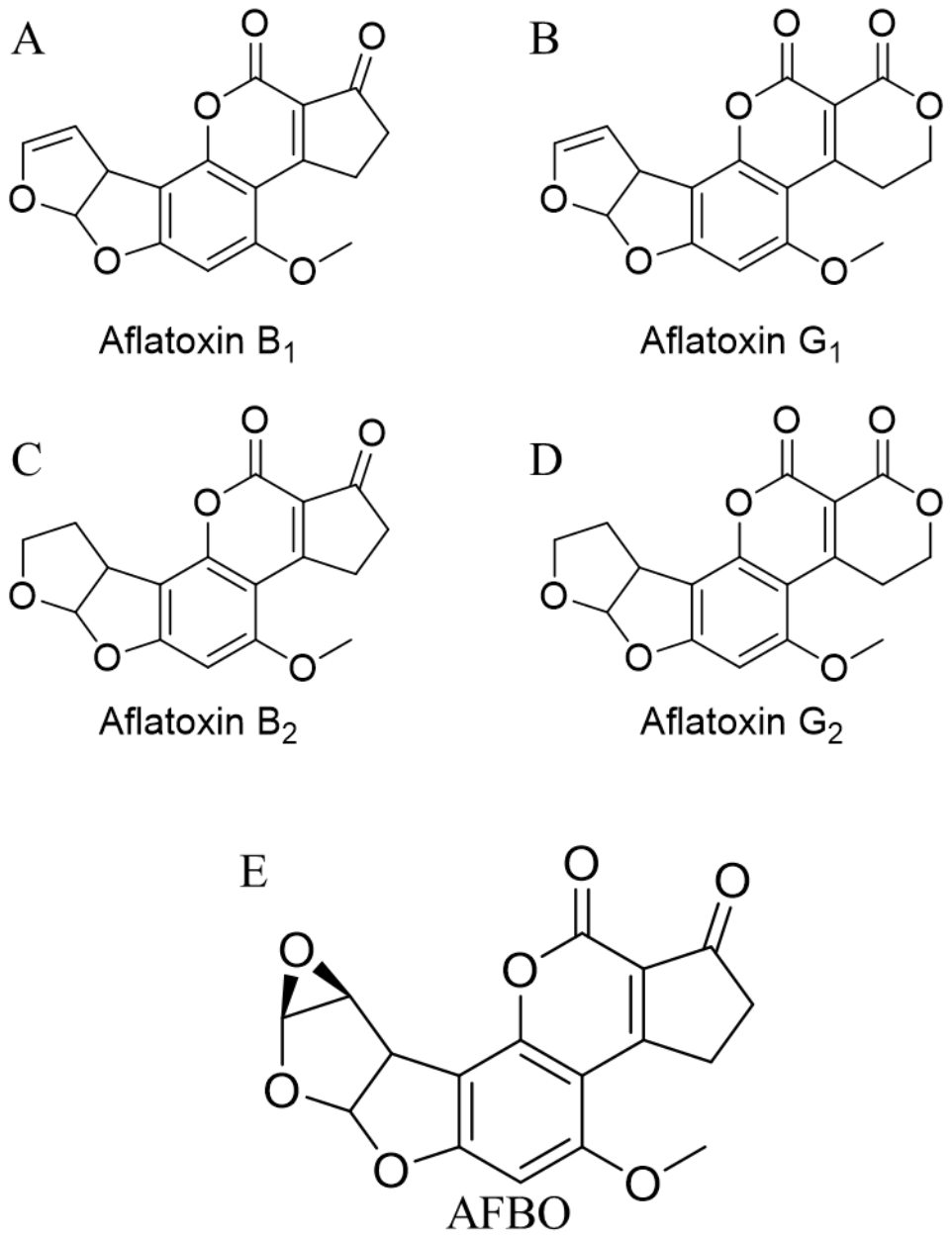

Figure 1.1: Structure of four types of aflatoxin and its metabolite AFBO.
(A) Alfatoxin B_1, (B) Alfatoxin G_1, (C) Alfatoxin B_2, (D) Alfatoxin G_2, (E) AFBO

Table 1.1 Summary of common liver diseases and the corresponding therapeutics.

Disease Names	Mainstream Therapeutics	Estimated Affected Population	References

Hepatitis A	No specific medication needs and will cure after several weeks or months	1.4 million per year	[40]
Hepatitis B	Antiviral medicines, such as entecavir, tenofovir, lamivudine, adefovir, and telbivudine can be used to protect the liver damages. The vaccine is usefully in prevention of hepatitis B.	About 257 million infections.	[41]
Hepatitis C	Antiviral medicines such as the sofosbuvir (sovaldi), simeprevir (olysio), daclatasvir (daklinza) and so on.	130-170 million.	[46]
Alcohol abuse	Stop drinking alcohol and could take some vitamins. Liver transplant is an available option if the liver damages are serious.	No published data showed the exact number of populations being affected. However, the amount of alcohol bigger than 14 g of	[42]

		alcohol (a 12 oz can of beer) is considered as the misuse of alcohol.	
NAFLD	No drug available.	882 million.	[49]
Autoimmune hepatitis	The drugs such as prednisone are used to suppress the immune system.	1-2 per 100,000 population per year.	[47]
Bile Duct Cancer	Surgery to remove the cancer.	It is not a common cancer; the incidences are varied in different areas. The highest incidence is in South Korea (3 per 100,000) while the lowest incidence is in UK (0.66 per 100,000)	[45]
Unclean food such as aflatoxin B1 contaminated peanuts	No therapeutic available.	4.5 billion people is affected.	[39]

1.2.2 Fatty liver diseases

Among the possible liver damages, the most common liver disease right now in the U.S. is non-alcohol fatty liver disease (NAFLD).[49] Unlike healthy liver contains a very limited amount of fats. Fatty liver diseases (FLDs) are a condition which excessive amounts of fat is found in the liver. Typical FLDs are usually referred to as a liver that contains more than 5-10% (total liver weights) of fat.[50] The FLDs can be divided into two categories based on the consumption of alcohol: the alcohol-induced fatty liver disease (ALD) and NAFLD, which the latter refers to fatty liver diseases that are alcohol-independent.[51] FLDs encompass a broad spectrum of liver diseases including steatosis, steatohepatitis, cirrhosis, and liver cancer.[52] The long-term over-dose consumption of alcohol accumulates the damages on the liver is still the major contributor to the pathogenesis of ALD.

NAFLD is a disease with a similar hepatic histologic pattern to that of alcohol-induced fatty liver disease, while the patients only intake a little amount of alcohol or even never consume the alcohol before. NAFLD is usually characterized into two subtypes: 1) non-alcoholic fatty liver (NAFL) which only shows excessive lipid accumulation, and 2) the more serious nonalcoholic steatohepatitis (NASH) which is the inflammatory condition indicated by lobular inflammation.[53] NAFLD is now the most common liver disease which affects about 25% of the general population in the world.[43] The prevalence of NAFLD in the United States has increased, which is expected to affect more than 100 million people by 2030.[54] Without proper treatments, NAFLD can develop into NASH and further develop into more life-threatening diseases such as liver fibrosis, cirrhosis, and even liver cancer. The pathogenesis of NAFLD is not fully understood which causes difficulties in drug development.[54] To date, no drug is approved by the FDA for

the treatment of NAFLD. The current first-line therapeutic strategy for NAFLD is aimed to reduce the patients' body weights via changing the lifestyle, i.e., a healthy diet and moderate exercise.

Recently, a "multi-hit" theory was proposed for the pathogenesis of NAFLD. According to this theory, pathogenesis results from the combination of factors including oxidative stress, lipid metabolism, immune response, dietary, gut bacteria-derived LPS, and so on.[54-56] Among those factors, oxidative stress is considered as the major factor which promotes the disease from NAFL to NASH. Thus, the antioxidants can be used as candidates for NAFLD therapy. In a clinical trial, vitamin E (800 IU/day) shows significant improvement in NASH when compared to the placebo (ClinicalTrials.gov number, NCT00063622.).[57]

Different types of liver cells are involved in the NAFLD development. In NAFLD, the hallmark is the extra accumulation of fats in the hepatocytes.[58] And this abnormal fatty acid accumulation can cause lipotoxicity to the hepatocytes by increasing the reactive species of oxygen (ROS) level.[56] In fact, ROS production is important in the NAFLD progression. In a clinical study, the ROS levels in the liver of obese volunteers (including the obesity without NAFL, obesity with NAFL, and obesity with NASH.) groups are found to be higher than that of the health volunteers' livers. In addition, only the ROS level in obesity with NASH is significantly higher than the level in the health group. A further study indicated the hepatic gene damages were only found in obesity with NASH.[59] The stresses on hepatocytes might lead to the release of cytokines such as the Monocyte chemoattractant protein-1 (MCP-1/CCL2), interleukin-6 (IL-6), IL-18, CD36, and tumor necrosis factor alpha (TNF-α). The upregulation of CCL2, which is observed in both ALD and NAFLD patients, promotes the macrophages recruitment in the liver and contributes to liver damage, inflammation, and steatosis.[30] Hepatic macrophages in liver sinusoids and the Kupffer cells play key roles in the development of NAFLD. According to the

"multi-hits" theory, the Kupffer cells can mainly mediate the inflammatory response (second hit). Recently studies support that the different subtypes of Kupffer cells played different roles in the immune response.[35] The M1 Kupffer cells play a role in the pro-inflammation effects in the NAFLD, while the M2 (M2a, M2b, and M2c) subtype exhibit a protective effect on the liver. As reported, the M1/M2 cell ratios are elevated in both NAFLD and ALD. The M2 Kupffer cells could decrease the M1 Kupffer cell-induced inflammation in the liver by causing the apoptosis of M1 Kupffer cells via secretion of IL-10.[60] The HSCs activation is the predominant cause for the development of liver fibrosis. Alpha smooth muscle actin (α-SMA) is used as a marker for activation of HSCs and the activated HSCs secrete collagen I. The morphology of HSCs in normal conditions is a star-like shape and the activated HSCs are in myofibroblast shape.[61] The molecular mechanism under the activation is complex which involves many proteins i.e., peroxisome proliferator-activated receptor gamma (PPARγ), Transforming growth factor-β1 (TGF-β1), LIM homeobox protein (Lhx2), platelet-derived growth factor (PDGF)-receptor, and so on.[62, 63] Current studies support that TGF- β1 plays a central role in enhancing the expression of α-SMA. The ligand of PPARγ showed potential for reducing the expression in TGF- β1-induced α-SMA and collagen expression.[62] In summary, the development of NAFLD is the result of the combination of many factors including the multi-stresses caused liver damages, hepatic macrophages activation, and the HSCs response (activation and collagen release). Those factors together promote the liver damages into NAFL to NASH, liver fibrosis, and even the liver cancer. This fact also implies that the ideal drug for NAFLD treatment should be able to modulate several signaling pathways and affect the different liver cells at the same time.

1.3 Lectin

Lectin, a set of proteins which bind to the specific carbohydrates, is produced by the animal, plant, fungi, and bacteria.[64-67] The interaction between lectins and carbohydrates is mediated by the carbohydrate recognition domain (CRD).[67, 68] Thus, the lectins are considered as the "antibody" for carbohydrates. Due to this unique recognition between lectin and carbohydrates, the lectins have been developed into important analytical techniques for carbohydrates research including the lectin array assay and the lectin affinity chromatography (LAC).[69, 70] For example, plant-derived lectins can be used as biochemical reagents to differentiate between different blood types in the ABO blood system; this is based on the lectin's abilities to differentiate the differences in terminal carbohydrate patterns on erythrocytes surface.[71] Carbohydrates are involved in many biological processes including nutrient, protein post-transcription modifications, and species recognition.[72] And the carbohydrates are found in the animal, plant, bacteria, and even virus.[72-75] Thus, it is not surprising that many interspecies recognitions are mediated by the lectin-carbohydrate interaction.[66, 67, 76] In addition, the functions of lectins are highly varied and dependent on the role of the carbohydrates and the glycoproteins. Glycosylation, an important method for proteins post-transcription modification, will affect the biological functions of proteins. The normal cells usually have different glycan modifications when compared to the cancer cells and the drug-resistant cancer cells.[70, 77] The lectin-carbohydrate recognitions also form the basis for innate immune response.[78] In summary, the biological function of lectin is varied and dependent on the functions of glycoproteins or carbohydrates.

1.3.1 Lectins derived from animals and plants

The lectin classification is complex since the criteria for the classification are various. The animal lectins are generally divided into two classes, the intercellular lectins, and

extracellular lectins which include the transmembrane lectins. Generally, in mammalian cells, intercellular lectins are involved in the regulation of inflammation and apoptosis, while extracellular lectins are considered to play the important role in signaling transduction.[79] Interestingly, the galectin-3, a beta-galactoside binding lectin, is found in both intercellular and extracellular space.[80] The intercellular galectin-3 inhibits cell apoptosis, while the extracellular galectin-3 serves as the ligand in activation of the surface glycoproteins including glycoprotein CD98, galectin-3 binding protein (G3BP), and so on.[79, 81-86] The asialoglycoprotein receptor is the transmembrane lectin on the surface of hepatocytes which shows a strong affinity to galactose. The function of the asialoglycoprotein receptor is to bind the proteins with galactose modification in the terminal.[87] This asialoglycoprotein receptor is reported to be mainly present on the surface of hepatocytes. Thus, this receptor is considered an important target in liver disease treatments.[88]

Plant lectins can be classified based on their subcellular location, binding substrates, structure similarity in CRDs, or their endogenous role.[89, 90] Based on the endogenous role, the plant lectins can be divided into three lectin families: 1) jacalin-related lectins family, 2) Cucurbitaceae phloem lectin family, 3) monocot mannose-binding lectin family.[90] Garlic is a monocotyledon and several different mannose-binding lectins have been identified from garlic including *Allium sativum* agglutinin (ASA) I (ASA I), ASA II, and ASA III. ASA II is a dimer formed by two II lectins. As shown in Figure 1.2, the garlic-derived lectin, II Lectin, is a protein with ten β-sheets that form the β-prism II fold pattern.[91] Three typical mannose-binding motifs (QXDXNXVXY) were found in the amino acid sequence.[92] Plants contain a large number of lectins which are considered as the plant strategies against bacteria, fungi, pests, and viruses.[93] For example, one group has designed pest-resistant transgenic rice by the incorporation of garlic

leaf lectin.[94] In addition to the lectin's role in interspecies communication, plant lectins are very important in glycan analysis. Most of the lectins used in the lectin array are derived from plants.[95]

A RNILTNDEGLYGGQSLDVNPYHLIM**QEDCNLVLY**DHSTAVWSSNTDIPGK
KGCKAVL**QSDGNFVVY**DAEGASLWASHSVRGNGNYVLVL**QEDGNVVIY**RS
DIWSTNTYR

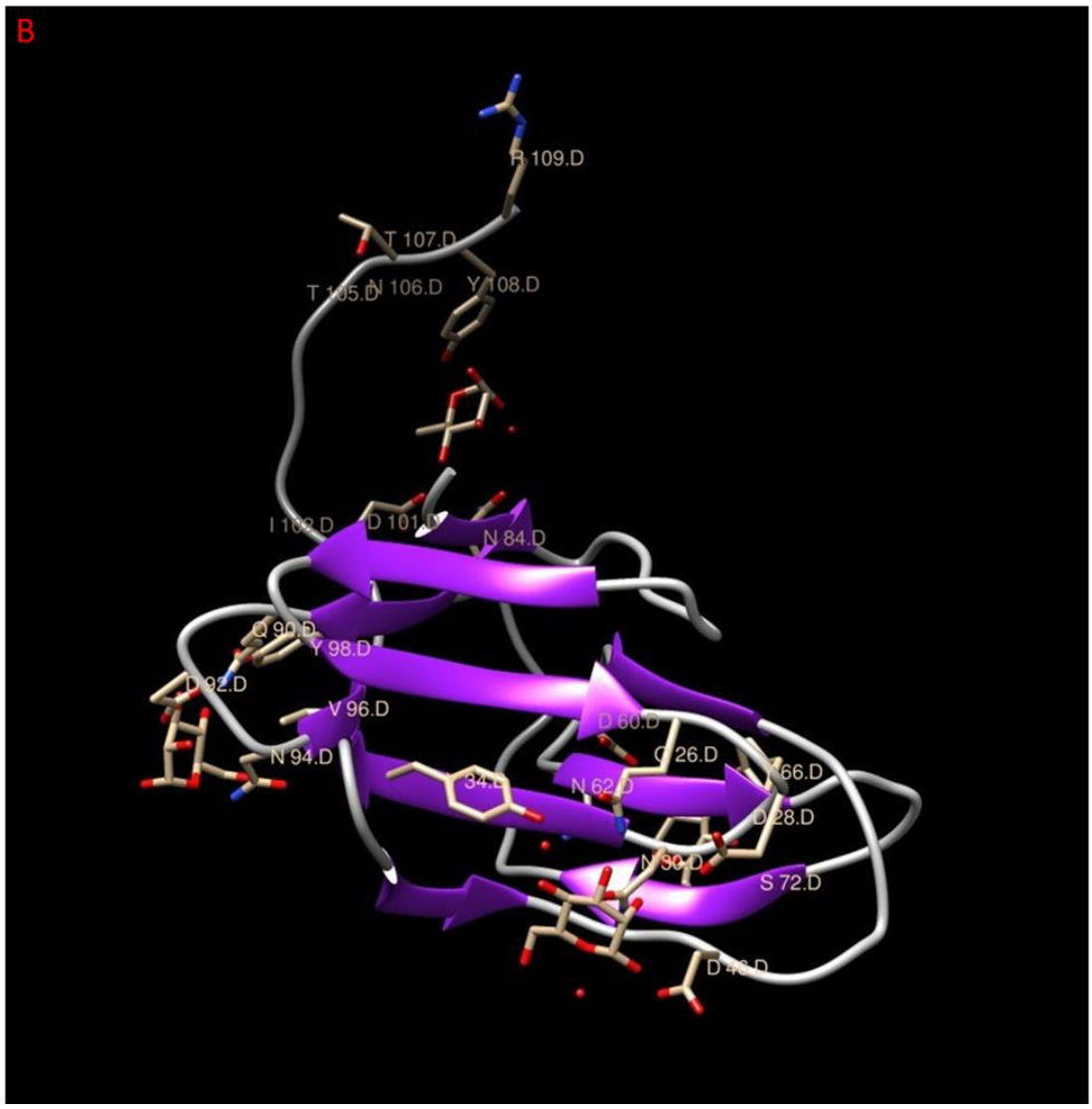

Figure 1.2: The amino sequence and structure of II Lectin.
(A) The sequence of II lectin. The motif of the mannose-binding site is in bold and underline.[91] (B) The structure of II Lectin. The β-sheets are shown in purple. The structure is

obtained from the protein data bank (PDB) with the PDB code 1BWU (chain D). The structure of 1BWU (chain D) is visualized by using Chimera.[96]

1.3.2 Lectins in disease treatment

Both plant and animal lectins show their potentials in treating diseases.[97] Lectins are mainly used in disease treatments in two distinct ways. The first strategy is to exert the lectin functions straightly. To date, accumulated studies have explored the potential treatments by using lectins in different diseases, including cancer, lung fibrosis, HIV infections, etc.[98-100] The other strategy is to take advantage of the strong affinity between carbohydrates and lectins to achieve drug targeting delivery. Nanoparticles (NPs) decorated with lectins or carbohydrates on the surface have shown enhanced delivery efficiency.[87, 97, 101] Significantly different carbohydrate profiles between the cancer cells and normal cells have been found.[102, 103] Screening the lectins which recognize the disease's unique carbohydrate patterns will contribute to developing the disease-targeted therapy in the future.

1.4 CD98

CD98 is a heterodimeric protein which is made by a heavy chain and a light chain (Figure 1.3).[104] The CD98 heavy chain (CD98hc) is encoded by the human *SLC3A2* gene. The light chain of CD98 (CD98lc) can be any of the following proteins: large amino acid transporter 1 (LAT1), large amino acid transporter 2 (LAT2), and glutamate transporter called system x_c^-.[105-107] The CD98hc and CD98lc are spatially close to each other and form the CD98 via ligation of a disulfate bond.[107-109] The CD98hc is required for the CD98lc to work functionally and in turn, the presence of CD98lc can protect CD98hc from degradation.[110] One fact is that CD98 is existed in all the actively proliferation cells.[111, 112] This indicates the important role of CD98 in maintaining cell proliferation and activation. Moreover, CD98 is involved in the

control of cellular internalization, nutrients intake, immune activation, and inflammation promotion.[81, 107, 113-118] CD98 is highly expressed in many diseases and multi-roles of CD98 make it a potential target for the development of therapeutics.

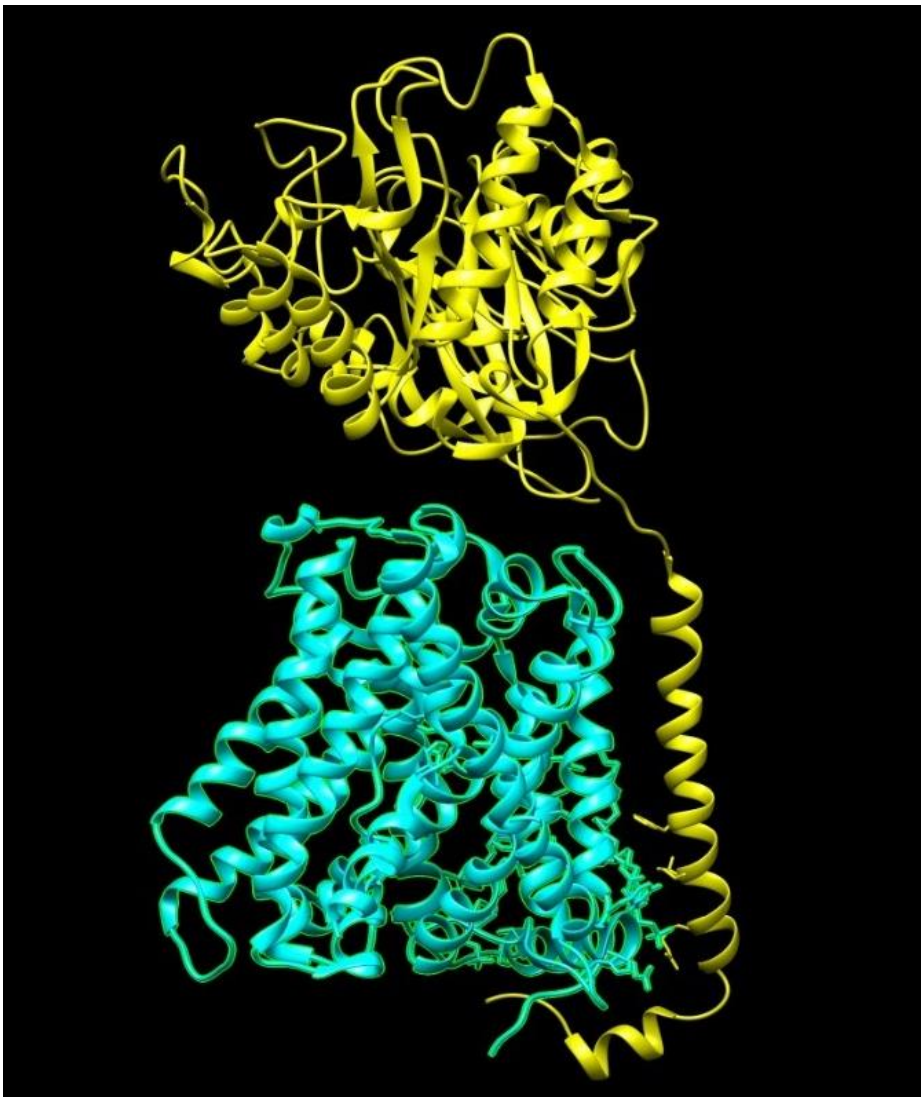

Figure 1.3: The structure of the CD98 (CD98hc and LAT1) complex.
The CD98hc is labeled in yellow and the LAT1 is labeled in cyan. The structure is obtained from the protein data bank (PDB) with the PDB code 6IRT. The structure of CD98 is visualized by using Chimera.[96]

1.4.1 CD98 heavy chain

The CD98hc is a single-pass transmembrane protein, and the sequence of CD98hc can be divided into four sections, i.e., the extracellular domain (ED), transmembrane domain (TM1'), juxtamembrane domain, and the cytoplasmic domain (N-terminal).[110, 119, 120] All four domains play important roles in CD98hc mediated biological functions. The ED of CD98hc is made of eight repeats (domain A) and eight β-streets (domain C).[110, 119] As reported, the ED of CD98 is important in maintaining the cellular adhesion of cells. The TM1' of CD98hc is the place for the binding of LAT1, and the TM1' is the most important section in interacting with the integrin β signal pathway. This integrin interaction was studied using the chimeric protein (C98T69E98, which has the ED and cytoplastic domain from CD98, and TM from CD69 protein) that has replaced the CD98 TM1' with a CD69 TM domain resulting in the disruption of the interaction with integrin β1. While the chimeric protein (C69T98E69, which has the ED and cytoplastic domain from CD69, and TM from CD98) shows the interaction with integrin β1. This fact indicated the TM of CD98 plays the center role in activating the integrin signal pathway. The sequence between the cytoplastic domain and TM is called the juxtransmembrane section. The juxtransmembrane and TM of CD98 are highly conserved, which suggested that they might play a key role in some unique cellular functions. The cytoplastic domain and juxtransmembrane sections show inhibition effects in the CD98hc-activated the integrin β signaling pathway.[113, 120]

The sequence of CD98 protein (human) is shown in Figure 1.4. The molar mass calculated from this CD98hc sequence is around 67 kDa. However, in most situations, the molar mass of CD98hc is about 85 kDa.[81] The difference in the mass is caused by the fact that CD98 is a protein with heavy glycosylation in the CD98hc.[81] Many sites in CD98hc are predicted as

potential sites for glycosylation. Recently, cryogenic electron microscopy (cryo-EM) has become a powerful tool in interpreting the structure of the protein, especially for the transmembrane proteins.[121] A study regarding illustration of CD98 (CD98hc-LAT1 complex) structure using cryo-EM confirmed that there are four new N-glycans modification sites on the ED of CD98hc.[119] Even though the CD98 used in this study was produced the HEK293 cells without the key enzyme to complete full glycosylation, heavy mannose modification on CD98hc was found in the N-glycans modifications on ED of CD98hc. The CD98hc ED mannose modifications are not likely to be necessary for the CD98 complex formation, however, the extracellular sugar antenna could act as potential binding sites for lectin-CD98 interaction.[81] The cryo-EM indicated that the TM1' forms a helix to helix interaction with the TM4 in the LAT1 and the N-terminal TM1' of CD98hc is closely interacting with the system x_c^-.[109, 119]

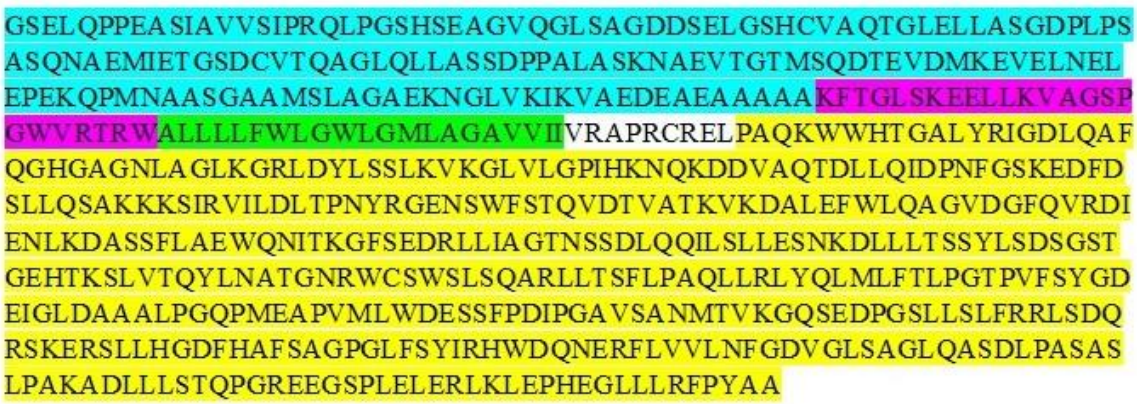

Figure 1.4: The amino acid sequence of full-length CD98.

The CD98hc protein can be divided into four sections by its location to the cell membrane. The four sections from extracellular to the cytosol are the extracellular domain (215-630), transmembrane domain (185-205), juxtransmembrane (161-184), and the cytosol domain (1-160). The sequence of CD98 is reported in the literature.[119]

1.4.2 CD98 light chain

To date, three complete CD98 heterodimeric structures have been characterized using the cryo-EM.[109, 119, 122] Those three light chains (LAT1, LAT2, and system x_c^-) are all bound to the CD98hc TM1' via the disulfate bridges, and all three light chains are identified as amino acid transporters. LAT1 and LAT2 are the larger amino acid transporters which are functionalized to transfer large neutral amino acid (L-leucine and L-tyrosine) in a Na^+-independent way. LAT1 affinities to large neutral amino acids are much higher than that of LAT2, while the LAT2 show a more broad ability in transporting the small amino acids such as alanine. Recently cryo-EM studies of CD98hc-LAT1 and the CD98hc-LAT2 contribute to the understanding of this difference in amino acid transport efficiency. The pocket, the substrate-binding site, is slightly different in the LAT1 and LAT2. The amino acids in the LAT2 pocket (Thr86, Tyr396, Tyr399, and Tyr430) are slightly larger than the amino acids in the LAT1 pocket (Ser96, Trp405, Val408, and Phe439). The large amino acids inside the pocket of LAT2 might contribute to the recognition of the small amino acids.[122] The system x_c^- is the amino acid transporter that can take the exocellular L-cystine into cells and export the intercellular L-glutamate out of the cells.[123] The system x_c^- is very important due to the cystine which is the key material for the production glutathione (GSH) that plays important roles in protecting cells from ROS.[124] As we know, the ROS level inside the cancer cells is usually higher than that in the normal cells because of the higher activities. System x_c^- is overexpressed in the tumor cells and contributes to maintaining intercellular redox status.[125] Thus, the inhibition of system x_c^- enhanced the cancer cell cisplatin-induced cytotoxicity synergistically.[126] Targeting the of system x_c^- can affect the nutrients and oxidative stress at the same time. Since all the three different CD98lcs are bound to the TM1' of

CD98hc to form the CD98, CD98 protein can be a very important target for modulation of redox status, nutrients, and other signaling pathways.

1.4.3 The role of CD98 in disease

CD98 biological functions are mainly related to fundamental functions of the CD98hc and CD98lc, which involves the nutrients intake, redox enhancement, and integrin signaling pathway modulation. Thus, it is no wonder that CD98 is upregulated in cancers and inflammatory diseases (colitis and NAFLD).[127-129] The upregulation of CD98 in cancer and inflammatory diseases promotes cell survivability against the harsh cell stresses. The role of CD98 in cancers includes the drug resistance to chemotherapeutic and the resistance to radio-chemotherapy.[14] In addition, the upregulation of CD98 may lead to poor prognostic outcomes.[130] CD98 inhibition increased the chemosensitivity in cancer cells when utilized in the design of the co-delivery nano-formulations to synergistically enhance chemotherapy.[131] Another CD98-based anticancer therapy is using an anti-CD98 antibody, IGN523. The *in vivo* study showed that the IGN523 decreased the amino acid uptake and increased the antibody-dependent cellular cytotoxicity.[118] CD98 is overexpressed in the colitis and governs the intestinal homeostasis via interacting integrin β1 proteins, leading to the activation of focal adhesion kinase (FAK).[128] Thus, decrease the expression of CD98 will be an effective way for attenuation of colitis.[132]

1.4.4 The role of CD98 in internalization regulation

CD98 trafficking is dependent on the clathrin-independent endocytosis (CIE) pathway, the recycled CD98 can be incorporated back into the membranes under the control of a small GTPase, Arf6.[113, 133] Thus, the CD98 dependent internalization requires the consumption of energy (GTP, Guanosine-5'-triphosphate). In normal tissue, the expression level of CD98 is relatively low, however, CD98 is usually overexpressed in cancer or inflammatory tissues (i.e., IBD

and colitis).[117, 128] In our recent study, CD98 has been found as a potential inducer for non-alcohol fatty liver disease (NAFLD).[129] NAFLD is a condition in which fat accumulation inside of the liver cells affects patients with little or no alcohol consumption. Our group also found that CD98 expression level is even higher in the hepatocellular carcinoma (HCC) patients' livers.[129] The differential expressions of CD98 between normal conditions and disease conditions make CD98 an ideal target for drug delivery and therapy. This idea has been verified by different research groups via targeting either CD98hc or CD98lc (LAT1). It was reported by Dr. Merlin's group that NPs modified with the CD98hc antibody Fab' sections on their surfaces were preferably taken into the colon tissues of the DSS-treated mice group.[115] Since the major role of LAT1 is transporting the neutral amino acid (such as glutamate) into the cells, glutamate has been added onto the surface of PLGA NPs to enhance the targeting ability to the tumor.[106] Taken together, glycoprotein CD98 can be a promising receptor for the internalization of NPs.

1.5 Nanoparticles for NAFLD treatments

Nanoparticles (NPs) refer to small particles which have a size up to 500 nm in diameter. The application of NPs is varied from therapy, biosensor, image contrast reagent, and diagnosis.[134-144] In this study, the NPs we discussed are referring the NPs used for drug delivery. The NPs for drug delivery usually consist of three elements including the matrix (NPs forming materials), cargoes (drugs or therapeutic molecules), and the surface ligands.[145, 146] The NPs can be made from many types of material, including metal, polymer, lipid, and silica.[145-149] Various drugs such as hydrophilic drugs, hydrophobic drugs, and large molecules (protein, mRNA) can be loaded into the NPs alone or in a combination way.[132, 150] In general, the advantages of drug delivery using NPs are drug protection, targeted delivery, and controlled release.[132, 151] As we discussed in the liver introduction section, one of the liver's functions is

to filtration of the toxic compounds (including drug molecules). Thus, most of the drugs will accumulate in the liver naturally and this property of the liver makes the drug delivery to other organs (except the liver) difficult. However, the study regarding the formulation of NPs in drug delivery to the liver using NPs is still necessary.[152] As mentioned before, the liver is made of different types of cells including the hepatocytes, HSCs, LESCs, and Kupffer cells. Different cells are playing different roles in the NAFLD. Thus, achieving the cellular targeted drug delivery to the liver will contribute to the therapeutic effects by increasing the drug concentration in desired cell types and reducing the side effects on other cells.

In general, the NPs internalization by cells is determined by many factors such as the size, shape, zeta potential, and surface modification (ligands).[153] Different cells have different preferences in the uptake of NPs. The NPs with a larger size (400-500 nm in diameter) will be eliminated by the Kupffer cells and the small size will reduce the macrophage depletion.[154] Interestingly, Kupffer cells prefer to uptake NPs with positive charges. However, negatively charged surfaces on NPs might interact with the protein in blood to form the protein corona, leading to macrophage clearance.[152] The Kupffer cells make up to 80% of the total macrophages in the whole body, thus, the Kupffer cells clearance of NPs should be taken into consideration if the NPs are designed to target other cells in the liver (exclude the Kupffer cells). One possible way to avoid the macrophages phagocytosis is to coat the NPs' surface with a poly (ethylene glycol) (PEG) layer.[155-157] These neutral hydroxy groups reduce the macrophages uptake *in vivo* by reducing the NPs interaction with the NPs. In addition to the Kupffer cells, another major barrier for NPs to be delivered to the hepatocytes is the sinusoid (LESCs). The sinusoid fenestrations (i.e., openings) size is about 100 to 150 nm in diameter.[158] In other word, NPs with a size smaller than 150 nm are capable of passing this physical barrier. In addition to

the size, the ligands on the surface of NPs could help to achieve the maximized hepatocyte delivery. For example, the asialoglycoprotein receptor (ASGPR) is a c-type lectin that is expressed on the surface of hepatocytes. This surface lectin (ASGPR) showed a strong binding affinity to the galactose and can capture the proteins with the galactose in the terminal. Thus, the galactose is chosen to modify the surface of NPs to enhance the hepatocytes targeting ability.[139] Other hepatocytes targeting ligands are summarized in the Table 1.2.

Table 1.2: Summary ligands and the receptors for hepatocytes targeted delivery

Ligands	Receptors	Reference
Galactose	Asialoglycoprotein receptors	[139, 140, 146, 159]
N-acetylgalactosamine	Asialoglycoprotein receptors	[137, 160]
Lactobionic acid	Asialoglycoprotein receptors	[148, 161, 162]
Pullulan	Asialoglycoprotein receptors	[163, 164]
Hyaluronic acid	CD44	[49, 138, 165]

Countless studies have been done to explore the NAFLD treatments using nanoparticle-based drugs. Those NPs can be both synthesized NPs or natural existing NPs which are referring to mammalian cells-derived exosomes and plant-derived nanovesicles.[166-169] The NPs for NAFLD treatment were summarized and categorized by the NPs materials.

1.5.1 The polymeric NPs for NAFLD treatment

The most famous polymers in drug delivery are the ploy (lactic acid) (PLA) and the poly (lactic-co-glycolic acid) (PLGA) (Figure 1.5). PLA and PLGA are both approved by the FDA for drug delivery and showing high biocompatibility and biodegradation.[170] Since CD98 plays an important role in the NAFLD progression, our group has designed a formulation of NPs

consisting of PLA to deliver CD98 siRNA to silence the CD98 *in vivo*. The average size of the NPs was about 270 nm and the zeta potential was slightly negative. The surface of the NPs was covered by the polyvinyl alcohol (PVA) to reduce the interaction with the macrophages *in vivo*. In the *in vivo* distribution assay, we found about NPs were accumulated in the 18% of hepatocytes of the high-fat diet (HFD) group and about NPs were accumulated in the 5% of macrophage-like cells in HFD mice group. This indicated the formulation we used can effectively deliver the drug into hepatocytes and avoid the macrophage depletions to some extent. This formulation decreased lipid accumulation in HFD mice and reduced the expression of pro-inflammation cytokine.[171] Along with the PLA and PLGA, many polymers are under evaluation. Wendi Teng et al. reported a formulation to deliver resveratrol to the liver for NAFLD treatment. They synthesized the NPs using a partially oxidized starch (30% oxidized) and enable the hepatocytes targeting ability by adding the galactose (gal) to the surface of NPs. They used the live image system to show the drug accumulation *in vivo* and found the gal-modified NPs accumulated more in the liver than that in free dye and non-targeted NPs treated groups.[172]

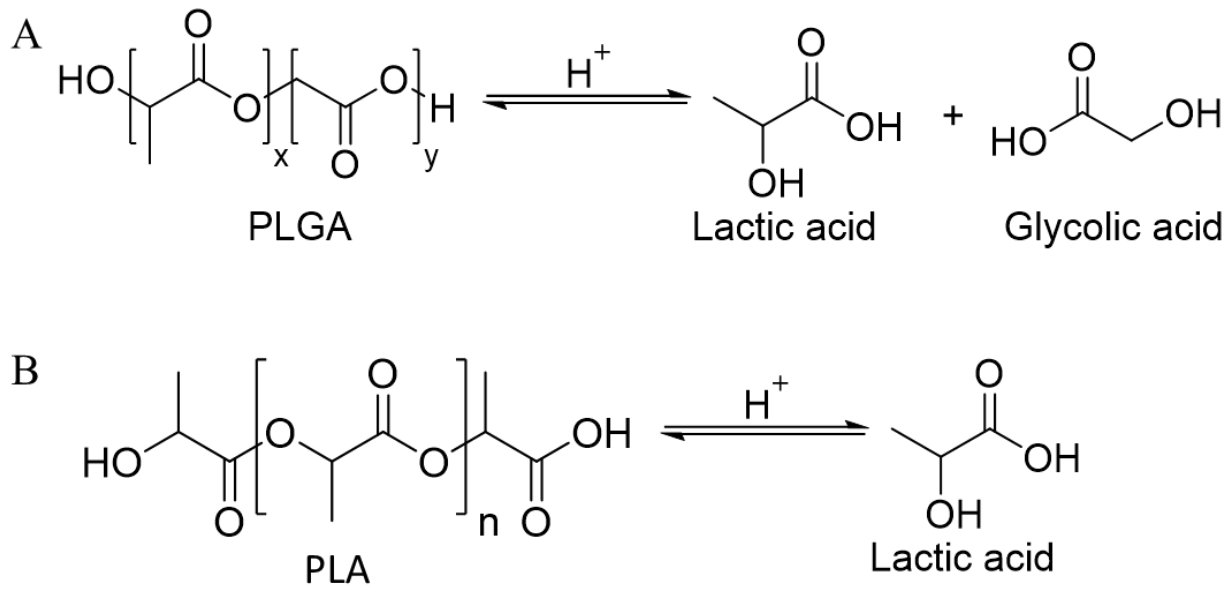

Figure 1.5: Structure of PLGA, PLA, and their breakdown products.
(A) Structure of PLGA and its breakdown products lactic acid and glycolic acid. (B) Structure of PLA and its breakdown products lactic acid. Both lactic acid and glycolic acid are existed in cells and can be metabolized.

1.5.2 The lipid-based NPs for NAFLD treatment

Muralidhara RaoMaradana et al. reported a liposome formulation in delivering curcumin. Their strategy was based on delivering the anti-inflammation compound (curcumin) into the dendritic cell (DCs) in the liver, leading to the inhibition of the inflammation environment and switch of the cell phenotypes. The liposomes were made by using the egg phosphatidylcholine (EPC) and cholesterol in the mass ratio of 7 to 3. The size of this liposome was about 120 nm, however, the macrophages targeting ability might be caused by the lack of PEG-coated on the surface. [173] Xiaona Liu et al. reported a liposomal formulation in NAFLD treatment by inhibiting fatty accumulation.[174] This liposome was made by L-α-phosphatidylcholine and cholesterol in the mass ratio of 20 to 1, and the average size of this liposome was about 70 nm. This

liposome showed strong accumulation in the liver *in vivo* and can retain in the liver up to 24 h after administration. And the delivery of liposomal deoxyschizandrin to adipocytes reduced the lipid droplet accumulations.

1.5.3 Inorganic NPs for NAFLD treatment

Unlike lipid-based or polymeric NPs mentioned which require the drug cargoes for treating NAFLD. The inorganic NPs have shown potential for NAFLD treatment due to their low cytotoxicity and unique physical properties. For example, the cerium dioxide (CeO_2) NPs (CNPs) exhibited strong anti-inflammatory effects based on the following reasons: 1) the small size of NPs caused a large ratio between surface area and volume, 2) the ability to switch the Ce^{3+} and Ce^{4+} on the surface of CNPs.[175] The biodistribution of CNPs is dependent on the administration routes. For intravenous administration, most of the CNPs are accumulated in the spleen followed closely by the liver. CNPs were also found in the lungs and the kidneys after the i.v. injection. The CNPs can stay inside the liver for up to a month, this enables the CNPs to exert the long-term anti-inflammation effects *in vivo*.[176] Silvia Carvajal et al. synthesized CNPs with the size of 4 nm, and they found those CNPs could decrease the lipid droplets, cholesterol, and cytokines accumulation in the liver after i.v. injection in the methionine and choline deficient diet (MCDD)-induced rats.[177]

2 CD98 SIRNA-LOADED NANOPARTICLES DECREASE HEPATIC STEATOSIS IN MICE

2.1 Introduction

Non-alcoholic fatty liver disease (NAFLD) is a common liver disease (with a prevalence of about 25%) in the world. Unfortunately, no drug is available for NAFLD treatment. The hallmark of NAFLD is the accumulation of excessive fat in the hepatocytes which are not the cells supposed to functionalize for large amount of fat storages. The NAFLD can be divided into two stages, the stage without inflammation is called NAFL and the stage with inflammation is called NASH. NASH can develop into more lethal diseases including fibrosis, cirrhosis, and liver cancer. Although the pathogenesis of NAFLD is not that clear, many different signaling pathways as well as different types of cells inside the body are related to the development of NAFLD. It has been shown that chronic liver inflammation can be the main driving force for this disease development.[178]

Currently, some therapeutic methods for NAFLD are under clinical evaluation. The exciting therapeutic effects of obeticholic acids (OCA) in the clinical trials are the best example to support the idea that NAFLD treatment may require a modulation of many signaling pathways at the same time. OCA, 6α-ethyl-3α,7α-dihydroxy-5-cholan-24-oic acid, is an agonist of the farnesoid-X-receptor (FXR) which has involved in many important biological processes including lipid metabolism, suppresses inflammation, and immune modulation in the NAFLD.[179-181] However, the serious side effects of the OCA might impair its therapeutic effects in NAFLD.[180] It is urgent to explore the new therapeutics for NAFLD treatment.

CD98 is a transmembrane glycoprotein which is existed in almost all types of cells, this fact implies the importance of CD98 in maintaining cell functions. Indeed, CD98 has shown broad functions in biology including the nutrients transportation, lipid metabolism,

inflammatory, innate immunity, and adaptive immunity.[104, 123, 132, 182, 183] Thus, it is rational to expect that many different signaling pathways in different cells can be modulated by targeting CD98. Moreover, CD98 is highly expressed in the disease condition and CD98 has shown the potential to be a target for disease treatment. For example, the signaling pathway in maintaining the acute myelogenous leukemia (AML) microenvironment is disturbed by CD98 antibodies.[184] Another CD98-targeting therapeutic approach is using the CD98 siRNA to silence the CD98 protein expression. This method requires the siRNA can be delivered into the cytosols of targeted cells. However, it is difficult for a bare siRNA to pass the membrane due to the negative charges, and the bare siRNAs might be degraded rapidly before they arrive at the lesions.

It has been proven that NPs can be an efficient platform for siRNA delivery with serval advantages: 1) nucleic acid protection, 2) targeted delivery, 3) controlled release. To date, siRNA has been loaded into many types of NPs including liposomes, polymeric NPs, and so on. Deliver CD98 siRNA to the lesions using NPs has been proven to be an effective way in the treatment of inflammation in the gastrointestinal systems including colitis and the inflammatory bowel disease (IBD).[114, 132] As demonstrated in the literature, the administration of CD98 siRNA NPs will lead to the small accumulation of NPs in unwanted tissues, and no damages were found in the major organs (heart, liver, lung, spleen, and kidney) by the H&E staining and the blood cells. These indicated that no serious side effects for the unwanted delivery of CD98 siRNA.[131]

The goal of this study is to verify the CD98 potential in NAFLD treatment. In this study, the CD98 siRNA loaded PLA NPs was fabricated using a double emulsion method. The size of NPs was examined by the dynamic light scattering method (DLS), scanning electron microscope

(SEM), and atomic force microscopy (AFM). The high-fat diet included NAFLD mice were used to evaluate the therapeutic effects of NPs.

2.2 Methods and materials

2.2.1 Materials

Machines:

The instruments used in this study included the Leo 1450VP scanning electron microscope (New York, NY), SPA 400 AFM (Seiko Instruments Inc., Japan), 90 Plus/BI-MAS sizer (Brookhaven Instruments Corporation, Holtsville, NY), ZetaPlus (Brookhaven Instruments Corporation, Holtsville, NY), Synergy H1 plate reader (BioTek, Winooski, USA), and Digital Sonifier 450 (Branson, Danbury, CT).

Reagents:

CD98 siRNAs (sc-35033 and sc-35034) were purchased from Santa Cruz. For the antibody, NF-κβ (sc-372) and CD98 (sc-9160) were purchased from Santa Cruz. CD11b (M1/70), CD11c (N418), and F4/80 (BM8) were purchased from eBioscience. TNF4α (MP6-XT22, 554419) and Ab 2.4G2 anti-FcγIII/II (553141) purchased from BD Biosciences. Albumin antibody (ab19196) was purchased from Abcam. GAPDH antibody (Millipore, AB2302, Temecula, CA) was purchased from Sigma-Aldrich. Human TNF-α ELISA kit (EH3TNFA, Kalamazoo, MI), Human IL-6 ELISA kit (EH2IL6, Kalamazoo, MI), and Human IFN-γ kit (EHIFNG, Kalamazoo, MI), Alexa Fluor 568 phalloidin (A12380), Hanks' Balanced Salt Solution (HBSS, 88284), Cytoseal XYL (94265), Hematoxylin 2, Maxima first strand cDNA synthesis kit (K1672), Maxima SYBR green/Rox (6-carboxyl-X-rhodamine) quantitative PCR Master Mix (K0221), and fixable Aqua Live/Dead cell staining kit (L34960) were purchased from Thermo

Fisher Scientific. Poly lactic acid (PLA, P1691-5G), polyethyleneimine (PEI, low molecular weight, Typical M_n 1800, Typical M_w 2000, 408700-250), WST-1 (11644807001), lipopolysaccharides (LPS, L7770), DAPI (4′,6-Diamidino-2-phenylindole dihydrochloride, D9542) Oil Red O (O0625) isopropanol (190764), primers, and collagenase VIII (C2139) were purchased from Sigma-Aldrich. 10% fat control diet and 60% fat diet were purchased from Research DIets (Research Diets, Inc, D12450B, New Brunswick, NJ). Polyvinyl alcohol (PVA, Stock #41238, 86-89% hydrolyzed low molecular weight) was purchased from Alfa Aesar. DMEM/Ham's F-12 medium was purchased from Invitrogen (Grand Island, NY). Penicillin and streptomycin (100X Corning) was purchased from Corning. Heat-inactivated fetal calf serum (10%, v/v) was purchased from Atlanta Biologicals (Atlanta, GA). Four-chamber tissue culture glass slides were purchased from BD Falcon (Bedford, MA, USA). Eosin Y Solution (Modified Alcoholic) was purchased from Scytek (EYB500, Logan, Utah). RNeasy Plus Mini Kit was purchased from Qiagen (Valencia, USA) and DNase I was purchased from Roche Diagnostics (Indianapolis, IN).

2.2.2 NPs fabrication

The NPs are fabricated using the double emulsion method which is usually referred to the W1/O/W2 emulsion. Twenty-nine μL of 5 μM CD98 siRNA is stabilized with 18 μL of 5mM polyethyleneimine (PEI) to achieve an N/P ratio of about 30 (N stands for the ammonium charge and the P stands for the phosphorous charges). The mixture is incubated at room temperature for 10 min to form the polyplex. The internal phase is formed by adding 750 μL of 50g/L BSA into the polyplex solution with a gentle mix. The PLA is dissolved in the dichloromethane (DCM) to make the stock with a concentration of 20 g/L. The internal phase is mixed with poly lactic acid (PLA) to make W1/O emulsion (first emulsion) after 1 min of ultrasonication with 50% active cycles at 70% power (Digital Sonifier 450, Branson, Danbury, CT) with the ice. Then the first

emulsion is added into the 0.3 g/L of polyvinyl alcohol (PVA) solution to form the W1/O/W2 emulsion. Then, the W1/O/W2 emulsion was added into the PVA solution (0.1g/L) with stirring and NPs will form during the evaporation of DCM. The NPs are centrifuged down at 9953 g for 1 h. And the pellets were rinsed 3 times and the samples were lyophilized after resuspension. The dried power was weighted and stored at -80 degree for further treatment usage and characterization.

For the fabrication of scramble siRNA NPs or the FITC-labelled siRNA loaded NPs, the same procedure was used, with replacing the cargoes from CD98 siRNA to the scramble siRNA or the FITC-labelled siRNA.

2.2.3 NPs size and zeta potential measurement

The size of NPs (diameter) is measured by light scattering (90Plus/BI-MAS, Brookhaven Instruments Corporation, Holtsville, NY). The zeta potential of NPs is measured in the zeta potential analyzer (ZetaPlus, Brookhaven Instruments Corporation, Holtsville, NY) by accessing the light scattering under an electric field. All the results were obtained from 3 measurements and each measurement is repeated 10 times.

2.2.4 SEM measurement

A drop of NPs solution is added onto a glass coverslip. After the samples were dried in room temperature, samples were sputter-coated with Au/Pd (Denton desktop sputter coater, Moorestown, NJ). The images were obtained using LEO 1450VP (New York, NY).

2.2.5 AFM measurement

A drop of NPs solution is added onto mica slides and the samples were dried in a hood at room temperature. The images were obtained using a SPA 400 AFM (Seiko Instruments Inc.,

Japan) with the following settings: 1) trapping mode with 150 kHz resonant frequency and 2) scanning frequency of 1 Hz.

2.2.6 Cytotoxicity assay (WST-1)

Even though the cytotoxicity of PLA is not a concern, the off-target effects of siRNA might cause cell death. To access the potential cytotoxicity of the CD98 siRNA NPs, the cell proliferation reagent, WST-1, is used. The cells were seeded on a 96-well plate with 5×10^4 cells per well and NPs were added into the culture medium at the final concentration of 1 mg/mL. After incubation, 10 µL of WST-1 reagent was added into the medium and the live cells will convert the WST-1 to form the purple formazan. The A440 was read by a plate reader and the viability in cells without any treatment was set to 1 (control).

2.2.7 Cell culture

Hep G2 (HepG2) cells, Caco2-BBe cells, and Raw264.7 cells were culture in the 37 °C incubator with 5% of CO_2 (v/v) in a humidified atmosphere. The culture medium used was DMEM/Ham's F-12 medium (Invitrogen, Grand Island, NY) with 10% (v/v) of heat-inactivated fetal calf serum, 1% of penicillin/streptomycin, and 2 mM of L-glutamine.

The Lipopolysaccharides (LPS) stimulation is done by adding the LPS into the culture medium for 24 h with the final concentration of 10 µg/mL.

2.2.8 NPs internalization studies

To track the NPs, the FITC-labeled siRNA was used to make the NPs. Thus, the signal of FITC inside of the NPs can be seen by using fluorescence microscopy. In this study, fluorescence microscopy was used to visualize the NPs. The internalization was studied both *in vitro* and *in vivo*.

For *in vitro* internalization study, the HepG2 cells were seeded in chamber tissue culture slides (BD Falcon, Bedford, MA, USA). Cells were incubated with 200 μg/mL of FITC-labeled siRNA-loaded NPs overnight. Then the medium was removed, and cells were rinsed with PBS for 3 times to remove the free NPs outside of cells. The cell samples were fixed with 4 % para-formaldehyde (PFA) at room temperature for 20 min in dark. The slide was sealed by the pro-long golden reagent with DAPI.

For *in vivo* internalization study, mice were sacrificed 4 h after the tail intravenous injection of FITC-labeled siRNA-loaded NPs. The major tissues were collected and treated properly for the next staining. The actin was stained by phalloidin with Alexa Fluor 568 (1: 60 diluted) for 45 min, and the nuclei were stained by DAPI for 5 min.

2.2.9 Mice experiment

All the mice experiments were approved by Georgia State University Institutional Animal Care and Use Committee (protocol number A13041).

C57BL/6 female mice (8 weeks of age) were purchased from the Jackson Laboratory and group-housed (5 mice per case) with the following condition: 25 °C, a 12 to 12 hours light-dark cycle, and allowed unrestricted access to potables and standard mouse chow.

The NAFLD model is built by feeding C57BL/6 mice with a 60% fat diet (high-fat diet, HFD). The control group mice were fed with a 10% fat diet (noted as the low-fat diet, LFD). Mice will receive a dose of NPs (CD98 siRNA-loaded NPs or the scrambled siRNA-loaded NPs) biweekly.

2.2.10 Oil red staining

The stock solution of 0.5% (w/v) Oil Red O is prepared by dissolving 0.5 g of Oil Red O in 100 mL of isopropanol. Before staining, the tissues are rinsed under the running water for 10

min and next, rinsed with 60% of isopropanol. Next, the slides were merged in the Oil Red O working better for 15 min. Hematoxylin 2 was used to stain the nuclei on the slides. Then, slides were rinsed with water and drying in the air. The slide was sealed by using a drop of cytoseal XYL reagent with a cover glass slide.

2.2.11 Hematoxylin and Eosin Y (H&E) staining

Before the staining, the paraffin-embedded tissues were dewaxed by the following procedures: 10 min of xylene wash for twice, 1 min of 100% ethanol wash for twice, 1 min of 95% ethanol wash for twice, and 1 min of 75% ethanol wash for twice. The dewaxed slides were stained with Hematoxylin for 5 min and followed by washing with DI water. The bluing reagent is used to enhance the color of nuclei. After the second rinse with DI water, the slides were rinsed with 100% ethanol before dipping into the Eosin Y solution. In the end, the excessive Eosin Y was removed by 100% ethanol washes and dry in the air. The slides were sealed using the cytoseal XYL reagent with a cover slide.

2.2.12 Liver grade calculation

The H&E stains were used to count the grade for liver damages by using the method reported by Kleiner et al.[185] The grading system is adding the scores from three subsystems: i.e., steatosis, lobular inflammation, and hepatocytes ballooning. The scores for steatosis and lobular inflammation were ranged from 0-3 and the score for hepatocyte ballooning was ranged from 0-2. The total scores were the sum of the scores in three subsystems, which is called the NAFLD activity score (NAS).

2.2.13 RT-qPCR

The total RNA was isolated from cells by using the RNeasy Plus Mini Kit under the manufacturer’s instructions. The quality of yield RNA was examined by checking the A260/A280

using a plate reader. The cDNA was synthesized for the same amount of total RNAs by using Maxima first strand cDNA synthesis kit. The expression level of certain mRNA is accessed by using the Maxima SYBR green (6-carboxyl-X-rhodamine) quantitative PCR Master Mix. The expression level of mRNA in the control group was set to 1 and the changing fold in the mRNA was calculated by a $2^{-\Delta\Delta CT}$ method. The sequence of primer was listed in table 1 in Appendix.

2.2.14 Western blot

The liver samples from mice with CD98 siRNA-loaded PLA NPs or the scramble siRNA-loaded NPs were homogenized with RIPA buffer to obtain the total proteins. 100 μg of total protein was loaded into the 12% SDS-PAGE gel. The membrane was blocked with 5% non-fat milk and then applied with the primary antibodies for 2 h at room temperature. Next, the membrane was washed 15 min for 3 times and applied with a secondary antibody with HRP conjugation (1: 4000 diluted). The films were developed by using a SERIES 2000A Processor film developer. The primary antibodies used in this studies are listed below: NF Kappa β (Santa Cruz,sc-9160, Dallas, TX), GAPDH (Millipore, AB2302, Temecula, CA) , and CD-98 (Santa Cruz, sc-9160, Dallas, TX).

2.2.15 ELISA for cytokines assay

HepG2 cells were culture with CD98 siRNA-loaded NPs for 12 h with or without LPS stimulation. The culture medium was collected for ELISA assay. Human TNF-α ELISA Kit, human IL-6 ELISA Kit, and human IFN-γ ELISA Kit were used to measure the cytokines secreted by the HepG2 cells. The cytokine secretion amounts in HepG2 cells without any treatment (no LPS, no NPs) were used as the control.

2.2.16 Flow cytometry

The liver samples were cut into small pieces and incubated in the HBSS with 5% FBS, 1.5 mg/mL of collagenase VIII, and 40 U/mL DNase I at 37 ℃ for 11 min in a shaker. Next, the solution was filtered by a 100 μm strainer to remove big particles and centrifuged at 300 g to get the cell pellets. The obtained cells were suspended in the PBS solution with 5% of FBS, and perform the live/death staining and antibody staining (4°C, 30 min). Flow cytometry analysis was performed using the LSR II.

2.2.17 Statistical analysis

Statistical analysis was performed using unpaired two-tailed Student's t-test by GraphPad software (v3.06). Values were expressed as means ± SEM from experiments performed in triplicate (n = 3), except for cytotoxicity tests and *in vivo* experiments (respectively n = 8 and n=5). Data are representative of n determinations. ***P < 0.001, **P < 0.01, *P < 0.05, and NS, not statically significant.

2.3 Results

2.3.1 Characterization of CD98 siRNA-loaded poly lactic acid (PLA) NPs

CD98 siRNA-loaded NPs were fabricated by using the double emulsion method, the size, and zeta potential of CD98 siRNA-loaded NPs or scramble siRNA-loaded NPs were detected by DLS, SEM, and AFM. As seen in Figure 2.1 A and B, the average size of CD98 siRNA-loaded NPs is about 273 nm with a zeta potential of -12.84 mV. The average size of scramble siRNA-loaded NPs is about 274 nm with a zeta potential of -15.60 mV. The SEM (Figure 2.1 C) and AFM (Appendix Figure 5-0.1) confirmed the shape of NPs was spherical with a size close to 280 nm in diameter.

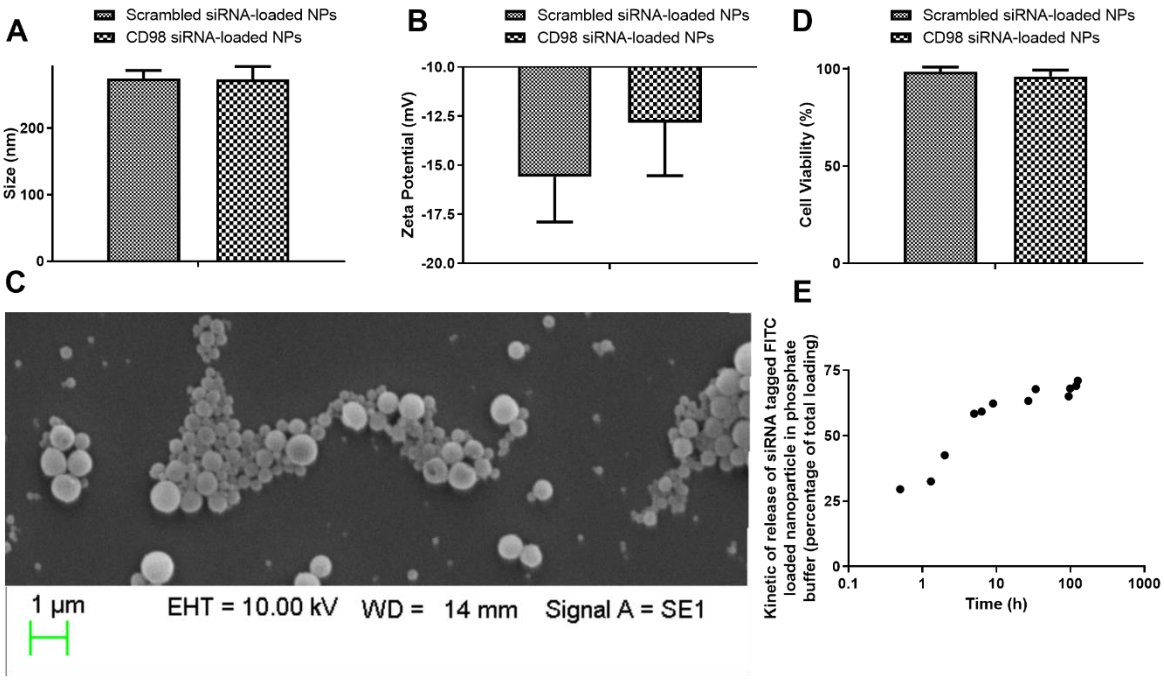

Figure 2.1: The characterization of CD98 siRNA-loaded NPs.
(A) Average size and (B) zeta potential (mV) of CD98 siRNA-loaded NPs and scrambled siRNA-loaded NPs were measured by light scattering analysis (values represent means ± SEM. Data are representative of n=3 determinations). (C) Scanning electronic microscopy image of CD98 siRNA-loaded NPs (The sample was prepared using a drop of NPs at a concentration of 500 µg/mL). (D) Cytotoxicity of 1 mg/mL CD98 siRNA-loaded NPs and scrambled siRNA-loaded NPs on HepG2 cells after 48h (values represent means ± SEM. Data are representative of n=8 determinations). (E) Kinetic of the release of CD98 siRNA complexed with PEI form NPs (PBS buffer, 37°C), the x-axis represents the log10 (Time).[171]

The drug release profile may affect the therapeutic effects.[186] As shown in Figure 2.1 E, the FITC-label siRNA accumulated release amount was plot versus the dialysis time. Within the beginning of 4 h, about 40% of the drug was released. This indicated the burst effects which refers to a large number of cargoes release from NPs at the beginning within a short period, were not observed in this formulation.[187] The further study indicated 4 h is enough for large

amounts of NPs to accumulate in the liver, thus, some of the 40% of siRNA can be released inside the cytosol. And the PEI/siRNA complex also contributes to the sustainable drug release inside cytosol (for the rest 60% siRNA). The result of CD98 siRNA-loaded NPs or scramble siRNA-loaded NPs cytotoxicity on HepG2 cells was showed in Figure 2.1 D.

No cytotoxicity was found in CD98 siRNA-loaded NPs (96.16%, 1 mg/mL) or scramble siRNA-loaded NPs (98.56%, 1 mg/mL) treated HepG2 cells for 72 h.

2.3.2 *In vitro* internalization of CD98 siRNA-loaded NPs

The internalization efficiency of NPs will affect the therapeutic outcomes. As seen in Appendix 5-0-2, the bright signals on the membrane and cytosol indicted the presence of FITC-label siRNA during the endocytosis and inside of cytosol. To test whether the CD98 siRNA could degrade the CD98 mRNA in the cells, the CD98 mRNA expression levels in different cell lines with or without LPS stimulation were accessed by using RT-qPCR. As shown in Figure 2.2, when compared to the CD98 expression level in the control group, the LPS increased the CD98 mRNA expression level significantly in the scramble siRNA-loaded NPs treated group. And the pre-treatment of CD98 siRNA-loaded NPs decreased the CD98 mRNA expression level in HepG2 cells, Raw264.7 cells, and Caco2-BBe cells for 6-, 7-, 8-times respectively when compared with the CD98 expression level in scramble siRNA-loaded NPs treated group. The significant decrease in the CD98 mRNA level with applying CD98 siRNA-loaded NPs further indicated the NPs could be taken by the cells with a high efficiency.

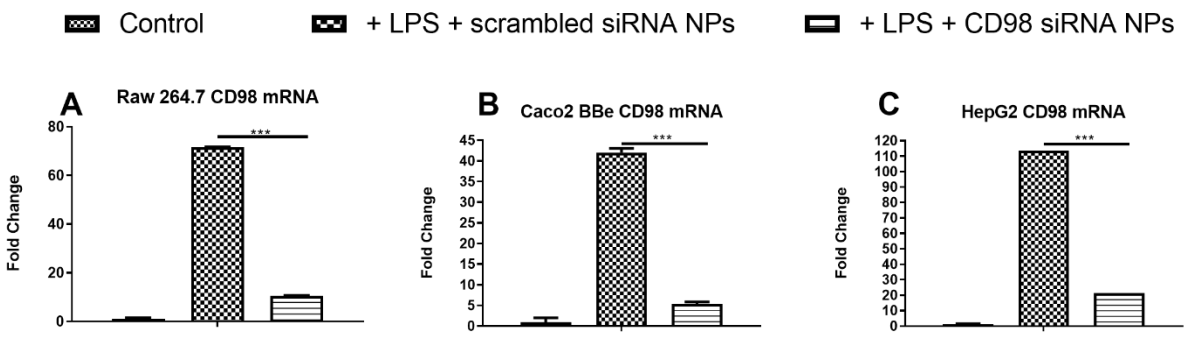

Figure 2.2: CD98 mRNA expression level was decreased after the incubation with CD98 siRNA-loaded NPs.

CD98 mRNA expression levels in three different cell lines (A) Raw 264.7, (B) Caco2 BBe, and HepG2 cells with different treatments were studied using the RT-qPCR. The cell without LPS-stimulation and NPs treatment were used as the control. The LPS-stimulated cells with CD98 siRNA-loaded NPs were showed with the legend in + LPS + CD98 siRNA NPs. The LPS-stimulated cells with scrambled siRNA-loaded NPs were showed with the legend in + LPS + scrambled siRNA NPs. The LPS stimulation was incubating cells with 10 μg/mL LPS for 24h. The NPs concentration for treatment is 200 μg/mL. Values represent means ± SE. Data are representative of n=3 determinations. ***P < 0.001, **P < 0.01, *P < 0.05, and NS, not statically significant.[171]

2.3.3 CD98 siRNA-loaded NPs inhibited the expression of the pro-inflammatory cytokines

As demonstrated in the literature, the CD98 has shown a pro-inflammatory effect. In this study, the mRNA expression level of IFN-γ, COX-2, and TNF-α were measured (Figure 2.3). Pre-treatment with scramble siRNA-loaded NPs in three cell lines showed an increased expression level of those cytokines with the LPS stimulation. While pre-treatment of CD98 siRNA-loaded NPs decreased the LPS-induced cytokine mRNAs expression. Pre-treatment of CD98 siRNA-loaded NPs decreased the TNF-α mRNA expression level in HepG2 cells, Raw264.7

cells, and Caco2-BBe cells for 10-, 90-, 10-times respectively when compared with the CD98 expression level in scramble siRNA-loaded NPs treated group (Figure 2.3 A-C). Pre-treatment of CD98 siRNA-loaded NPs decreased the COX-2 mRNA expression level in HepG2 cells, Raw264.7 cells, and Caco2-BBe cells for 4-, 5-, 5-times respectively when compared with the CD98 expression level in scramble siRNA-loaded NPs treated group (Figure 2.3 D-F). Pre-treatment of CD98 siRNA-loaded NPs decreased the IFN-γ mRNA expression level in HepG2 cells, Raw264.7 cells, and Caco2-BBe cells for 6-, 10-, 2-times respectively when compared with the CD98 expression level in scramble siRNA-loaded NPs treated group (Figure 2.3 G-I).

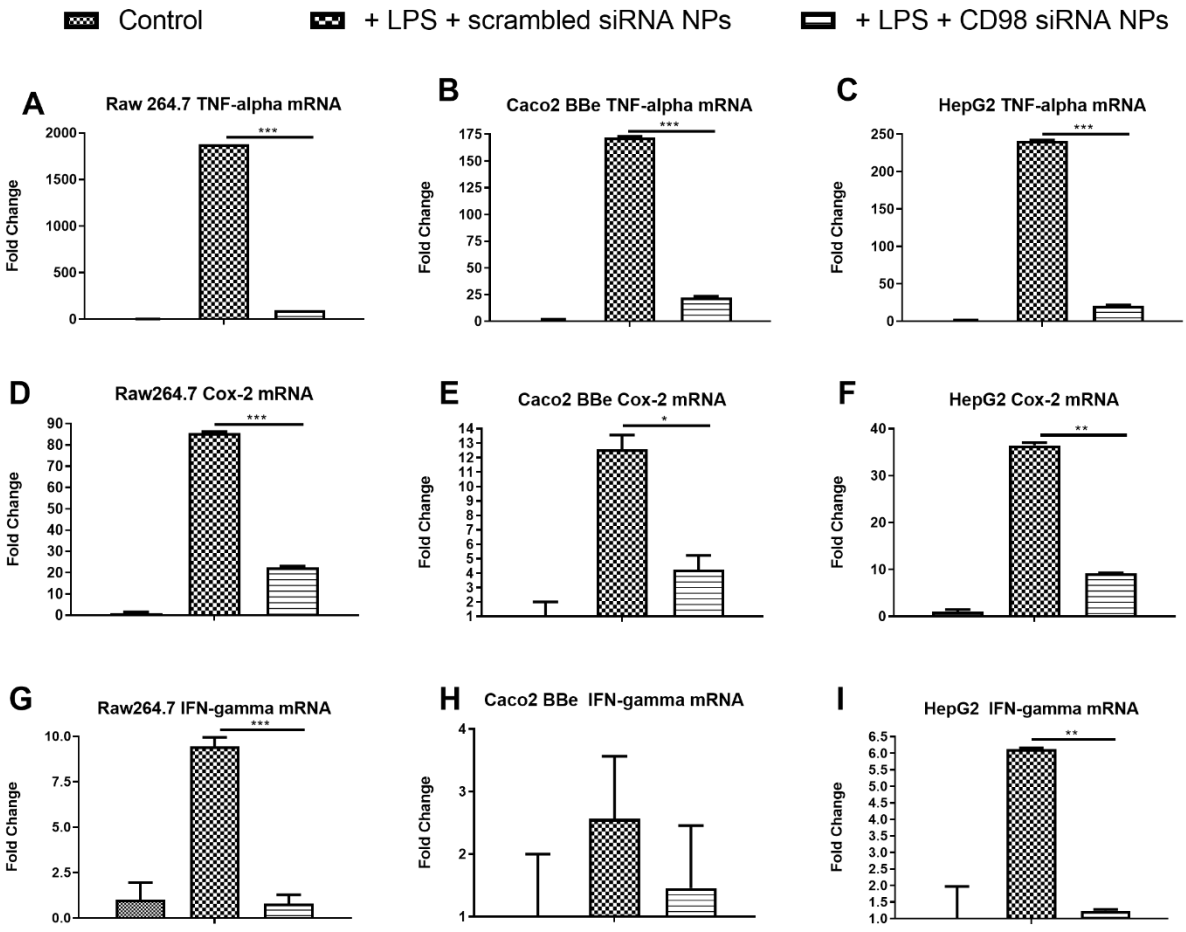

Figure 2.3: CD98 siRNA-loaded NPs treatments decrease the expression of pro-inflammatory cytokines.

TNF-α, COX-2, and IFN-γ mRNA expression levels in three different cell lines (A) Raw 264.7, (B) Caco2 BBe, and HepG2 cells with different treatments were studied using the RT-qPCR. The cell without LPS-stimulation and NPs treatment were used as the control. The LPS-stimulated cells with CD98 siRNA-loaded NPs were showed with the legend in + LPS + CD98 siRNA NPs. The LPS-stimulated cells with scrambled siRNA-loaded NPs were showed with the legend in + LPS + scrambled siRNA NPs. The LPS stimulation was incubating cells with 10 μg/mL LPS for 24 h. The NPs concentration for treatment is 200 μg/mL. Values represent means ± SEM. Data are representative of n=3 determinations. ***P < 0.001, **P < 0.01, *P < 0.05, and NS, not statically significant.[171]

The expression of the secreted cytokines was also studied by using the corresponding ELISA assays. As shown in Figure 2.4, the uptake of CD98 siRNA-loaded NPs decreased the expression levels of TNF-α (14% decrease, $p<0.05$), IL-6 (6% decrease, NS), and IFN-γ (500% decrease, $p<0.001$) when compared to the control group.

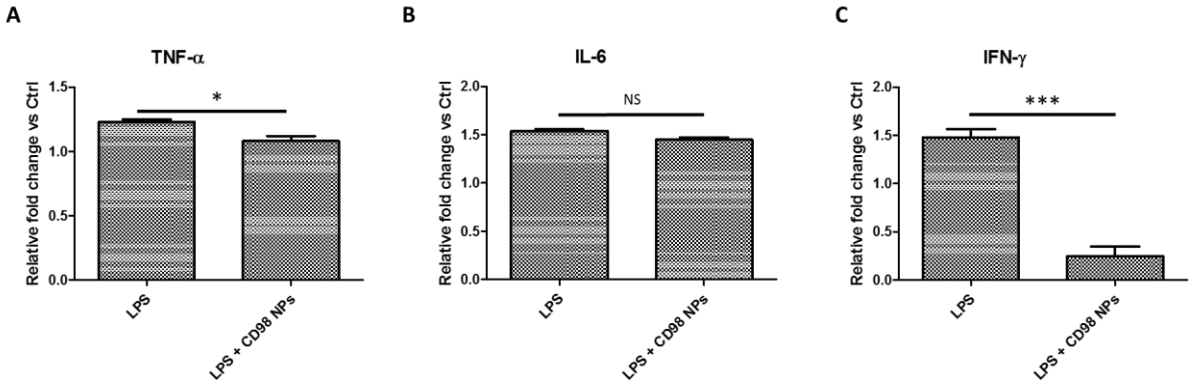

Figure 2.4: CD98 siRNA-loaded NPs inhibited the secretion of LPS-induced pro-inflammatory cytokines, TNF-α, IL-6, and IFN-γ.
(A) TNF-α, (B) IL-6, and (C) IFN-γ expression levels in LPS-stimulated HepG2 cells with or without the treatment of CD98 siRNA-loaded NPs. The LPS stimulation was incubating cells with 10 μg/mL LPS for 24 h. The NPs concentration for treatment is 200 μg/mL. Values

represent means ± SEM. Data are representative of n=3 determinations. ***P < 0.001, **P < 0.01, *P < 0.05, and NS, not statically significant.[171]

Taken together, the CD98 siRNA-loaded NPs showed a strong CD98 silence effect and the potential in anti-inflammatory. As mentioned, the inflammatory could be the major driving force in the NAFLD development. Therefore, the NAFLD mice were used to evaluate the therapeutic effects of CD98 siRNA-loaded NPs.

2.3.4 CD98 siRNA-loaded NPs are accumulated in the liver

The FITC-labeled siRNA NPs were used for NPs biodistribution in major organs including heart, lung, brain, colon, kidney, spleen, and the liver. The biodistribution of NPs in both HFD mice and LFD mice was studied and the signal of FITC was only found in the kidney, spleen, and liver after the tail vein injection.

As shown in Appendix Figure 5-0.3, the kidney, spleen, and liver from the HFD mice without treatment of FITC-labeled siRNA NPs were used to control the autofluorescence. The red signals indicated the actin, and the blue signals indicated the nuclei. In LFD mice, no strong signal of FITC was found in the spleen (Figure 2.5 C), and slightly intensity of FITC signals was found in the liver (Figure 2.5 E), and kidney (Figure 2.5 A). However, the biodistribution profiles in HFD mice showed the huge difference when compared with those in LFD mice. The fluorescent signal was found in Figure 2.5 show in the yellow color which indicated the overlapping of FITC-labeled siRNA NPs and the actin. A clear intensity of FITC was found in the spleen (Figure 2.5 D) which was not obviously seen in the spleen of LFD mice. In HFD mice, the kidney (Figure 2.5 B) and liver (Figure 2.5 F) showed a stronger accumulation of FITC-labeled siRNA NPs when compared spleen. Those results implied the HFD might cause changes in the

spleen. As known, the spleen plays important role in the immune responses and the changes in the spleen might be involved in the NAFLD.

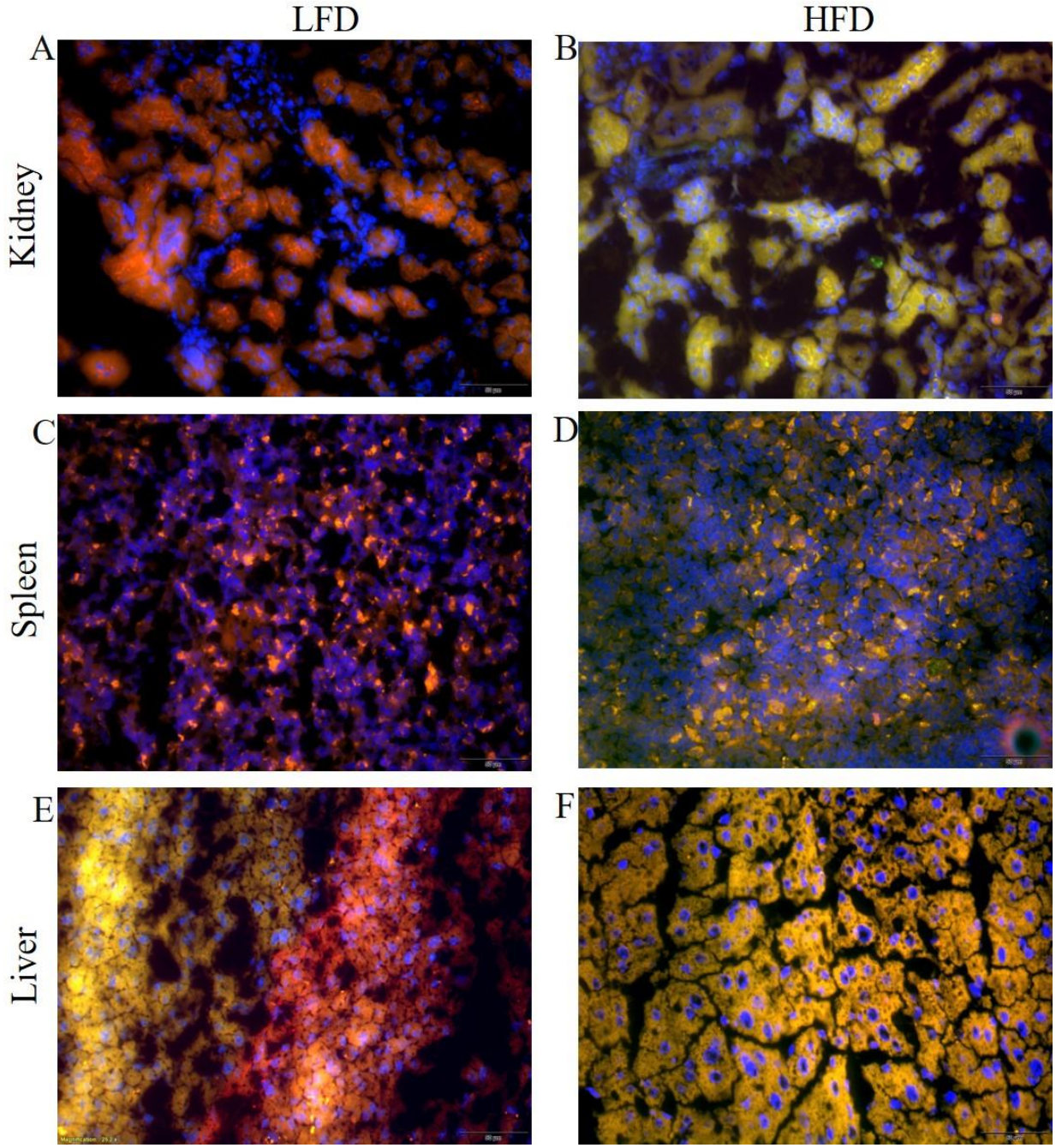

Figure 2.5: Biodistribution of NPs in mice at 4 h after the i.v. the administration indicated the liver in HFD group uptake most of NPs.

Among the major organs, the signal of FITC was only found in the kidney (A&B), spleen (C&D), and liver (E&F). The FITC-labeled siRNA-loaded NPs (green) was used to track the

presence of NPs. The actin was stained with Alexa Fluor 568 conjugated phalloidin (red) and DAPI was used to stained the nuclei (blue). The scale bar is 50 μm.

2.3.5 The NPs are specifically accumulated in macrophages-like cells and hepatocytes

As mentioned, different cells in the liver played different roles in NAFLD. Thus, the biodistribution of NPs inside the liver was measured. As shown in Figure 2.6, the upper panel is the biodistribution profiles derived from HFD mice and the lower panel is the biodistribution profiles derived from LFD mice. When compared the column B, C, and D, the percentages of FITC-positive (NP-positive) macrophages-like cells, dendrite cell, and hepatocytes in HFD mice is 2.2-fold, 0.95-, and 1.68-fold higher than that in the LFD mice, respectively. This is the same as what we found in the whole body biodistribution study, that more NPs accumulation was found in the HFD mice than that in LFD mice. In the liver, hepatocytes and macrophages-like cells uptake most of the NPs. A very limited amount of uptake percentage was found in the dendrite cells.

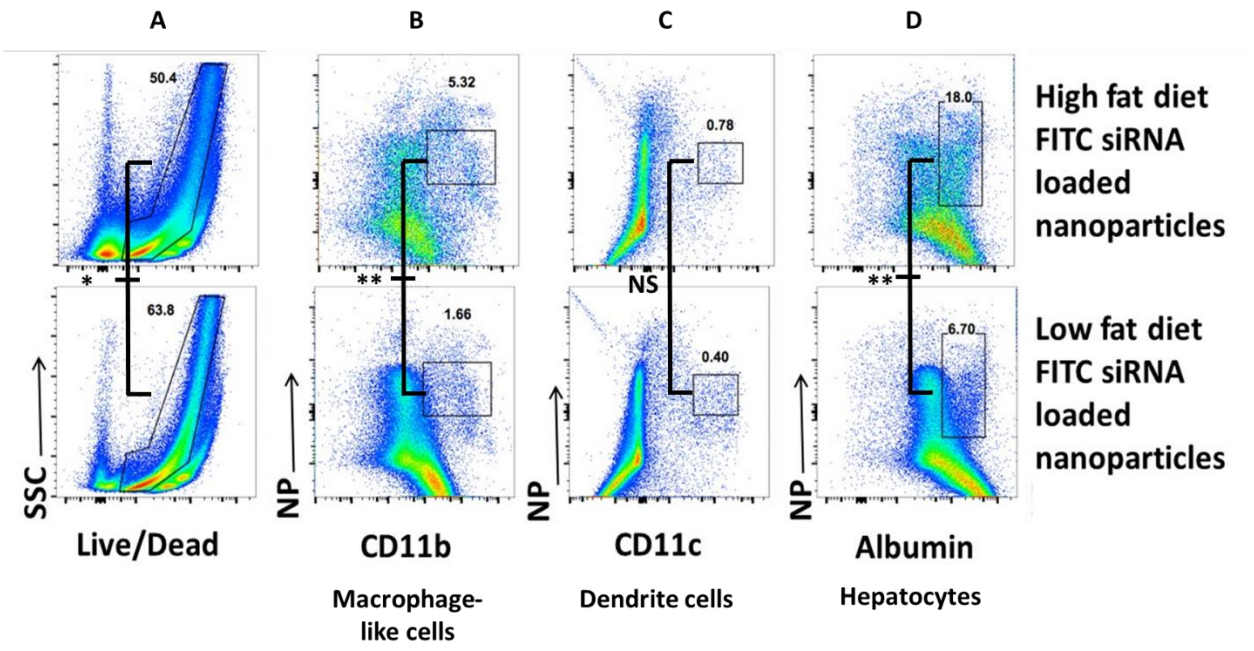

Figure 2.6: The biodistribution of NPs inside of the liver at 4 h after the *i.v.* administration indicated the NPs are majorly taken by Kupffer cells and hepatocytes.

Representative FACS plots showing the percentage of FITC-positive cells in each cell populations, including (A) live cells, (B) macro-phages like cells, (C) dendritic cells, and (D) hepatocytes in HFD mice (upper panel) or LFD mice (lower panel) after administration of FITC-labeled siRNA-loaded NPs. Cells were gated as followed: hepatocytes (CD45-MHC class II- F4/80-CD11b-CD11c-albumin+), macrophages-like cells (CD45+MHC class II+F4/80+CD11b+CD11c-), and dendritic cells (CD45+MHC class II+F4/80-CD11b+CD11c+). Values represent means ± SEM. Data are representative of n=5 mice per group. **P < 0.01, *P < 0.05 and NS, not statically significant.[171]

2.3.6 The CD98 expression level was decreased after delivery of CD98 siRNA loaded NPs

After a large amount of FITC-labeled-siRNA-loaded NPs found in the liver, the expression level of CD98 protein in live was accessed by western blot. As seen in Figure 2.7, the injection of CD98 siRNA-loaded NPs decreased the CD98 expression. Quantification results

indicated the CD98 siRNA-loaded NPs can reduce CD98 expression by about 90%. The expression of NF-κB was decreased after the CD98 siRNA-loaded NPs administration indicated the NF-κB is likely among one of the downstream targets of CD98 signaling pathway.

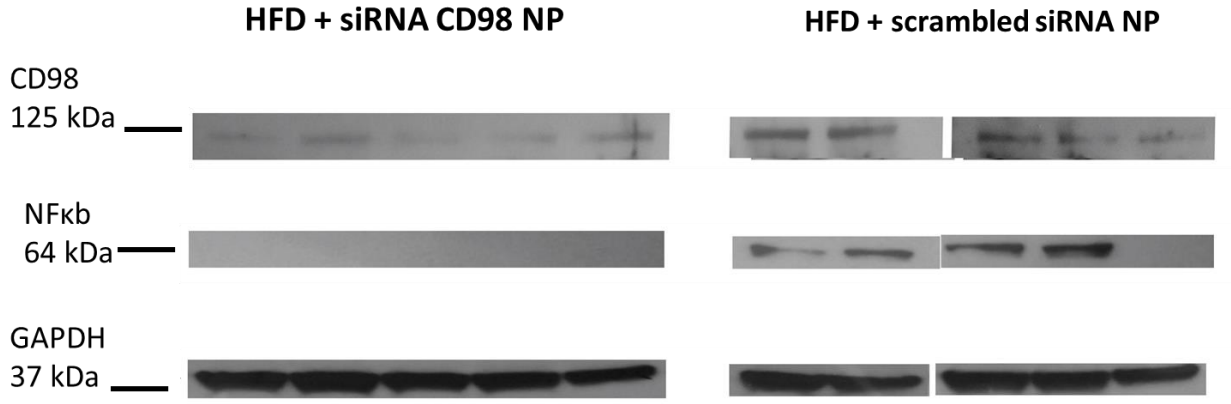

Figure 2.7: CD98 siRNA-loaded NPs silenced the CD98 protein expression level in the liver. CD98 and NF-κB expression levels in HFD mice livers were examined by the western blot after treated with CD98 siRNA-loaded NPs or scrambled siRNA-loaded NPs twice a week. The dose of NPs is 500 μg of NPs per mice.[171]

2.3.7 CD98 siRNA-loaded NPs alleviated the NAFLD symptoms

As seen in Figure 2.8, the serum level of ALT in HFD mice with CD98 siRNA-loaded NPs treatment was significantly lower (about 45%, $p < 0.01$) than that in the HFD mice with scramble siRNA-loaded NPs. The serum level of ALT in HFD mice with CD98 siRNA-loaded NPs treated groups was close to that in the mice with a regular diet (healthy mice, Figure 2.8 A). The amount of cholesterol (Figure 2.8 B), triglycerides (Figure 2.8 E), and glucose (Figure 2.8 C) in CD98 siRNA-loaded NPs treated HFD mice were significantly decreased when compared with those in scramble siRNA-loaded NPs treated groups. The HDLc in CD98 siRNA-loaded NPs treated HFD mice was slightly decreased (NS) when compared with that in scramble siRNA-loaded NPs treated groups (Figure 2.8 D).

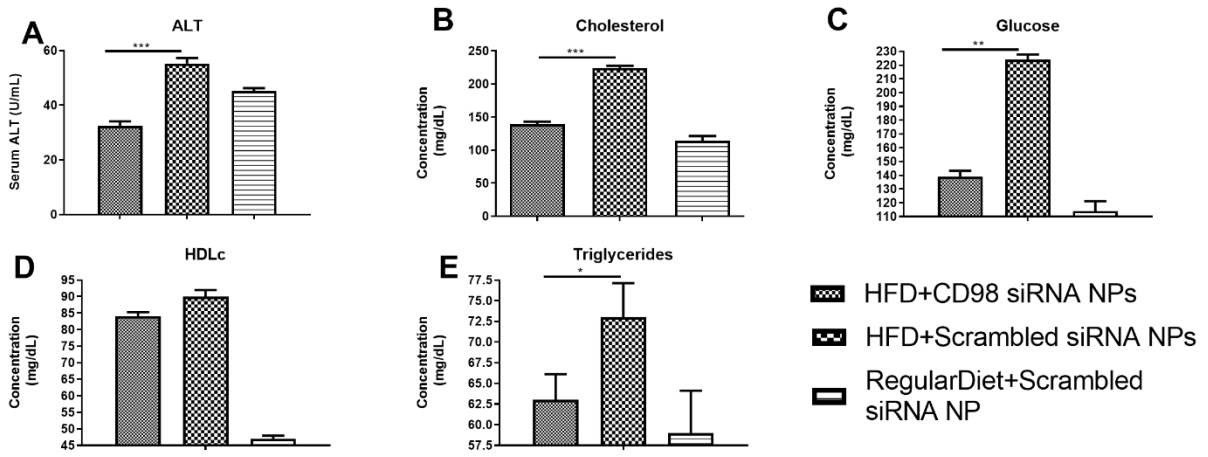

Figure 2.8: CD98 siRNA-loaded NPs decreased the pro-steatosis markers in NAFLD mice. The pro-steatosis makers including the (A) serum ALT, (B) cholesterol, (C) glucose, (D) HDLc, and (E) triglycerides are analyzed in mice with different diets (HFD or regular diet) and received different treatments (CD98 siRNA-loaded NPs or scrambled siRNA-loaded NPs biweekly. The dose for each treatment was 500 μg of NPs. Values represent means ± SEM, n= 5. **P < 0.01, *P < 0.05, and NS, not statically significant.[171]

Since the biopsy is the golden standard for NAFLD diagnosis, the image of the liver was visualized by Sirius red and H&E stains (Figure 2.9).[188] Clear lipid vacuoles (Figure 2.9 B) and the collagens (Figure 2.9 A) are seen in the liver from HFD with scramble siRNA-loaded NPs treatment. While no collagen (Figure 2.9 C) or the lipid vacuoles (Figure 2.9 D) was found in the liver from HFD mice with CD98 siRNA-loaded NPs treatment. The total NAFLD Activity Score (NAS) in HFD mice with scramble siRNA-loaded NPs treatment is 7 which indicates a serious level of liver damage (Figure 2.9 E). While the NAS equals zero in the CD98 siRNA-loaded NPs treated HFD mice indicated the liver is under healthy condition.[185]

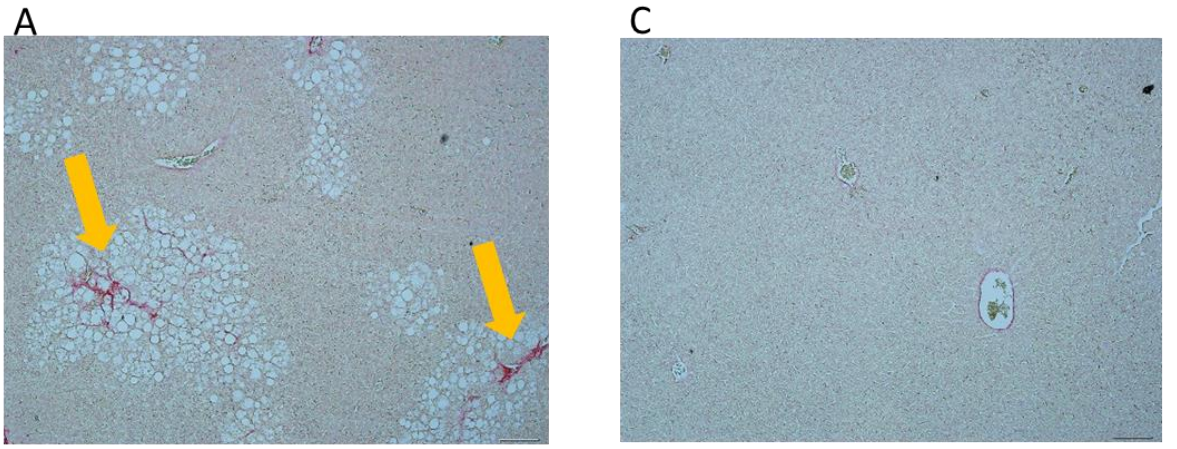

E

NAFLD Activity Score	Scrambled siRNA-loaded NPs	CD98 siRNA-loaded NPs
Steatosis	3	0
Lobular inflammation	2	0
Hepatocytes Ballooning	2	0
Total NAFLD Activity Score	7	0

Figure 2.9: CD98 siRNA-loaded NPs significantly improved HFD-caused liver damages. Sirius Red stains showed the fibrotic collagens in the HFD mice received CD98 siRNA-loaded NPs (C) or scrambled siRNA-loaded NPs (A) twice a week. The H&E stains showed the hall-mark of NAFLD (lipid vacuolization) in the HFD mice CD98 siRNA-loaded NPs (D) or scram-bled siRNA-loaded NPs (B) twice a week. Each group contains 5 mice. The scale bar is 50 μm. (E) The NAFLD activity scores were calculated based on the methods reported by Kleiner.[171, 185]

2.4 Discussion

CD98 is more than just an amino acid transporter.[14, 81, 104, 115, 116] The CD98 has been well identified as the marker and promoter protein in inflammatory disease including colitis and IBD. In the colitis, the upregulation of CD98 was found as well as the upregulation of proinflammatory cytokines such as TNF-α, IFN-γ, IL-1β, and IL-6.[182, 189, 190] And silencing of CD98 by delivery in the CD98 siRNA into the gastrointestinal site showed a decreased level of pro-inflammatory cytokines.[132] In the liver, the pro-inflammatory cytokines have shown the ability in promoting NAFLD development. According to the most accepted NAFLD pathogenesis theory (multiple hit theory), the stresses such as nutrients and the inflammation showed a high impact on the NAFLD developments.[191] For example, the most-well studied pro-inflammatory cytokine in NAFLD, TNF-α, is highly correlated with fibrosis level in NASH patients and liver damages (NAS) in NAFLD. But no significant improvement was found in the clinical trial by using an anti-TNF-α reagent, pentoxifylline, for NAFLD or NASH treatment. The failure of this trial might be caused by a single type of cytokines is not enough for the treatment of NAFLD, since many types of cytokines are involved in the development of NAFLD. Also, without specific targeting ability, the side effects of immune-related diseases might impair the application of this anti-TNF-α reagent.[192]

The targeting delivery feature of NPs allowed most drugs accumulated in the lesion or the lesion-related sites. Thus, enhancing the therapeutic effects by the high presence of the drug in the lesion and decrease the side effects on other tissues.[193] Decreased CD98 expression in the liver specifically decrease serval pro-inflammatory cytokines expression, leading to the NAFLD alleviation. In addition, the CD98 siRNA reduced expression level of NF-κB, leading to the shutdown of pro-inflammatory cytokines productions.[194]

The average size of CD98 siRNA-loaded NPs is around 270 nm. The SEM image indicated the some CD98 siRNA-loaded NPs were less than 150 nm while some are larger than 300 nm. The size and surface modifications will affect the biodistribution of NPs inside of the liver. The Kupffer cells are preferring the NPs with sizes bigger than 200 nm while only small NPs (smaller than 150 nm) can pass the LESCs barriers to target the hepatocytes. Also, the hydroxyl group on the surface of NPs helps reduce the clearance by macrophages. Decreased the CD98 expression in macrophage-like cells showed a significant decrease in pro-inflammatory secretion. The Kupffer cells are the macrophages inside the liver. Targeting the Kupffer cells and hepatocytes at the same time could show strong therapeutic effects on NAFLD since different types of cells (hepatocytes, stellate cells, Kupffer cells, etc.) were involved in NAFLD progression.

In conclusion, CD98 can be a potential therapeutic target for NAFLD treatment, and the NPs can be an effective way in delivering the CD98 siRNA to the liver. And more studies on the formulations are required to improve the drug targeting delivery to different hepatic cells, which can help us to find out the most effective way in curing the NAFLD via targeting CD98 or other molecules.

3 THE INTERNALIZATION OF GARLIC-DERIVED NANOVESICLES ON LIVER CELLS IS TRIGGERED BY INTERACTION WITH CD98

3.1 Background

Recently, plant-derived nanovesicles were isolated from several edible plants such as grapefruits, gingers, carrots, apples, and lemons.[7-10] Those plant-derived nanovesicles resembled their mammalian exosome counterparts in that they carried functional cargos such as small molecules, proteins, mRNA, and miRNA which can modulate the fate of recipient cells.[15] Several plant-derived nanovesicles have been reported to be effectively used for cancer therapy, changing the gut microbiota composition, and protecting mice from DSS-induced colitis and inflammatory bowel disease.[9, 11, 15] These reports indicate that plant-derived nanovesicles are involved in interspecies communication for their biological effect.[7] Although plant-derived nanovesicles are promising in anti-inflammatory and cancer therapy, the uptake mechanism of the plant-derived nanovesicles has yet to be determined.

Understanding the mechanisms of the mammalian exosomes can elucidate potential mechanisms of plant-derived nanovesicles. The main uptake mechanisms for mammalian exosomes include phagocytosis, clathrin-dependent, or clathrin-independent pathways.[18, 19, 195] Heparan sulfate proteoglycans (HSPG) on cell surfaces could be a possible receptor for exosome endocytosis, but it has been reported that the HSPG on the surface of exosomes is not involved in the internalization of exosomes.[20] Another study revealed that fibronectins on the surface of myeloma cell-derived exosomes have interactions with HSPG on target cells.[21] Also, proteins on both the surface of ovarian cancer cell-derived exosomes and ovarian cancer cells are important for uptake.[22]

CD98 is a transmembrane, glycoprotein heterodimer, consists of the CD98 heavy chain (CD98hc) and several light chains (CD98lc), such as large amino acid transporter 1 (LAT 1).[104]

The glycan on CD98hc consists of tetra-antennary with terminal fucosylation and mannose oligosaccharides (oligomannose).[104, 196] CD98 has various functions which include mediating cell proliferation through activating the integrin-β pathway, importing amino acid to support cell growth, and regulating cell fusion in several types of cell lines (BeWo cells, Peripheral blood mononuclear cells, and L929 cells).[104, 197, 198] CD98 has been reported to play an important role in the internalization of human β-defensin 3 and endocytosis of mature vaccinia virus particles. Recently, a study has shown that the LAT 1 may be involved in the uptake of nanoparticles.[106, 113, 116] CD98 was used as a targeted protein to enhance the internalization of therapeutic nanoparticles due to its overexpression in tumor and inflammatory tissues.[114] These reports indicate that CD98 played an important role in the uptake process. CD98 has also been linked to inflammatory bowel disease (IBD) and plays a potential role in chronic liver disease, *e.g.*, non-alcoholic fatty liver disease (NAFLD).[129] Thus, CD98 can be a promising target for both therapeutic and drug delivery.

Lectin, a type of protein with a specific binding affinity to saccharides, plays an important role in interspecies recognition. For example, the innate immune recognition of coronaviruses was mediated by the interaction of certain lectins on cell membranes and the oligomannose from coronaviruses.[199] A lectin from *Sparassis latifolia* (a mushroom) has shown antibacterial activity against E. coli and other drug-resistant strains.[200] Inspired by those lectin-carbohydrates mediated interspecies communications, it is hypothesized that the interactions between plant-derived nanovesicles and mammalian cells are mediated by the interaction of lectins and saccharides.

Several dietary lectins have been found to exert health benefits through the induction of apoptosis after binding to the membrane. Among various edible plants, garlic is enriched in the lectins (1 mg of lectins per 1 g of garlic)[201] and has well-documented health benefits in many

epidemiology studies.[202, 203] In this study, the HepG2 cell line has been shown the internalization of garlic-derived nanovesicles (GDVs). The GDVs were isolated by the differential centrifugation method. And the resultant GDVs were identified by size, zeta potential, and morphology of previous studies.[7, 9, 11, 204] Surface proteins from GDVs were removed by incubation of GDVs with trypsin, and internalization properties were examined in HepG2 cells over various time points leading to the finding that the surface proteins from GDVs were involved in the internalization. Mass spectrum-based protein identification indicated that a mannose-specific binding lectin (II Lectin) is located on the surface of GDVs. Saturation of the II lectins with mannose and blocking CD98 receptors with CD98 antibody significantly impairs the GDV internalization. In addition, co-localization between GDVs and CD98 reduces significantly after trypsin digestion of GDVs' the surface protein. Taken together, those results indicate both proteins in the surface of GDVs (majorly II Lectin) and CD98 from cell membranes have directly interacted during the internalization of GDVs. The undigested GDVs treated group showed stronger *in vitro* anti-inflammatory effects when compared to the digested GDVs due to the changes in GDV uptake. This study contributed to understanding a part of the interspecies communication and provided new angles in understanding the benefit of dietary garlic.

3.2 Methods

3.2.1 Cell culture

HepG2 cell lines were cultured in the 1 g/L L-glutamine DMEM medium with 10% FBS, 5% penicillin, and streptomycin (100X Corning) at 5% CO2 and 37°C. LPS stimulation was conducted by adding 10 µg/mL of LPS into the culture medium for 24 h.[171] CD98 siRNA specific downregulation was performed following oligofectamine transfection procedure. Briefly, a serum-free medium (SFM) was gently mixed with oligofectamine and let for incubation at room

temperature for 5 min. The diluted CD98 siRNA were combined with the Oligofectamine/SFM mix and incubated for 15 min at room temperature to form a complex. The complex was then added into cells for a 4h-incubation at 37°C (the final concentration of siRNA is 100 nM). After the 4h-incubation, the reaction was completed by adding concentrated FBS to reach a final concentration of 10% of FBS in the medium.

3.2.2 Isolation of the Garlic-derived Nanovesicles (GDVs)

Garlic was washed 3 times with 1X PBS buffer and then homogenized using a blender with refrigerated PBS (4°C). The collected juice was centrifuged according to a multistep procedure optimized in our laboratory to get GDVs. The mixture was centrifuged at 5,000g for 20 min 3 times, 10,000 g for 1 h, and centrifuged at 120,000 g for 70 min. The pellet was washed with cold PBS 3 times and resuspended in PBS. The size was detected using the dynamic light scattering (DLS) method, atomic force microscope (AFM), and transmission electron microscopy (TEM). The zeta potential was measured by Malvern Nano ZS90.

3.2.3 Digest the surface protein of GDVs

The concentration of the GDVs was calculated by the total protein concentration using the DC assay (BIO-RAD, Hercules, CA). GDVs were incubated with trypsin (0.25%, Corning) at a mass ratio of 2:1 at 37°C for 1, 2, 3, 4h. After digestion, the pellets were collected by ultracentrifugation at 120,000 ×g for 2 hours. The pellets were washed with cold PBS 3 times and resuspended with 1X PBS and labeled as T1, T2, T3, and T4 GDVs respectively for 1h, 2h, 3h, and 4h of enzymatic digestion.

3.2.4 TEM measurement

A drop of the sample (10 μg of protein) was deposited onto the surface of a formvar-coated copper grid, after which 1% uranyl acetate was added and the sample was drying at room temperature for further imaging.

3.2.5 AFM Measurement

A drop of the sample (10 μg of protein) was deposited onto a freshly cleaved mica slide and drying in a cleaning vacuum hood with a cover at room temperature. AFM images were acquired using a SPA 400 AFM instrument (Seiko Instruments Inc., Chiba, Japan).

3.2.6 In-gel digestion and MS experiments

The concentration of the GDVs was calculated by the total protein concentration using the DC assay (BIO-RAD, Hercules, CA). GDVs were incubated with trypsin (0.25%, Corning) at a mass ratio of 2:1 at 37°C for 1, 2, 3, 4h. After digestion, the pellets were collected by ultracentrifugation at 120,000 ×g for 2 hours. The pellets were washed with cold PBS 3 times and resuspended with 1X PBS and labeled as T1, T2, T3, and T4 GDVs respectively for 1h, 2h, 3h, and 4h of enzymatic digestion.

After ultracentrifugation, GDVs were lysis in RIPA buffer for protein extraction. The gel was run and then stained using Denville protein blue stain. The gel was microwaved first with the 250 mL of DI water for 3min twice, then microwaved with 50 mL of Denville protein blue stain solution for 2 min, another 2 min in 250 mL of DI water.

The in-gel digestion was conducted by the method described previously.[205] Gel spots were picked from the 1 D gel and rinsed with double distilled water for 3 times. The spots were washing with 400 μl of 25 mM ammonium bicarbonate/methanol for 1 min. The destaining of Coomassie Blue was conducted by incubating the gel spots in 400 μl of 25 mM ammonium

bicarbonate/acetonitrile for 5 min and 100% acetonitrile for 1 min, respectively. The acetonitrile was removed and gels were dried via speed-vacuum. The gel spots were completely covered with trypsin for 10 min to saturate them with trypsin. After that, 60 µl of 50 mM ammonium bicarbonate was added and the tubes were placed in an air circulation thermostat and incubated overnight at 37°C. Then the samples were transferred to a new microcentrifuge tube and added 60 µl of 2.5% TFA to extra spots for 10 min. The volume of the combination was reduced to 20 µl and submitted to mass spectroscopy analysis (MS/MS).

Nano RP HPLC-MS experiments were performed on an LTQ-Orbitrap Elite mass spectrometer (Thermo Fisher) equipped with EASY-spray source and nano-LC UltiMate 3000 high-performance liquid chromatography system (Thermo Fisher) as described previously. EASY-Spray PepMap C18 Column (75 µm × 15 cm, 3 µm, ThermoFisher, US) was used for separation. The separation was achieved with a linear gradient from 3 to 40 % mobile phase B for 80 min at a flow rate of 300 nL/min (mobile phase A: 1.95 % ACN, 97.95 % H2O, 0.1 % formic acid (FA); mobile phase B: 79.95 % ACN, 19.95 % H2O, 0.1 % FA). LTQ-Orbitrap Elite mass spectrometer was operated in the data-dependent mode. A full-scan survey MS experiment (m/z range from 400 to 1600; automatic gain control target, 1,000,000 ions; resolution at 400 m/z, 60,000; maximum ion accumulation time, 50 ms) was acquired by the Orbitrap mass spectrometer, and ten of the intense ions were fragmented by collision-induced dissociation (CID). The other conditions used included: capillary temperature of 200°C and collision energy of 35 eV.

A Uniprot's garlic database fasta file (3155 items, May 2017) was used for MS/MS spectra matching as reported.[206] Raw data were analyzed by using Proteome Discoverer 1.4 (ThermoFisher) to search against Uniprot's garlic database (3155 items, May 2017). Searching

parameters were used as followed: fixed modification, carbamidomethyl (Cys); variable modifications, deamination (Asn), and oxidation (Met). Trypsin was selected as the enzyme, and two missed cleavages were allowed. The mass tolerance for the precursor ions and the fragment ions was set to 20 ppm and 0.5 Da, respectively. A false discovery rate (FDR) of 1 % was applied to all data sets at the peptide level.

3.2.7 Western Blot

The cells (treated or not) were lysed with RIPA Buffer (150 mM NaCl, 1.0% Triton X-100, 0.5% Sodium deoxycholate, 0.1% SDS, 50mM Tris pH 8.0, Roche phoSTOP and EDTA-free protease tablets). The concentration of protein was analyzed using a DC assay. The samples were loaded into the 4-20% SDS-PAGE and transferred the samples to a nitrocellulose membrane. After 1 h blocking, the membrane was incubated with primary antibody at room temperature for 2 hours. The membrane was rinsed 3 times with TBST buffer. The membrane was incubated with a secondary antibody for 1 h at room temperature. Primary antibodies CD98, β-actin, and GAPDH were diluted in 1:1000. The secondary antibodies goat anti-Rabbit IgG (H+L) ads-HRP, and goat anti-Mouse IgG (H+L) HRP Conjugate were diluted at 1:5000. The films were developed using a SERIES 2000A Processor film developer.

3.2.8 MTT Assay

To assess the potential toxicity of GDVs and digested GDVs, MTT assays were performed. HepG2 cells were seeded in 96-well plates at a density of 5×10^5 cells per well and exposed to 100 µg/mL of GDVs for 24 hours. The MTT (3-[4,5-dimethylthiazol-2-yl]-2,5-diphenyltetrazolium bromide) is added to wells for 4 hours of incubation and reduced by metabolically active cells to form the purple formazan dye crystals. The detergent solution was then added to the wells, solubilizing the crystals so that absorbance can be read using a spectrophotometer. The wavelength for

measuring the absorbance of the formazan product was 570 nm. Untreated cells (controls) were set to 100% viability.

3.2.9 Cell Uptake Assay

GDVs (100 µg) were incubated with 1 µM coumarin-6 at room temperature for 30 min and the pellets were collected by ultracentrifugation after 3 rinses. The labeled GDVs were resuspended in cold PBS buffer and incubated with HepG2 cells at 37°C or 4°C.

Uptake studies were conducted by treating HepG2 cells at a concentration of 100 µg/mL labeled GDVs for 1 to 6 h. The blocking test was carried by pre-incubating HepG2 with 10 µg/mL of CD98 antibody for 1h before incubation with GDVs for 2 hours.[118, 184] GDVs were incubated with carbohydrates for 30 min before uptake assay.[22] The carbohydrates were D-glucose, D-mannose, D-galactose, D-fructose, N-acetylglucosamine, lactose, and maltose. The results of uptake were visualized and analyzed by immunofluorescence microscopy and flow cytometry described below.

3.2.10 Immunofluorescence Microscopy

For CD98 staining, the cells were fixed with 4% paraformaldehyde for 15 min at room temperature. The chamber slides were then rinsed 3 times using the DPBS. The cells were incubated with 5% BSA for 1 h at room temperature (Blocking solution). Then, the cells were incubated with CD98 (1:1000 containing 1% BSA and 0.01% of tween-20) antibody overnight at 4°C. The cells were washed 3 times and incubated with the anti-rabbit IgG (1:4000) for 1 h at room temperature. After 3 washes with the DPBS, the cells were stained with DAPI for 5 min. Finally, the cells were washed with DPBS for 3 times and sealed with prolong gold antifade reagent.

After the uptake incubation, the medium was removed and the cells were washed with DPBS 3 times. The cells were fixed with 4% paraformaldehyde for 15 min at room temperature. Then,

the slides were rinsed 3 times and incubated with the Alexa Fluor 568 phalloidin (1:1000) for 1 h at room temperature, and the cells were stained with DAPI for 5 min. Finally, the cells were washed with DPBS 3 times and sealed with prolong gold antifade reagent for fluorescent microscopy.

3.2.11 Flow Cytometry

After incubation with GDVs, the growth medium was removed and cells were rinsed 3 times DPBS. Cells were fixed with 4% paraformaldehyde acid (PFA) for 10 min at room temperature. After, the cells were resuspended in PBS with 5% FBS. Flow cytometric analysis was performed on a BD LSRFortessa flow cytometer (BD Biosciences), and data were analyzed using FlowJo version 10. The gate was set using cells without any treatment (negative control) versus Labeled GDVs-treated (positive control) cells measured by the FITC channel. The intensity of uptake was calculated using the geometric mean of the population (n=10).

3.2.12 RT-qPCR

Total RNA was extracted from HepG2 cells using SpinSmart RNA mini purification kit under the manufacture's manual. The RNA was quantified by Synergy H1 plate reader (BioTek, Winooski, USA). cDNA was synthesized from the total RNA using cDNA synthesis master mix according to the manufacturer's instructions. Gene-specific cDNAs were quantified by RT-qPCR using SB-Green qPCR Master Kit. The GAPDH gene was used as a housekeeping gene in RT-qPCR. Fold-induction was calculated using the Ct method: ΔΔCt= (CtTarget gene- CtHousekeeping gene) treatment-(CtTarget gene- CtHousekeeping gene) nontreatment, and result was calculated using the formulation $2^{-\Delta\Delta Ct}$.

Primers used for qRT-PCR: IL-6 Fwd: 5'-CAATCTGGATTCAATGAGGAGAC-3', IL-6 Rvs: 5'-CTCTGGCTTGTTCCTCACTACTC-3', IFN-γ Fwd: 5'-GCTT-GAATCTAAATTATCAGTC-3', IFN-γ Rvs: 5'-GAAGATTCAAATTGCATCTTTAT-3'.

3.2.13 Statistical Analysis

Data are presented as mean and standard deviation (SD). A two-way ANOVA Analysis was performed to obtain statistical differences among groups. The t-test was used for comparison between the two groups and a P-value less than 0.05 was considered significant.

3.3 Results

3.3.1 The Physicochemical Properties of the GDVs

The size and shape of GDVs (Figure 3.1 A) and T4 GDVs (4h incubation with trypsin) (Figure 3.1 B) were identified by TEM. Both sizes were less than 150 nm with a spheroid shape. The T4 GDVs showed a multi-vehicle body structure. This might be caused by digestion which destroyed surface proteins and rearranges the lipid structure.[204, 207] AFM study has shown the morphology of digested GDVs and GDVs had no significant difference. The shapes of GDVs (Figure 3.1 C) and T4 GDVs (Figure 3.1 D) were similar but not uniform, which may be a result of the different membrane protein compositions due to enzymatic digestion. As shown in Figure 3.1 E and 3.1 F, the blue curve shows the size distribution by number and the red curve shows size distribution by intensity. The size of GDVs by intensity ranged from 70-200 nm and the average size was 191.8 ± 2.0 nm (Figure 3.1 E) and the size of T4 GDVs was ranged from 70-200 nm and the average size is 178.6 ± 1.8 nm (Figure 3.1 F). The size distributions of GDVs and T4 GDVs by number showed that GDVs or T4 GDVs have a diameter of around 100 nm.

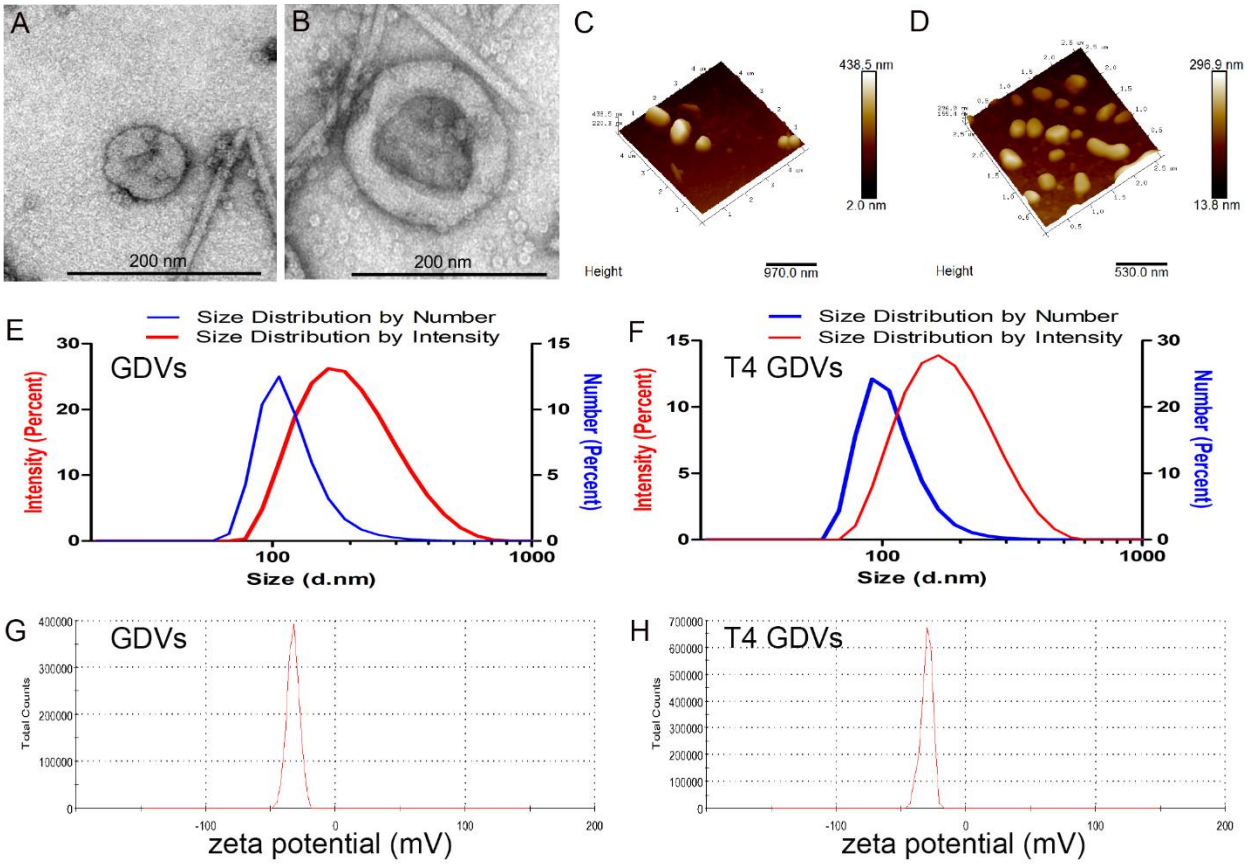

Figure 3.1: The physicochemical properties of garlic-derived nanovesicles (GDVs).

(A) The intact GDVs and (B) GDVs, which the surface proteins have been trypsin-digested for 4h (T4 GDVs) were visualized by transmission electron microscopy (TEM). Atomic force microscopy images of (C) GDVs and (D) T4 GDVs were captured. The average size was measured by the dynamic light scattering (DLS) method as well as the zeta potential respectively (E) The size distribution of GDVs was measured by intensity (red) and number (blue), (F) The size distribution of T4 GDVs was measured by intensity (red) and number (blue), as well as the (G) Zeta potential distribution of GDVs and, (H) Zeta potential distribution of T4 GDVs.

The curves show a narrow size distribution listed in Table 2.1. The analysis of the size curves after trypsin digestion showed that T4 GDVs slightly decreased. The DLS showed the sizes were homogenous. The zeta potential analysis showed that the zeta potential of digested or

undigested GDVs was negative, and around -31 mV (Figure 3.1 G and 3.1 H). It has been reported that particles derived from edible plants (such as carrot, grape, grapefruit, and ginger) were quite stable in simulated gastrointestinal solutions.[7, 204] Moreover, plant-derived nanovesicles showed intact biology effects after oral administration indicating their stability *in vivo*. This latter observation is interesting as such particles (size of 200 nm such as GDVs) are suitable for both active and passive internalizations.[208, 209] Altogether, these observations established that the differences in GDVs uptake by cells were only due to the deletion of surface membrane proteins on GDVs.

Table 3.1: Summary of GDVs' and Trypsin-digested GDVs' size and zeta potentials.

Sample	size (d. nm)	PDI	Zeta (mV)
GDVs	191.8±2.0	0.217±0.011	-32.3±0.86
T1 GDVs	178.6±1.8	0.171±0.017	-31.5±1.2
T2 GDVs	175.7±4.2	0.199±0.008	-34.9±0.60
T3 GDVs	170.8±1.6	0.170±0.015	-33.2±0.70
T4 GDVs	175.2±1.7	0.188±0.018	-30.8±1.0

Table 2.1: Summary of the size and zeta potentials of the intact GDVs and GDVs which the surface proteins have been trypsin-digested for 4h.

3.3.2 Uptake kinetics of GDVs is correlated to the surface expression of CD98 on HepG2 cells

The global incidence of nonalcoholic fatty liver disease (NAFLD) is 25%, which induced a strong burden on society.[44] In the United States, this increased incidence of NAFLD was associated with increased liver disease mortality.[210] The goal of this paper is to develop a preliminary understanding of the uptake mechanisms of the GDVs and their potential therapeutic effects

to apply them further as a nanotherapeutic for inflammatory and liver disease. Thus, HepG2 cell was used in this study. As shown in Figure 3.2 A, we studied the cytotoxicity of GDVs on HepG2 cells and found that both the undigested and digested GDVs were not cytotoxic in HepG2 cells after 24-hour incubation with 100 µg/mL of GDVs (more than 98% of viable cells). Hence, GDVs uptake within 24 hours of exposure was used to track GDVs endocytosis.

The uptake of GDVs by HepG2 cells was concentration- and time-dependent. As shown in Figure 3.2 B, the uptake of GDVs by HepG2 cells was investigated by flow cytometry. GDVs were tagged with coumarin-6. The kinetics uptake was studied at the range of concentration of coumarin-6 tagged GDVs of 25 to 150 µg/mL for 6 h. GDVs were incubated with HepG2 cells for different periods (1h to 6h at 100 µg/mL of GDVs). The uptake was measured by flow cytometry (Figure 3.2 C), and it showed the GDVs uptake was fast and reached a plateau after 1 hour of incubation.

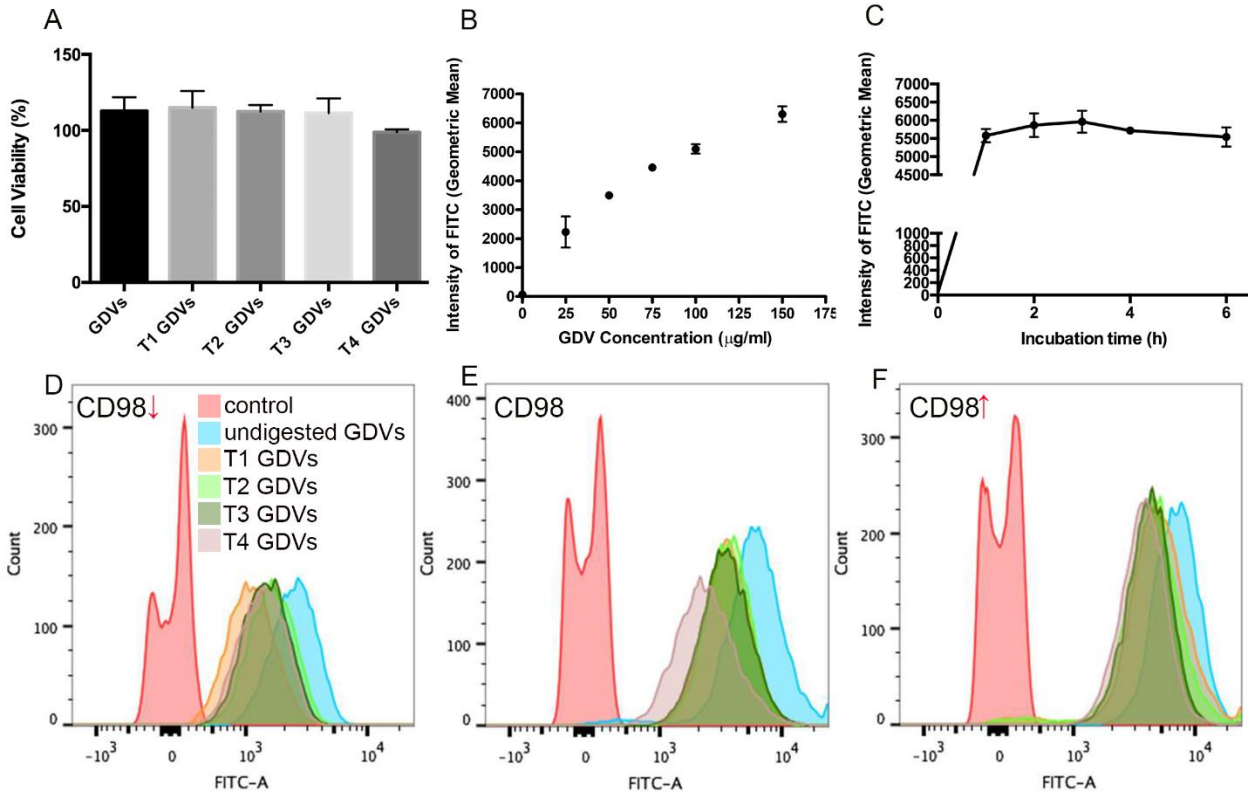

Figure 3.2: Uptake of GDVs is dependent on the GDVs surface protein integrity and CD98 expression level in HepG2 cells.

(A) MTT cell viability assay on HepG2 cells after incubation with GDVs for 24h (the concentration of GDVs was 100 μg/mL, the values represent means ± SD. Data represents of n=6 determinations). The uptake of GDVs was (B) concentration-dependent and (C) time-dependent for the first hour and reached a plateau after 2h. (B) GDVs were incubated with HepG2 cells for 6 hours and (C) HepG2 cells were incubated with GDVs at a concentration of 100 μg/mL. The values represent means ± SD. Data represents n=3 determinations). (D-F) illustrates the uptake of GDVs as a function of the CD98 level of expression. (D) The lowest level of CD98, as the downregulation, was conducted by CD98 siRNA using oligofecatmine, (E) basal level of CD98 expression on HepG2 cell, and (F) the highest level of expression of CD98 in HepG2 cells (stimulation by 10 μg/mL of LPS for 24 h).

The study also investigated the kinetics uptake of GDVs on cells (HepG2) expressing differential levels of CD98 expression. Many groups have found that LPS stimulation increased the expression level of CD98 mRNA.[132, 171, 211] In this study, the three differential expression levels of CD98 proteins were accessed by LPS-stimulation (upregulation), regular condition, and CD98 siRNA (downregulation). Both immunofluorescent images and Western blot successfully confirmed that CD98 express at different levels on the HepG2 cell surface. The basal level (HepG2 cells under regular culture condition) was set as the control (Figure 3.3 B). A higher CD98 expression level was observed by supplementing the cell medium with LPS (Figure 3.3 A), while a lower level was found by transfecting cells with CD98 siRNA (Figure 3.3 C). The western blot (Figure 3.3 D, Appendix Figure 5-0.4 A) verified that the experiment was able to generate differential CD98 expression with HepG2 cells (control, LPS, siRNA). Since the CD98 is already highly

overexpressed in liver cancer cells, changes in the amount of CD98 were further investigated by the quantification of the western blot films. The quantification of western blots (Appendix Figure 5-0.4 B) showed that LPS can increase the expression of CD98 by 10% when compared with the control group (HepG2 cell under regular culture condition). In contrast, CD98 siRNA significantly decreased CD98 expression by 37%.

By comparing Figure 3.3 A-C, the effect of CD98 cell expressions on the uptake of GDVs was able to be observed. The intensity of uptake was detected by using CD98 silenced HepG2 cells (Figure 3.2 D), untreated HepG2 (Figure 3.2 E) cells and LPS stimulated HepG2 cells (Figure 3.2 F). As shown in Figure 3.2 D-F, the GDVs uptake was proportionally increased with the expression of CD98 as shown by the position of the peak maximum and the area under the curve of each flow cytometry experiment. Comparing each line within the same plot, it was displayed that for any CD98 expression, the surface protein digestion reduced the uptakes of GDVs. Similarly, in literature, proteins on membranes of exosomes were digested by protease K which inhibited the uptake by cells.[22] Trypsin-digested GDV uptake was significantly decreased compared to native GDVs demonstrating the importance of ligands present on the surface. Also, comparing each curve of the same color in the 3 different experiments, it was shown that for the same GDVs surface proteins profile, the uptake of GDVs was correlated to CD98 expression. This result was further demonstrated by investigating the uptake of GDVs with differential CD98 expression by fluorescent microscopy (Figure 3.4).

The intensity of uptake was also quantified by the geometric mean and as shown in Figure 3.3 E. T4 GDVs were uptaken less than intact GDVs by HepG2 cells. For the uptake of GDVs, it was shown that silencing CD98 significantly decreased the uptake of GDVs by 33.85% compared with that in HepG2 cells under regular culture conditions. In contrast, LPS-stimulated HepG2

increased the uptake of GDVs by 17.16%. These results together showed the uptake of GDVs by HepG2 cells was correlated to the level expression of CD98 on HepG2 cells.

The uptake of GDVs was visualized by fluorescence microscopy (Figure 3.4). Figure 3.4 showed the uptake of GDVs (i) by LPS-stimulated HepG2 cells (first panel), (ii) by regular HepG2 cells (second panel), and (iii) by HepG2 cells treated with CD98 siRNA (third panel). As expected, there is no coumarin-6 signal (GDVs) in the cells without GDVs (PBS column in Figure 3.4). The fluorescent study showed clearly that the intact GDVs group was significantly uptaken more than trypsin-digested GDVs groups. Within the GDVs supplemented cells column, it was also observed that the kinetics of GDV uptake by HepG2 cells directly correlated with the CD98 expression levels. CD98 downregulation (line 3 in Figure 3.4) showed a significant decrease in the endocytosis of GDVs. These indicated that CD98 expression in the HepG2 cell plays an important role in the recognition and uptake process of GDVs.

3.3.3 Important Presence of II Lectin on GDVs Surface

After establishing that CD98 expression in HepG2 cells is a key factor for GDVs uptake, a proteomics study was carried out to investigate which proteins on the GDVs' surface might interact with CD98.

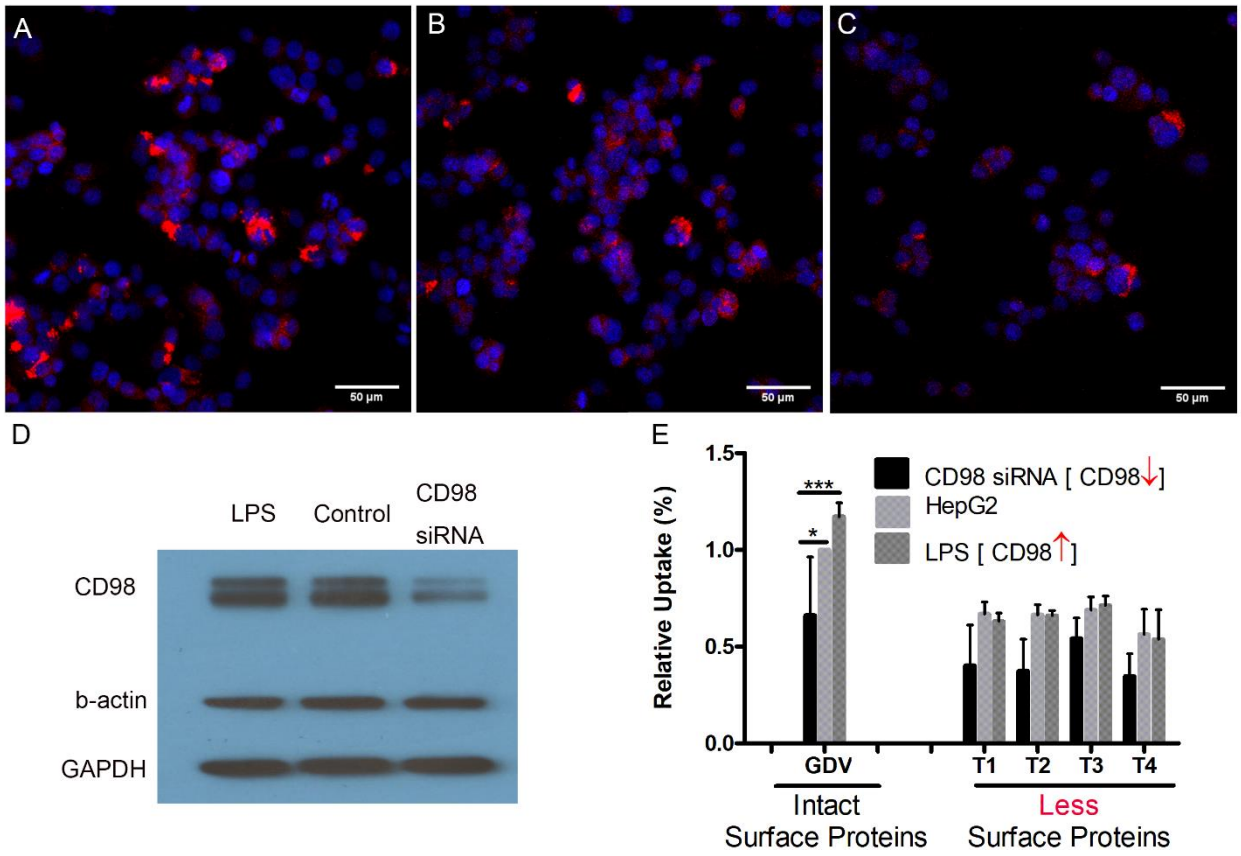

Figure 3.3: CD98 expression level is significantly involved in GDVs uptake.

Differential levels of expression of surface CD98 (red) were stained by stimulating HepG2 cells with 10 µg/mL of LPS for 24 h (A, the highest expression of CD98), by regular cell culture of HepG2 (B, basal CD98 expression), and by treating HepG2 cells with CD98 siRNA using oligo-fectamine (C, lowest expression of CD98). The CD98 was stained in red and the nuclear was stained in blue (DAPI). (D) Western blot showed a level of CD98 after different treatments (LPS, control, and siRNA). (E) CD98 expression is directly correlated with GDVs uptake. Uptake was monitored by flow cytometer and the result was calculated relatively to the uptake without treat-ment, considered as 1.0.

GDVs' Surface proteins were isolated using a standard protocol of membrane isolation for cells. GDVs' surface proteins were digested using trypsin (0.25%) and separated using SDS-Page (4-15%, 135 V, 80 min). As shown in Figure 3.5 A, the channels from left to right are respectively

protein markers, undigested plasma proteins from GDVs (undigested), and GDVs' plasma proteins digested by trypsin for 4h (digested). While fewer bands in the GDVs' plasma membranes digested by the trypsin channel indicate that most proteins were degraded, the "undigested" plasma membrane proteins show interesting significant bands (corresponding to dominant presence surface proteins). As shown in Figure 3.5 A, the bands between 110 kDa, 55kDA, 25-37 kDa, 20-25 kDa, and 15kDa were observed. These bands were cut off the gel and analyzed by mass spectroscopy (MS/MS) as described in the supplemental method section. The result of protein identification is shown in Figure 3.5 B (table section). Some proteins (abundant in garlic) were found from protein identification, such as alliinase, ribulose bisphosphate carboxylase large chain, and ATP synthase subunit beta. Interestingly, a mannose high-affinity lectin, i.e., II Lectin was found. Because II Lectin had been investigated prior for specific interaction with certain surface cell receptors,[65, 212] it was decided to further study the specific interaction.

3.3.4 Specific Interaction Between GDVs Surface Ligands (II Lectin) and CD98

The mechanism of extracellular vesicle endocytosis is diverse, including membrane fusions, protein interactions, and lipid raft-mediated internalization.[19] As shown in Figure 3.6 A, a significant "left"-shift of the fluorescent channel peak was observed when the GDVs were exposed to cells (2 h) at 4°C versus 37°C. This observation supports the fact that the uptake of GDVs by mammalian cells was significantly inhibited under 4°C, indicating that a predominant part of the uptake of GDVs by cells was energy-dependent. In Figure 3.6 B, the co-localization study of CD98 (stained in red) and undigested GDVs (stained in green) showed significant co-localization clusters visualized in yellow. To confirm that plasma membrane proteins were playing a key role in endocytosis, the same experiments (6-hour incubation, 37°C) were conducted after respectively 1h- (Figure 3.6 C) and 4h- (Figure 3.6 D) digestion of GDVs' plasma membranes proteins by

trypsin. The results of this fluorescent microscopy study showed that T1 GDVs (1h trypsin-digestion, Figure 3.6 C) and T4 GDVs (4h trypsin-digestion, Figure 3.6 D) had significantly fewer co-localization signals than the undigested GDVs (Figure 3.6 D). Combining the scientific literature with the results of the flow cytometry, mass spectroscopy, and fluorescent microscopy experiments, it was concluded that lectin family proteins present on GDVs playing a major role in the endocytosis of GDVs mediated by CD98 interactions. As a reminder, lectins are a type of protein that can bind to glycoproteins including CD98 glycoprotein, and lectins are found in mammalian, bacteria, and plants. Animal lectin such as galectin-3 was proven to be a ligand of CD98 and plant lectin such as GSL-IB4 has been reported to have similar carbohydrate-binding specificities with galectin-3.[81, 82, 213]

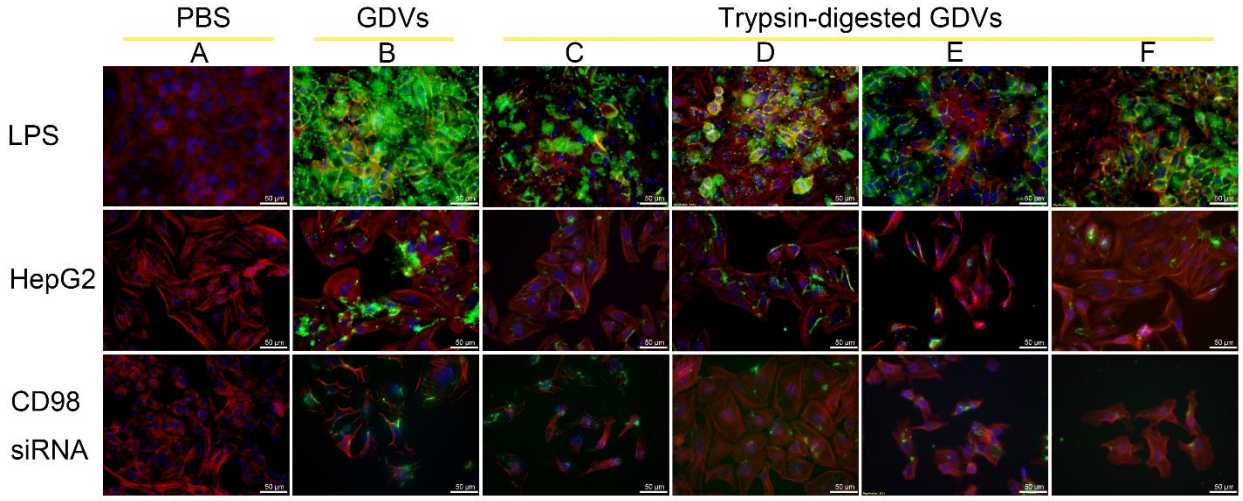

Figure 3.4: Cross study of the modulation of GDVs endocytosis by HepG2 cells by tuning the expression level of CD98 on HepG2 cells and the integrity of surface proteins of GDVs.

HepG2 cells were incubated with 100 µg/mL GDVs for 6 h excepted column A (noted PBS) which represents HepG2 cells without GDVs. The GDVs were labeled with coumarin-6 (green), HepG2 cells were stained for actin with Phalloidin (red) and nuclei were stained with DAPI (blue).

Vertically**,** other columns (B, C, D, E, and F) represent a different "type" of GDVs treatment. B, C, D, E, and F columns represent respectively intact GDVs (GDVs in B), 1h-trypsin-digested GDVs (T1 GDVs in C), 2h-trypsin-digested GDVs (T2 GDVs in D), 3h-trypsin-digested GDVs (T3 GDVs in E), and 4h-trypsin-digested (T4 GDVs in F). Horizontally, line 1 (noted LPS) represents LPS-stimulated HepG2 cells (overexpressing surface CD98 on HepG2 cells). The second line (noted HepG2) represents the basal expression of CD98 on HepG2 cells. Finally, line 3 (noted CD98 siRNA) shows HepG2 cells with lower expression of CD98 (blocked by pre-treatment with CD98 siRNA).

Based on the literature and the corroborating results, it is concluded that the interaction between a ligand (II Lectin) on GDVs and CD98 glycoprotein determines the uptake of GDVs in HepG2 cells.[19] The next step aims to demonstrate that CD98 is the receptor involved on the side of the HepG2 and that the specific ligand on GDVs is II Lectin significantly found on the surface of GDVs by MS/MS.

3.3.5 CD98 is the Main Receptor of GDVs via II Lectin Coated GDVs

As shown previously in this study (Figure 3.3 E), the downregulation of CD98 by its specific siRNA significantly inhibit the uptake of GDVs by 33% and decreased the co-localization of CD98 and GDVs demonstrating that the uptake was highly related with CD98 on the side of the HepG2 membrane. To further confirm this, HepG2 cells were pre-incubated with CD98 antibodies before conducting the flow cytometry uptake assay. As observed in Figure 3.6 E, a significant "left-shift" of the fluorescent signal related to endocytosis of GDVs by HepG2 cells was noticed. Based on Figure 3.6 E, the uptake of GDVs after blocking CD98 receptors on HepG2 cells with a specific CD98 antibody (10 μg/mL, 1h), decreased as much as 47.01%. These results

combined with the previously described data in this study definitively set CD98 as the main receptors on HepG2 cells involved in endocytosis.

Thus, the goal was to demonstrate that "on the other side', II Lectin protein was the ligand of CD98. To confirm this hypothesis based on MS/MS results and scientific literature, we deduced that if the hypothesis was right, the uptake of GDVs could be inhibited by pre-incubated GDVs with free mannose highly bounding lectin.[22] The strategy was to block lectin *via* free mannose and observe the potential effects on the endocytosis of GDVs by HepG2 cells. To complete the study, it was decided to experiment on the different types of carbohydrates (mono- or disaccharides). The choice of free carbohydrates was defined by literature search where it is clearly shown that lectins are a family of proteins with a high affinity to mannose and other carbohydrates (i.e., glucose,[214] mannose,[215] galactose,[216] fructose,[217] N-Acetylgalactosamine (noted GalNac),[218] lactose,[219] and maltose. [220]). It was demonstrated that the II Lectin has a high affinity for mannose compared with other sugars.[91, 221] The uptake of GDVs after pre-incubation with free carbohydrates (150mM) was investigated using flow cytometry (Figure 3.6 F). The GDVs without incubation with carbohydrates (noted control in Figure 2.6F) was normalized as 100%. As shown in Figure 3.6 F, the highest relative decrease (-44% compared to control) of the uptake of GDVs by HepG2 cells was caused by pre-incubation of GDVs with the mannose. Notably, galactose pre-incubation decreased uptake by 30%, while glucose did not affect the uptake efficiency. Lactose-, GalNac-, Maltose-, and Fructose- pre-incubations did not significantly modify the uptake of GDVs by HepG2 (less than 5% change). The structures of those different carbohydrates are shown in Figure 3.7. The data indicates that the uptake of GDVs was highly inhibited by mannose pre-incubation strongly supporting the role of the lectins on GDVs surfaces. Taken together, it can be concluded that CD98 is a key receptor

for GDVs uptake and that mannose pre-incubation coupled with MS/MS results strongly supports that the interaction with CD98 is lectins-dependent on GDVs surface side.

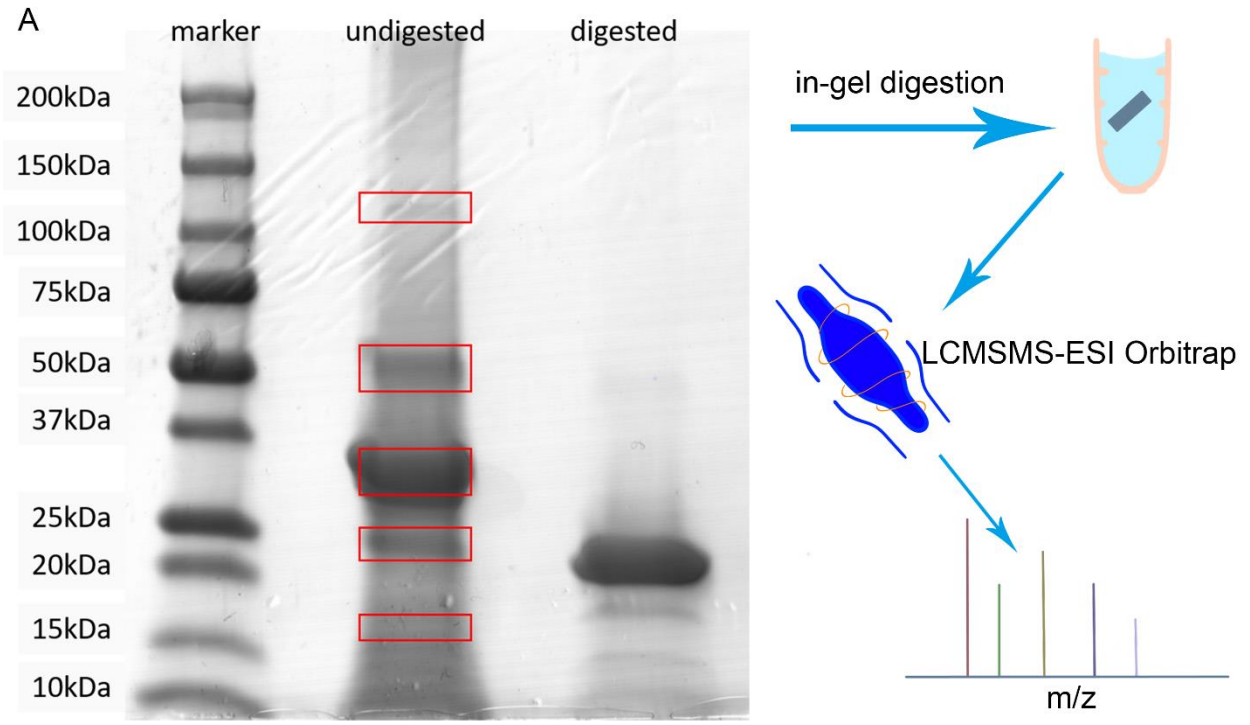

B

Description	MW [kDa]	# AAs
Alliinase [A0A0G2YMQ1_ALLSA]	54.9	480
ATP synthase subunit beta [A0A1D8RD23_ALLSA]	53.8	498
Unspecific 9/13 divinyl ether synthase [Q2WE96_ALLSA]	52.8	472
Ribulose bisphosphate carboxylase large chain [O98661_BIGAE]	51.5	466
Cysteine synthase [Q3L195_ALLSA]	36.1	339
GTP-binding nuclear protein [A9X4K0_ALLSA]	24.9	220
II lectin [Q38784_ALLSA]	15.4	144

Figure 3.5: II Lectin presence on the surface of intact GDVs.

(A) Gel analyses have shown that the surface proteins of GDVs were digested and the gel was stained with Coomassie blue. The three lanes of protein samples from left to right are a marker, intact GDVs, and T4 GDVs (4h-trypsin-digested GDVs) respectively. **(B)** represent proteins found in protein identification.

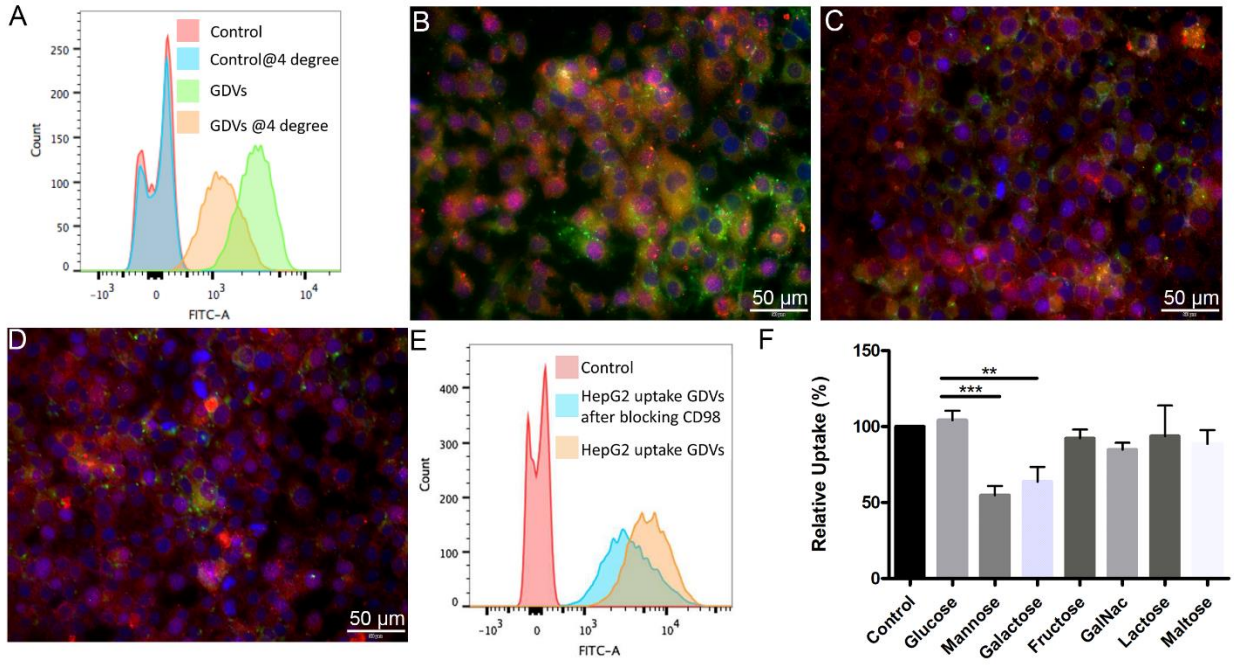

Figure 3.6: CD98 is the main receptor of GDVs *via* II Lectin-coated GDVs.

(A) Uptake of GDVs by HepG2 cells were temperature-sensitive as shown by the endocytosis studied through flow cytometry at 4°C versus 37°C. The "left-shift" signal of fluorescence at 4°C showed a decrease of intact GDVs uptake by HepG2 cells compared to 37°C. (B) Co-localization of intact GDVs (green) with CD98 expressed on HepG2 cells (red), (C) co-localization of 1h-trypsin-digested GDVs (T1 GDVs in green) with CD98 expressed on HepG2 cells (red), (D) co-localization of 4h-trypsin-digested GDVs (T4 GDVs in green) with CD98 expressed on HepG2 cells (red). HepG2 cells were incubated with 100 µg/mL GDVs for 6 h. The GDVs were labeled with coumarin-6 (green), CD98 was stained in red and cell nuclei were stained with DAPI (blue). The co-localization GDVs-CD98 appears in yellow. (E) Uptake of GDVs by HepG2 cells were CD98-sensitive as shown by the endocytosis studied by flow cytometry with a pre-incubation of cells with CD98 antibody (CD98 Ab) versus no blocking. The "left-shift" signal of fluorescence with the CD98 Ab showed a decrease of intact GDVs uptake by HepG2 cells compared to cells without Ab. (F) Flow cytometry quantification of the GDVs uptake by HepG2 cells after pre-

incubation of GDVs with 150 mM of different saccharides were glucose, mannose, galactose, fructose, N-Acetylgalactosamine (noted GalNac), lactose, and maltose. Relative Uptake was calculated and standardized to the uptake of GDVs by HepG2 cells without treatment considered as 100%. Results are displayed in relative percentages ± S.D. The results shown are representative of three independent experiments performed in duplicate.

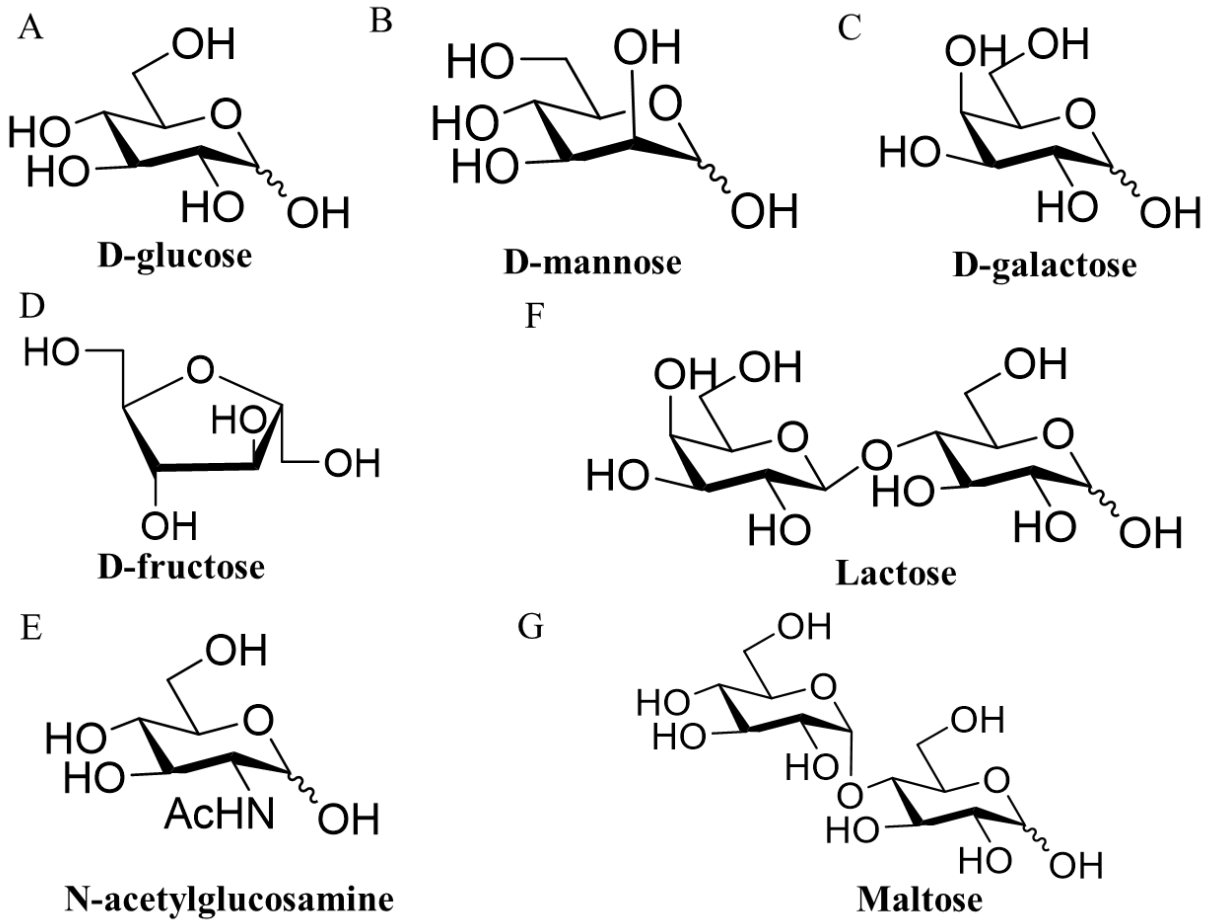

Figure 3.7: The structure of carbohydrates used in the GDVs pre-incubation.
(A) D-glucose, (B) D-mannose, (C) D-galactose, (D) D-fructose, (E) N-acetylglucosamine, (F) Lactose, (G) Maltose.

3.3.6 GDVs Uptake by HepG2 Cells Reduced the LPS-induced Inflammatory

Knowing the biological effect of GDVs on liver cells could help understand the benefit of garlic in the human diet. The IFN-γ and IL-6 have been reported to play an important role in many pathological conditions, such as inflammatory, carcinogenic, and infectious.[171, 222-224] The *in vivo* amount of LPS was majorly produced by the gut gram-negative bacteria and the LPS was considered as the inducer of hepatic inflammation and colitis (gut-liver axis).[225-227] LPS mainly stimulated the liver cell by interacting with the different toll-like receptors. The induction of IL-6 by LPS is through the MyD88-dependent signaling pathway, while the generation of IFN-γ was in a MyD88-independent way.[228] As shown in Figure 3.8, the anti-inflammatory effects of GDVs or T4 GDVs were tested on HepG2 cells with different expression levels of CD98. The regular HepG2 cells control group was treated with PBS only and their relative expressions of IFN-γ (Figure 3.8 A) and IL-6 (Figure 3.8 B) mRNA were used as the baseline and set to 1. After the treatment of GDVs or T4 GDVs, the expression levels of IFN-γ were reduced by 42% ($p< 0.001$) and 29% ($p< 0.05$), respectively. A similar result was observed in the IL-6 mRNA expression. Moreover, more inhibition on the expression of IFN-γ and IL-6 was found in GDVs treated groups. The LPS stimulation increased the expression level of IFN-γ and IL-6.[229] The expression of IFN-γ and IL-6 mRNA on LPS-treated HepG2 cells was significantly inhibited by applying GDVs or T4 GDVs. Interestingly, the expression level of IFN-γ mRNA in GDVs treated LPS-stimulated HepG2 cells was significantly lower than that induced by its counterpart (T4 GDVs). The stronger anti-inflammatory effects were observed on GDVs treated groups rather than the T4 GDVs treated groups, confirming the higher internalization was of GDVs rather than T4 GDVs by HepG2 cells. After the treatment of GDVs, the level of IFN-γ and IL-6 mRNA was close to the baseline, indicating the strong anti-inflammatory effect of GDVs. Silencing CD98 decreased the

expression of IFN-γ and IL-6. Thus, even treated with GDVs or T4 GDVs, there was no significant difference in the expression level of IFN-γ and IL-6. Recently, it was reported that CD98 could be an inducer receptor in non-alcoholic fatty (NAFLD) liver disease, and CD98 siRNA-loaded nano-particles were shown therapeutic potential for this disease. These nanoparticles downregulated the expression CD98 both *in vitro* and *in vivo*, decreasing the level of NAFLD-related pro-inflammatory cytokines such as TNF-alpha, IFN-gamma, and IL-1beta.[171] These results associated with previous conclusions suggested that GDVs showed broad anti-inflammatory potentials against the LPS-induced inflammatory on liver cells. Taken together, GDVs could be a promising strategy to reduce the anti-inflammatory process in pathologies like fibrosis or colitis.

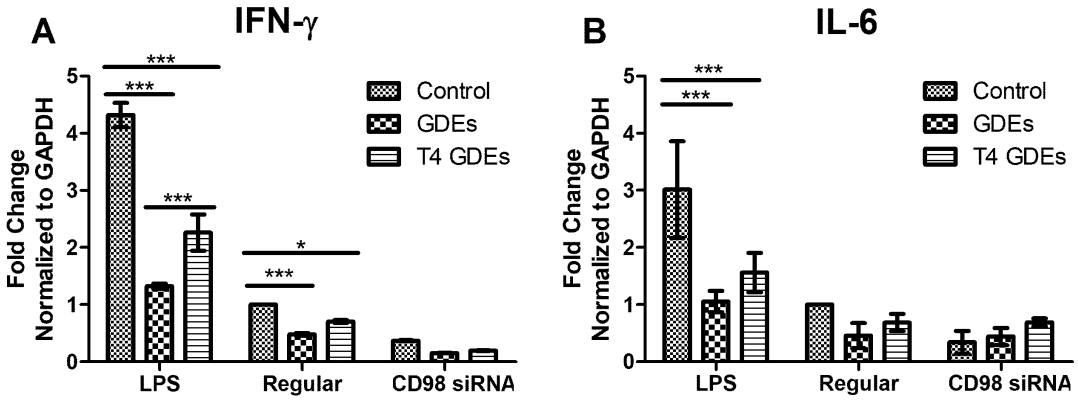

Figure 3.8: Intact GDVs had a biological effect on reducing the expression of an anti-inflammatory gene (Interferon γ noted IFN-γ and Interleukin 6 noted IL-6).

HepG2 cells were incubated without GDVs or digested GDVs (control noted control), with GDVs (100 µg/mL), or with T4 GDVs (100 µg/mL) for 24 hours, and total RNAs were isolated by using the RNA extraction Kits. The CD98 expression was regulated by LPS, CD98 siRNA, and without any treatment (Regular). HepG2 cells without any treatments were set as 1. Values represent means ± S.D. Data are represents n = 3 determinations, * $p<0.05$, ***$p<0.001$. Normalization of results

has been done over a gene known as stable expression (housekeeping gene) of gene glyceraldehyde 3-phosphate dehydrogenase (GAPDH).

3.4 Discussion

This study contributes to understanding the communications between GDVs and mammalian cells. Edible plants have been consumed by humans for thousands of years, which shows the great biosafety of garlic and how the provided dietary antioxidants show benefits to many types of chronic disease including NAFLD.[230, 231] Garlic has been shown to provide broad anti-inflammatory effects *via* many different bioactivated compounds. However, no histologically clear results were found in the garlic NAFLD trials.[232] This might be caused by the difficulty for bioactivated compounds to access the cytosol.[233] Many types of cargoes have been found in mammalian cell-derived vesicles. As reported, the exosomes contained more than 1000 types of proteins and RNA.[234, 235] The PDNs carry small molecular, RNA, and proteins, similar to their animal cell counterparts. Unlike the free compounds, PDNs not only protect the compounds but also enhance the bioactive compounds' penetration into deep tissues.[11] Thus, PDNs can amplify the benefits of the edible plant by enhancing the bioactive compounds delivery efficiency.

The GDVs were characterized by DLS, TEM, and AFM, which are the most common technologies for characterizing nanoparticles. The DLS showed that the size and zeta potential of GDVs are not significantly changed after trypsin digestion. The AFM study has shown that the morphology of digested GDVs and GDVs has no significant difference. Thus, it can be concluded that the digested proteins were surface proteins of GDVs. Together with the nontoxic properties of GDVs, it can be concluded that GDVs can be the promising oral administrative formulation for drug delivery as other PDNs.[8, 11]

In the literature, a variety of fluorophores (PHK-26, PHK-67, CFSE, Dil, coumarin-6, and DiD) have been used to label the lipid-based vesicles for the microscope visualization and flow cytometry analysis.[9, 236-239] Excess unincorporated dyes were removed by ultracentrifugation or column before carrying the uptake studies, which proved the fluorescent signals detected in cells were caused by the internalization of labeled vesicles. Our results showed the CD98 expression level was highly associated with the labeled GDVs internalization amount. Previous studies showed that CD98 played an important role in regulating drugs to pass the blood-brain barriers (BBB) and drug delivery.[115, 240]

The CD98 receptor is connected to II Lectin by exploring surface proteins via MS/MS and blocking II Lectin via mannose pre-incubation with GDVs. As reported, the interactions between lectin and sugar are involved in the uptake of exosomes. The interactions can be affected by appearing corresponding sugars or lectins. For example, the mechanism for dendritic cells uptake dendritic cells-derived exosomes is *via* the C-type lectin/mannose (glucosamine)-rich CLR interaction. Thus, this internalization can be inhibited by presenting mannose.[241] In another research study, researchers found that galectin-5 was present in the surface of rat reticulocyte cell exosomes and the internalization by macrophages was inhibited after adding galectin-5.[239] Plant lectins could have a biological function on mammalian cells such as inducing apoptosis and autophagy [242]. GSL-IB4, a plant lectin, could bind to CD98, stimulating Ca^{2+} channels on Jurkat cell membranes [82]. It has been reported that garlic lectins showed a high affinity to mannose and as stated before, some parts of glycans on CD98 consist of mannose oligosaccharides [221]. The co-localization and II Lectin blocking by mannose studies showed that the lectins on GDVs interact with HepG2 cells via CD98 glycoprotein.

As said, many factors parallelly lead to inflammation in the NASH, leading to difficulty in the development of an effective drug. The potential anti-inflammatory benefits of GDVs were demonstrated by using HepG2 cells. Hepatic IL-6 level in NASH patients is significantly higher when compared with that in healthy volunteers or NAFLD patients.[243] The IFN-γ-deficient mice were more resistant to a methionine- and choline-deficient high-fat-induced hepatic inflammatory. And IFN-γ might promote the development of NASH by stimulating the macrophages secreting TNF-α.[244] GDVs carrying a mixture of natural bioactive compounds, making them able to mediate the anti-inflammation effect via different pathways.

3.5 Conclusion

In summary, this study demonstrated that the CD98 glycoprotein (rich in mannose motifs) on HepG2 cells is involved in the internalization of GDVs *via* binding with lectin-type proteins. As CD98 is highly expressed in many types of cancers, intestinal inflammation, and non-alcoholic fatty liver disease, the potential therapeutic interests of oral administration of native GDVs in different disease models can be investigated. GDVs are great therapeutic potentials to target CD98 based on their significant anti-inflammatory effect and high non-toxicity. GDVs may open a novel therapeutic platform for acute or chronic diseases *via* oral administrations.

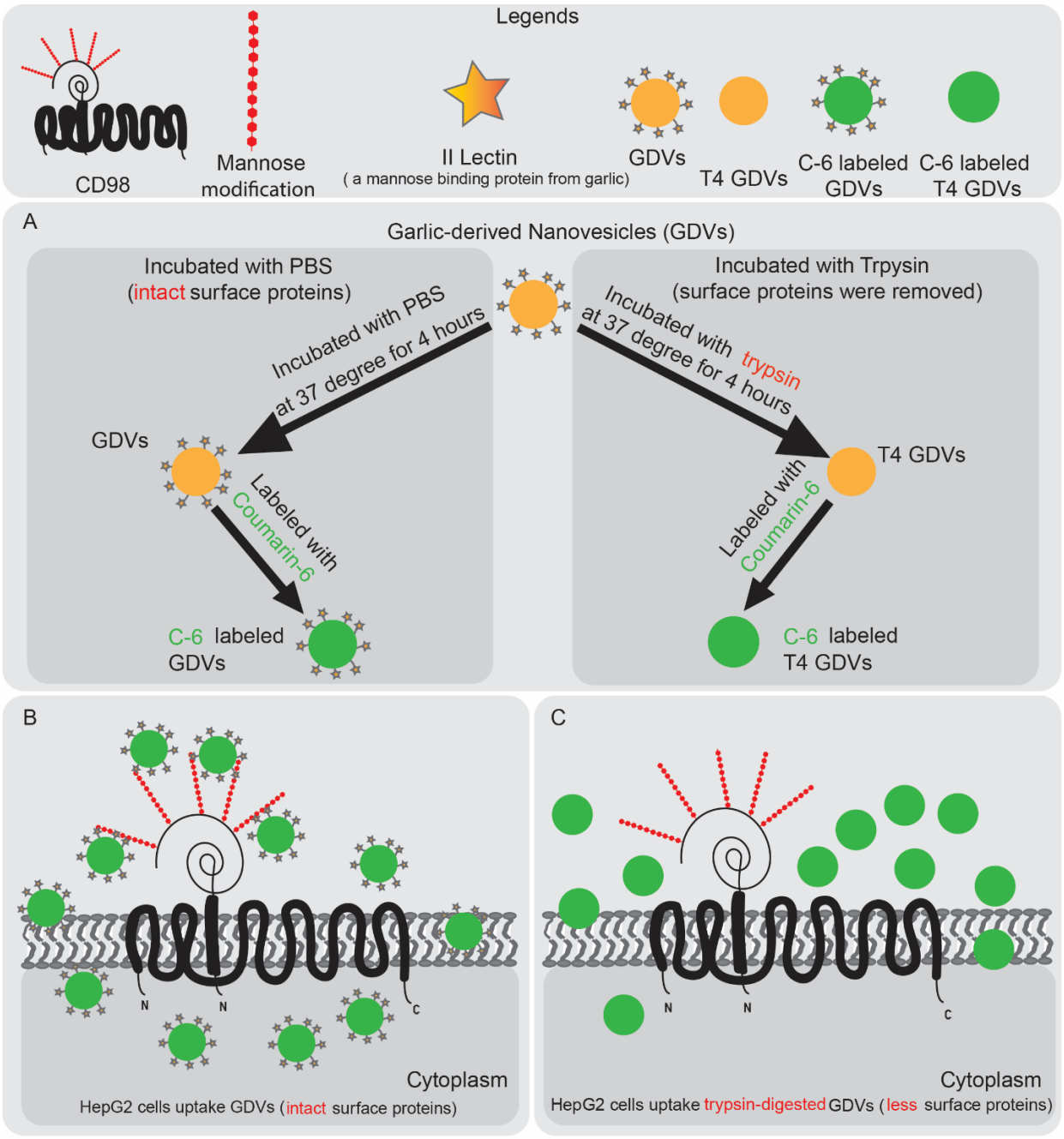

Scheme 1: Internalization of Garlic-derived Exosome-like Nanovesicles (GDEs) by HepG2 is triggered by interaction with CD98

4 CONTRIBUTIONS AND FUTURE DIRECTIONS

4.1 Plant-derived nanovectors and their effects on anti-inflammation and steatosis

Upon joining the laboratory, great efforts were being made on the testing of plant nanovectors and their effects on inflammation and steatosis in NAFLD. The training was obtained in all forms of nanovector isolation to the biological testing (Western blot, PCR, ect). Major contributions to the project were carried out during the late stages of the project where the *in vivo* experiments were progressed. Assistance was given to performing the daily gavage of the garlic-derived nanovectors to the mice in addition to the daily weight monitoring. These experiments were carried out as a 9-week concurrent treatment with the high-fat diet and as an 8-week on the high-fat diet followed by 2 weeks of daily gavages of the garlic-derived nanovectors. The goal of the study was to determine the overall effect of the garlic-derived nanovectors as a preventative and therapeutic method for managing the development and progression of NAFLD. At the end of the experiments, the blood was collected via terminal blood collection and the liver, colon, kidney, and spleen were harvested for further analysis. The procedure and weights are depicted in Figure 4.1. It was documented that the overall weight of the mice was not significantly different between the PBS and the garlic gavage groups (Figure 4.1 B). This demonstrates that the garlic-derived nanovectors did not affect overall visceral fat as was seen through daily monitoring. It is also worth noting that the weight loss of the mice in the post-treatment was most likely due to the shock of the mice being gavaged after the initial 8-week period on the high-fat diet. Weights gradually increased at a similar rate after the initial gavage.

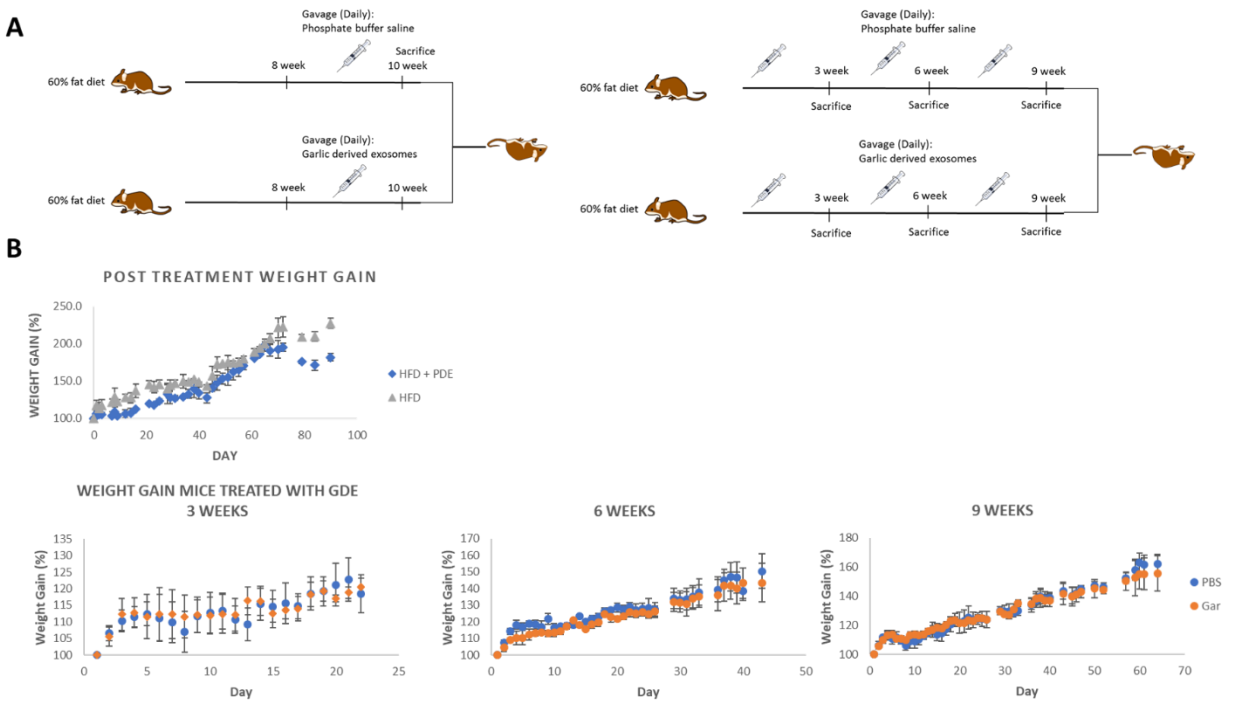

Figure 4.1: Mice treated with garlic-derived nanovectors exhibited similar weight loss trends to that of the control mice group.

A) Mice were fed with an HFD for 9-10 weeks with a daily gavage of 0.5 mg/mL garlic-derived nanovectors and 1x PBS after week 8 and throughout HFD for 9 weeks. B) Weight gain trends for mice recorded periodically through diet and treatment. (Figure used from Brandon Canup's dissertation with permission to allow for an overview [245])

The overall results will be highlighted in Brandon Canup's dissertation and possible future publication.[245] The initial results that were obtained in the laboratory showed that the garlic-derived nanovectors were very good at suppressing CD98 upregulation in HepG2 cells after LPS and palmitic acid stimulation. The results from these experiments were promising for the directions of the *in vivo* experiments. The results of the *in vivo* experiments showed that CD98 was successfully downregulated in both the concurrent and post-treatment with the garlic-derived nanovectors (Figure 4.2). This response to the garlic-derived nanovectors was similar to the prior results in the laboratory.

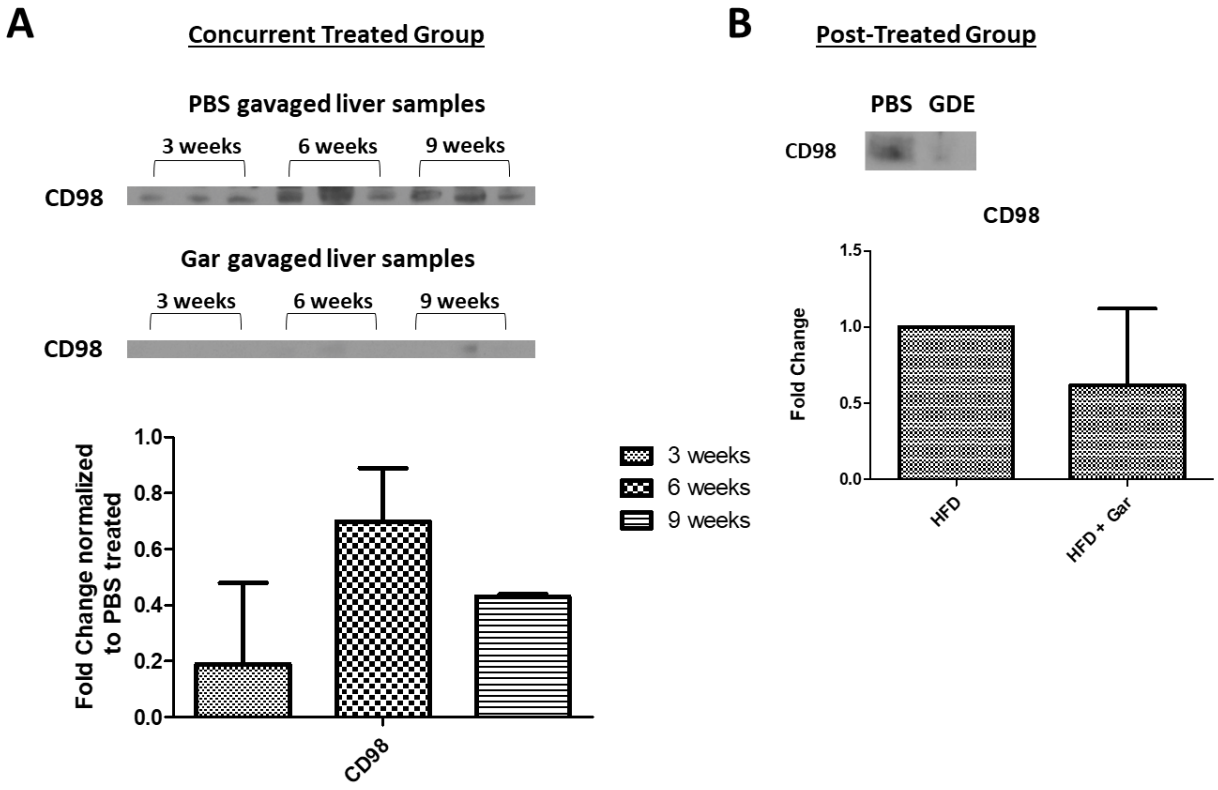

Figure 4.2: Mice treated with garlic derived nanovectors exhibited downregulation of CD98 mRNA and protein expression

A) Mice were fed with an HFD for a period of 9 weeks with a daily gavage of 0.5 mg/mL garlic-derived nanovectors and 1x PBS for 9 weeks. B) Mice were fed with an HFD for a period of 10 weeks with a daily gavage of 0.5 mg/mL garlic-derived nanovectors and 1x PBS after week 8 and throughout HFD for a total of 10 weeks. (Figure derived from data in Brandon Canup's dissertation with permission [245])

Since the downregulation of CD98 was observed in the liver tissue of the treated mice, the overall effect on the liver was examined by histology. The results of the CD98 downregulation demonstrated downregulation in the lipid vacuoles in the liver tissue as analyzed by H&E staining (Figure 4.3) which was similar to the results reported in the work produced using the CD98 siRNA-loaded polymer nanoparticles.[171]

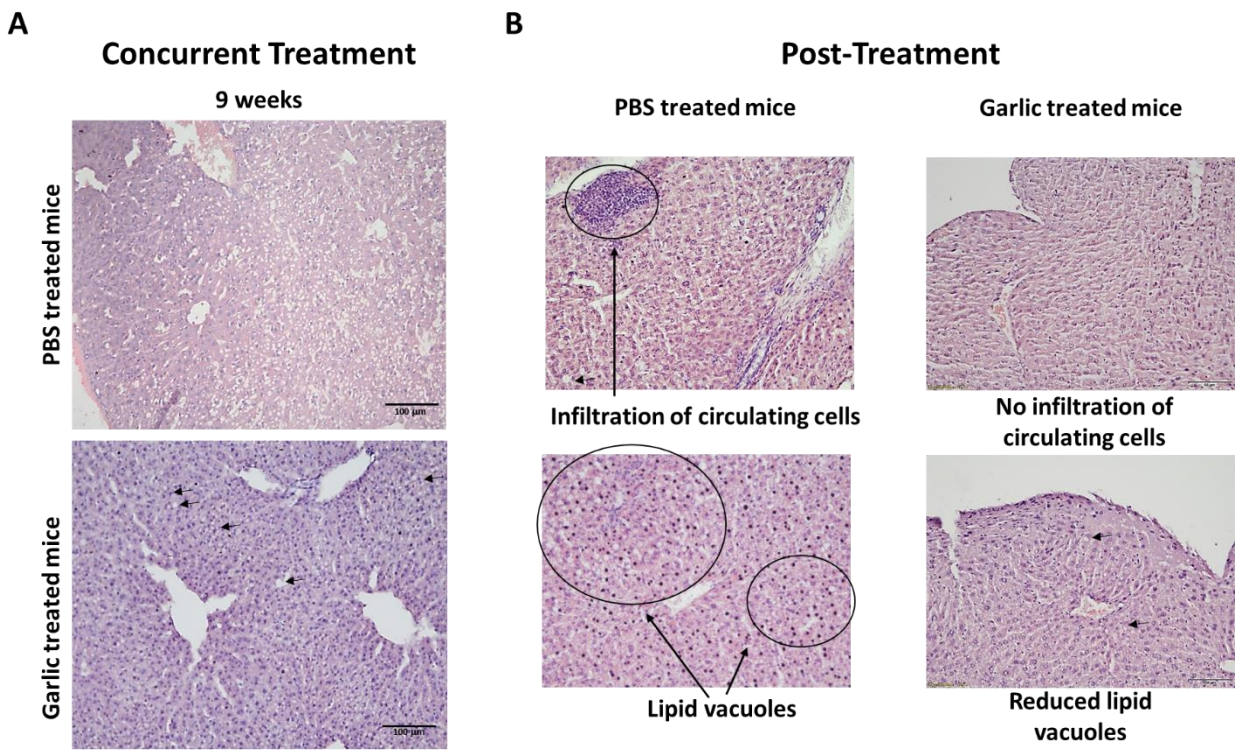

Figure 4.3: Mice treated with garlic derived exosomes exhibited attenuation of lipid vacuoles in the livers of high-fat-diet-fed mice

Hematoxylin and Eosin staining of liver tissue from *in vivo* experiments. A) Mice were fed with an HFD for a period of 9 weeks with a daily gavage of 0.5 mg/mL garlic-derived nano-vectors and 1x PBS for 9 weeks. B) Mice were fed with an HFD for a period of 10 weeks with a daily gavage of 0.5 mg/mL garlic-derived nanovectors and 1x PBS after week 8 and throughout HFD for a total of 10 weeks. (Figure derived from data in Brandon Canup's dissertation with permission [245])

The promising results obtained during the training period propagated the project outlined in Chapter 3 and which was published in ACS Omega.[246] The goal was to question if CD98 played a role in the internalization of the garlic-derived nanovectors. Due to the initial increase in CD98 expression in the *in vitro* and *in vivo* models that were tested, it was speculated that the in-creased expression of CD98 would also allow for increased garlic-derived nanovectors uptake.

Thereby allowing the garlic-derived nanovectors to enact their therapeutic benefits. With this prior knowledge in hand, the anti-inflammatory characteristics of the garlic-derived nanovectors were also confirmed. Thus, the experiments described in Chapter 2 and the material presented in Brandon Canup's dissertation allow for the understanding of the uptake mechanism and overall benefit of utilizing garlic-derived nanovectors for the downregulation of CD98 in the liver.

4.2 Future directions

The endeavors undertaken to investigate the roles of CD98 in liver inflammation and its association with plant nanovectors internalization in the laboratory are still incomplete. Herein, the role of CD98 and its interaction with garlic-derived nanovectors was investigated. Other reports for CD98 and its relation to the plant-derived nanovectors have been documented, but not published [1]. One of the issues that using plant-derived nanovectors as therapeutic tools is the lack of information on characteristics such as lipid constitution, protein cargo, nucleic acid cargo, and small molecule cargo. Screening multiple plant-derived nanovectors then becomes a costly endeavor. In addition, the controversy over the identity of plant-derived nanovectors as associated with plant-derived exosomes. Currently, there are a lot of reports that have demonstrated commonality between exosomes derived from mammalian species such as similar surface markers and cargos. This is not the case with the plant-derived nanovectors which as of writing this dissertation, there are not similar surface markers that can be used to identify if the plant nanovector is an exosome. The biogenesis of the plant-derived exosome has yet to be fully unraveled since the mechanism may or may not be similar to that of the mammalian counterpart. Great efforts must be made to analyze these fundamental problems to ensure quality control and reproducibility among research laboratories.

The logical steps of the experiments thus far would be to analyze the other plant-derived nanovectors studied in the laboratory. The lab has analyzed grapefruit and carrot-derived exosomes in the *in vitro* models. It would provide great insight to see if they would behave similarly with CD98. For the progress of the internalization experiment, a knockout study of CD98 using mice would elucidate if the results could be translated *in vivo*. The experiment could be determined using flow cytometry analysis after the successful development of the CD98 knockout mice. The knockout mice could also be fed with a high-fat diet for a period of 9 weeks with a daily 1X PBS and garlic-derived nanovectors to validate the previous publication and study performed in the lab. The next step would be optimizing the garlic-derived nanovectors to be a therapeutic vehicle to sites with known upregulation of CD98. There is a great variety of different avenues in which the project could progress given time and funding.

REFERENCES

1. Cui, Y., et al., *Plant extracellular vesicles.* Protoplasma, 2020. **257**(1): p. 3-12.
2. Robinson, D.G., Y. Ding, and L. Jiang, *Unconventional protein secretion in plants: a critical assessment.* Protoplasma, 2016. **253**(1): p. 31-43.
3. Kim, J., H.Y. Gee, and M.G. Lee, *Unconventional protein secretion – new insights into the pathogenesis and therapeutic targets of human diseases.* Journal of Cell Science, 2018. **131**(12): p. jcs213686.
4. Hwang, I. and D.G. Robinson, *Transport vesicle formation in plant cells.* Current Opinion in Plant Biology, 2009. **12**(6): p. 660-669.
5. Robinson, D.G. and P. Pimpl, *Clathrin and post-Golgi trafficking: a very complicated issue.* Trends in Plant Science, 2014. **19**(3): p. 134-139.
6. Tuso, P.J., et al., *Nutritional update for physicians: plant-based diets.* Perm J, 2013. **17**(2): p. 61-6.
7. Mu, J., et al., *Interspecies communication between plant and mouse gut host cells through edible plant derived exosome‐like nanoparticles.* Molecular nutrition & food research, 2014. **58**(7): p. 1561-1573.
8. Zhuang, X., et al., *Grapefruit-derived nanovectors delivering therapeutic miR17 through an intranasal route inhibit brain tumor progression.* Molecular Therapy, 2016. **24**(1): p. 96-105.
9. Raimondo, S., et al., *Citrus limon-derived nanovesicles inhibit cancer cell proliferation and suppress CML xenograft growth by inducing TRAIL-mediated cell death.* Oncotarget, 2015. **6**(23): p. 19514.
10. Fujita, D., et al., *Apple-derived nanoparticles modulate expression of organic-anion-transporting polypeptide (OATP) 2B1 in Caco-2 cells.* Molecular pharmaceutics, 2018. **15**(12): p. 5772-5780.
11. Ju, S., et al., *Grape exosome-like nanoparticles induce intestinal stem cells and protect mice from DSS-induced colitis.* Molecular Therapy, 2013. **21**(7): p. 1345-1357.
12. Zhang, M., et al., *Plant derived edible nanoparticles as a new therapeutic approach against diseases.* Tissue barriers, 2016. **4**(2): p. e1134415-e1134415.
13. Deng, Z., et al., *Broccoli-Derived Nanoparticle Inhibits Mouse Colitis by Activating Dendritic Cell AMP-Activated Protein Kinase.* Molecular therapy : the journal of the American Society of Gene Therapy, 2017. **25**(7): p. 1641-1654.
14. Digomann, D., et al., *The CD98 Heavy Chain Is a Marker and Regulator of Head and Neck Squamous Cell Carcinoma Radiosensitivity.* Clin Cancer Res, 2019. **25**(10): p. 3152-3163.
15. Teng, Y., et al., *Plant-Derived Exosomal MicroRNAs Shape the Gut Microbiota.* Cell Host Microbe, 2018. **24**(5): p. 637-652.e8.
16. Chernomordik, L.V. and M.M. Kozlov, *Mechanics of membrane fusion.* Nat Struct Mol Biol, 2008. **15**(7): p. 675-83.
17. Chandler, K.B. and C.E. Costello, *Glycomics and glycoproteomics of membrane proteins and cell-surface receptors: Present trends and future opportunities.* Electrophoresis, 2016. **37**(11): p. 1407-19.
18. Tian, T., et al., *Exosome uptake through clathrin-mediated endocytosis and macropinocytosis and mediating miR-21 delivery.* Journal of Biological Chemistry, 2014. **289**(32): p. 22258-22267.
19. Mulcahy, L.A., R.C. Pink, and D.R.F. Carter, *Routes and mechanisms of extracellular vesicle uptake.* Journal of extracellular vesicles, 2014. **3**(1): p. 24641.
20. Christianson, H.C., et al., *Cancer cell exosomes depend on cell-surface heparan sulfate proteoglycans for their internalization and functional activity.* Proceedings of the National Academy of Sciences, 2013. **110**(43): p. 17380-17385.

21. Purushothaman, A., et al., *Fibronectin on the surface of myeloma cell-derived exosomes mediates exosome-cell interactions.* Journal of Biological Chemistry, 2016. **291**(4): p. 1652-1663.
22. Escrevente, C., et al., *Interaction and uptake of exosomes by ovarian cancer cells.* BMC cancer, 2011. **11**(1): p. 108.
23. Danfær, A., *Nutrient metabolism and utilization in the liver.* Livestock Production Science, 1994. **39**(1): p. 115-127.
24. Rui, L., *Energy metabolism in the liver.* Comprehensive physiology, 2011. **4**(1): p. 177-197.
25. Seal, C. and C. Reynolds, *Nutritional implications of gastrointestinal and liver metabolism in ruminants.* Nutrition research reviews, 1993. **6**(1): p. 185-208.
26. Grant, D., *Detoxification pathways in the liver.* Journal of inherited metabolic disease, 1991: p. 421-430.
27. Carriaga, M.T. and D.E. Henson, *Liver, gallbladder, extrahepatic bile ducts, and pancreas.* Cancer, 1995. **75**(S1): p. 171-190.
28. Nishida, N. and M. Kudo, *Liver damage related to immune checkpoint inhibitors.* Hepatology international, 2019: p. 1-5.
29. Ong, J.P., A. Pitts, and Z.M. Younossi, *Increased overall mortality and liver-related mortality in non-alcoholic fatty liver disease.* Journal of hepatology, 2008. **49**(4): p. 608-612.
30. Zhou, Z., M.-J. Xu, and B. Gao, *Hepatocytes: a key cell type for innate immunity.* Cellular & Molecular Immunology, 2016. **13**(3): p. 301-315.
31. Shetty, S., P.F. Lalor, and D.H. Adams, *Liver sinusoidal endothelial cells—gatekeepers of hepatic immunity.* Nature Reviews Gastroenterology & Hepatology, 2018. **15**(9): p. 555-567.
32. Baffy, G., *Kupffer cells in non-alcoholic fatty liver disease: the emerging view.* J Hepatol, 2009. **51**(1): p. 212-23.
33. Cha, J.-Y., D.-H. Kim, and K.-H. Chun, *The role of hepatic macrophages in nonalcoholic fatty liver disease and nonalcoholic steatohepatitis.* Laboratory animal research, 2018. **34**(4): p. 133-139.
34. Dixon, L.J., et al., *Kupffer cells in the liver.* Comprehensive Physiology, 2013. **3**(2): p. 785-797.
35. Nguyen-Lefebvre, A.T. and A. Horuzsko, *Kupffer Cell Metabolism and Function.* Journal of enzymology and metabolism, 2015. **1**(1): p. 101.
36. Tsuchida, T., *[Mechanisms of hepatic stellate cell activation as a therapeutic target for the treatment of non-alcoholic steatohepatitis].* Nihon Yakurigaku Zasshi, 2019. **154**(4): p. 203-209.
37. Washington, K., et al., *Hepatic stellate cell activation in nonalcoholic steatohepatitis and fatty liver.* Hum Pathol, 2000. **31**(7): p. 822-8.
38. Senoo, H., et al., *Hepatic stellate cell (vitamin A‐storing cell) and its relative‐past, present and future.* Cell biology international, 2010. **34**(12): p. 1247-1272.
39. Hamid, A.S., et al., *Aflatoxin B1-induced hepatocellular carcinoma in developing countries: Geographical distribution, mechanism of action and prevention.* Oncology letters, 2013. **5**(4): p. 1087-1092.
40. Wang, Z., et al., *Changing Epidemiological Characteristics of Hepatitis A in Zhejiang Province, China: Increased Susceptibility in Adults.* PloS one, 2016. **11**(4): p. e0153804-e0153804.
41. Hyun Kim, B. and W. Ray Kim, *Epidemiology of Hepatitis B Virus Infection in the United States.* Clin Liver Dis (Hoboken), 2018. **12**(1): p. 1-4.
42. Mellinger, J.L., *Epidemiology of alcohol use and alcoholic liver disease.* Clinical liver disease, 2019. **13**(5): p. 136.
43. Sherif, Z.A., et al., *Global Epidemiology of Nonalcoholic Fatty Liver Disease and Perspectives on US Minority Populations.* Dig Dis Sci, 2016. **61**(5): p. 1214-25.
44. Younossi, Z.M., et al., *Global epidemiology of nonalcoholic fatty liver disease—Meta-analytic assessment of prevalence, incidence, and outcomes.* Hepatology, 2016. **64**(1): p. 73-84.

45. Wang, H., P. Sun, and K. Baria, *The world-wide incidence of biliary tract cancer (BTC).* Journal of Clinical Oncology, 2020. **38**(4_suppl): p. 585-585.
46. González-Grande, R., et al., *New approaches in the treatment of hepatitis C.* World J Gastroenterol, 2016. **22**(4): p. 1421-32.
47. Jepsen, P., L. Gronbaek, and H. Vilstrup, *Worldwide Incidence of Autoimmune Liver Disease.* Dig Dis, 2015. **33 Suppl 2**: p. 2-12.
48. Szmuness, W., et al., *Hepatitis B vaccine: demonstration of efficacy in a controlled clinical trial in a high-risk population in the United States.* New England Journal of Medicine, 1980. **303**(15): p. 833-841.
49. Ge, X., et al., *Prevalence trends in non-alcoholic fatty liver disease at the global, regional and national levels, 1990–2017: a population-based observational study.* BMJ Open, 2020. **10**(8): p. e036663.
50. Yari, Z. and A. Hekmatdoost, *Chapter 20 - Dietary Interventions in Fatty Liver*, in *Dietary Interventions in Gastrointestinal Diseases*, R.R. Watson and V.R. Preedy, Editors. 2019, Academic Press. p. 245-255.
51. Dietrich, P. and C. Hellerbrand, *Non-alcoholic fatty liver disease, obesity and the metabolic syndrome.* Best Practice & Research Clinical Gastroenterology, 2014. **28**(4): p. 637-653.
52. Dickson, I., *Full-spectrum transcriptomics in NAFLD.* Nature Reviews Gastroenterology & Hepatology, 2021. **18**(2): p. 82-82.
53. Oseini, A.M. and A.J. Sanyal, *Therapies in non-alcoholic steatohepatitis (NASH).* Liver Int, 2017. **37 Suppl 1**(Suppl 1): p. 97-103.
54. Friedman, S.L., et al., *Mechanisms of NAFLD development and therapeutic strategies.* Nature Medicine, 2018. **24**(7): p. 908-922.
55. Chen, Z., et al., *Role of oxidative stress in the pathogenesis of nonalcoholic fatty liver disease.* Free Radical Biology and Medicine, 2020. **152**: p. 116-141.
56. Rada, P., et al., *Understanding lipotoxicity in NAFLD pathogenesis: is CD36 a key driver?* Cell Death & Disease, 2020. **11**(9): p. 802.
57. Sanyal, A.J., et al., *Pioglitazone, vitamin E, or placebo for nonalcoholic steatohepatitis.* N Engl J Med, 2010. **362**(18): p. 1675-85.
58. Kwon, M., et al., *Meroterpenoid-rich fraction of an ethanolic extract from Sargassum serratifolium alleviates obesity and non-alcoholic fatty liver disease in high fat-fed C57BL/6J mice.* Journal of Functional Foods, 2018. **47**: p. 288-298.
59. Koliaki, C., et al., *Adaptation of hepatic mitochondrial function in humans with non-alcoholic fatty liver is lost in steatohepatitis.* Cell Metab, 2015. **21**(5): p. 739-46.
60. Chen, J., et al., *Kupffer Cells in Non-alcoholic Fatty Liver Disease: Friend or Foe?* International journal of biological sciences, 2020. **16**(13): p. 2367-2378.
61. Lee, U.E. and S.L. Friedman, *Mechanisms of hepatic fibrogenesis.* Best practice & research. Clinical gastroenterology, 2011. **25**(2): p. 195-206.
62. Vallée, A. and Y. Lecarpentier, *TGF-β in fibrosis by acting as a conductor for contractile properties of myofibroblasts.* Cell & Bioscience, 2019. **9**(1): p. 98.
63. Gandhi, C.R., *Hepatic stellate cell activation and pro-fibrogenic signals.* Journal of hepatology, 2017. **67**(5): p. 1104-1105.
64. Eriksson, O., et al., *Mannose-Binding Lectin is Associated with Thrombosis and Coagulopathy in Critically Ill COVID-19 Patients.* Thrombosis and haemostasis, 2020. **120**(12): p. 1720-1724.
65. Clement, F. and Y.P. Venkatesh, *Dietary garlic (Allium sativum) lectins, ASA I and ASA II, are highly stable and immunogenic.* Int Immunopharmacol, 2010. **10**(10): p. 1161-9.
66. Pistole, T.x., *Interaction of bacteria and fungi with lectins and lectin-like substances.* Annual Reviews in Microbiology, 1981. **35**(1): p. 85-112.

67. Zhan, M.-Y., et al., *A single-CRD C-type lectin is important for bacterial clearance in the silkworm.* Developmental & Comparative Immunology, 2016. **65**: p. 330-339.
68. Drickamer, K. and M.E. Taylor, *Recent insights into structures and functions of C-type lectins in the immune system.* Current Opinion in Structural Biology, 2015. **34**: p. 26-34.
69. Satish, P.R. and A. Surolia, *Exploiting lectin affinity chromatography in clinical diagnosis.* Journal of biochemical and biophysical methods, 2001. **49**(1-3): p. 625-640.
70. Zhao, R., et al., *Lectin array and glycogene expression analyses of ovarian cancer cell line A2780 and its cisplatin-resistant derivate cell line A2780-cp.* Clinical proteomics, 2017. **14**: p. 20-20.
71. Khan, F., et al., *Lectins as markers for blood grouping.* Med Sci Monit, 2002. **8**(12): p. Ra293-300.
72. Varki, A., *Biological roles of glycans.* Glycobiology, 2017. **27**(1): p. 3-49.
73. Dyason, J.C. and M. von Itzstein, *Viral surface glycoproteins in carbohydrate recognition: Structure and modelling.* Microbial Glycobiology, 2010: p. 269-283.
74. Herget, S., et al., *Statistical analysis of the Bacterial Carbohydrate Structure Data Base (BCSDB): characteristics and diversity of bacterial carbohydrates in comparison with mammalian glycans.* BMC structural biology, 2008. **8**: p. 35-35.
75. Wu, Y., et al., *Non-structural carbohydrates in maize with different nitrogen tolerance are affected by nitrogen addition.* PloS one, 2019. **14**(12): p. e0225753-e0225753.
76. Van Breedam, W., et al., *Bitter-sweet symphony: glycan–lectin interactions in virus biology.* FEMS Microbiology Reviews, 2014. **38**(4): p. 598-632.
77. Stowell, S.R., T. Ju, and R.D. Cummings, *Protein glycosylation in cancer.* Annual review of pathology, 2015. **10**: p. 473-510.
78. Ip, W.K., et al., *Mannose-binding lectin and innate immunity.* Immunol Rev, 2009. **230**(1): p. 9-21.
79. Lichtenstein, R.G. and G.A. Rabinovich, *Glycobiology of cell death: when glycans and lectins govern cell fate.* Cell Death & Differentiation, 2013. **20**(8): p. 976-986.
80. Bänfer, S., et al., *Molecular mechanism to recruit galectin-3 into multivesicular bodies for polarized exosomal secretion.* Proceedings of the National Academy of Sciences, 2018. **115**(19): p. E4396-E4405.
81. Dalton, P., et al., *Membrane trafficking of CD98 and its ligand galectin 3 in BeWo cells–implication for placental cell fusion.* The FEBS journal, 2007. **274**(11): p. 2715-2727.
82. Dong, S. and R.C. Hughes, *Galectin-3 stimulates uptake of extracellular Ca2+ in human Jurkat T-cells.* FEBS Lett, 1996. **395**(2-3): p. 165-9.
83. MacKinnon, A.C., et al., *Regulation of alternative macrophage activation by galectin-3.* The Journal of Immunology, 2008. **180**(4): p. 2650-2658.
84. Ohshima, S., et al., *Galectin 3 and its binding protein in rheumatoid arthritis.* Arthritis & Rheumatism, 2003. **48**(10): p. 2788-2795.
85. Inohara, H., et al., *Interactions between galectin-3 and Mac-2-binding protein mediate cell-cell adhesion.* Cancer research, 1996. **56**(19): p. 4530-4534.
86. Wang, L., et al., *Galectin-3 is a nuclear matrix protein which binds RNA.* Biochemical and biophysical research communications, 1995. **217**(1): p. 292-303.
87. Hu, J., et al., *Physiological roles of asialoglycoprotein receptors (ASGPRs) variants and recent advances in hepatic-targeted delivery of therapeutic molecules via ASGPRs.* Protein Pept Lett, 2014. **21**(10): p. 1025-30.
88. D'Souza, A.A. and P.V. Devarajan, *Asialoglycoprotein receptor mediated hepatocyte targeting - strategies and applications.* J Control Release, 2015. **203**: p. 126-39.
89. Tsaneva, M. and E.J.M. Van Damme, *130 years of Plant Lectin Research.* Glycoconjugate Journal, 2020. **37**(5): p. 533-551.

90. Van Damme, E.J.M., et al., *Cytoplasmic/nuclear plant lectins: a new story.* Trends in Plant Science, 2004. **9**(10): p. 484-489.
91. Chandra, N.R., et al., *Crystal structure of a dimeric mannose-specific agglutinin from garlic: quaternary association and carbohydrate specificity.* Journal of molecular biology, 1999. **285**(3): p. 1157-1168.
92. Ramachandraiah, G. and N.R. Chandra, *Sequence and structural determinants of mannose recognition.* Proteins, 2000. **39**(4): p. 358-64.
93. Surya, P.H., M. Deepti, and K.K. Elyas, *Plant Lectins: Sugar-Binding Properties and Biotechnological Applications*, in *Plant Metabolites: Methods, Applications and Prospects*, S.T. Sukumaran, S. Sugathan, and S. Abdulhameed, Editors. 2020, Springer Singapore: Singapore. p. 401-439.
94. Saha, P., et al., *Transgenic rice expressing Allium sativum leaf lectin with enhanced resistance against sap-sucking insect pests.* Planta, 2006. **223**(6): p. 1329.
95. Hu, S. and D.T. Wong, *Lectin microarray.* Proteomics. Clinical applications, 2009. **3**(2): p. 148-154.
96. Pettersen, E.F., et al., *UCSF Chimera--a visualization system for exploratory research and analysis.* J Comput Chem, 2004. **25**(13): p. 1605-12.
97. Sharma, A., S. Sharma, and G.K. Khuller, *Lectin-functionalized poly (lactide-co-glycolide) nanoparticles as oral/aerosolized antitubercular drug carriers for treatment of tuberculosis.* J Antimicrob Chemother, 2004. **54**(4): p. 761-6.
98. Liu, B., M.W. Min, and J.K. Bao, *Induction of apoptosis by Concanavalin A and its molecular mechanisms in cancer cells.* Autophagy, 2009. **5**(3): p. 432-3.
99. Kulkarni, G.V. and C.A. McCulloch, *Concanavalin A induced apoptosis in fibroblasts: the role of cell surface carbohydrates in lectin mediated cytotoxicity.* J Cell Physiol, 1995. **165**(1): p. 119-33.
100. Garred, P., et al., *Mannose‐binding lectin (MBL) therapy in an MBL‐deficient patient with severe cystic fibrosis lung disease.* Pediatric pulmonology, 2002. **33**(3): p. 201-207.
101. Mukwaya, V., et al., *Lectin-Glycan-Mediated Nanoparticle Docking as a Step toward Programmable Membrane Catalysis and Adhesion in Synthetic Protocells.* ACS nano, 2020. **14**(7): p. 7899-7910.
102. Mazalovska, M. and J.C. Kouokam, *Plant-derived lectins as potential cancer therapeutics and diagnostic tools.* BioMed Research International, 2020. **2020**.
103. Beckwith, D.M. and M. Cudic, *Tumor-associated O-glycans of MUC1: Carriers of the glyco-code and targets for cancer vaccine design.* Seminars in Immunology, 2020. **47**: p. 101389.
104. Cantor, J.M. and M.H. Ginsberg, *CD98 at the crossroads of adaptive immunity and cancer.* Journal of cell science, 2012. **125**(6): p. 1373-1382.
105. Robert, S.M. and H. Sontheimer, *Peritumoral Epilepsy ☆*, in *Reference Module in Neuroscience and Biobehavioral Psychology*. 2017, Elsevier.
106. Li, L., et al., *Targeting tumor highly-expressed LAT1 transporter with amino acid-modified nanoparticles: Toward a novel active targeting strategy in breast cancer therapy.* Nanomedicine, 2017. **13**(3): p. 987-998.
107. Rossier, G., et al., *LAT2, a new basolateral 4F2hc/CD98-associated amino acid transporter of kidney and intestine.* J Biol Chem, 1999. **274**(49): p. 34948-54.
108. Scalise, M., et al., *The human SLC7A5 (LAT1): the intriguing histidine/large neutral amino acid transporter and its relevance to human health.* Frontiers in chemistry, 2018. **6**: p. 243.
109. Oda, K., et al., *Consensus mutagenesis approach improves the thermal stability of system xc− transporter, xCT, and enables cryo‐EM analyses.* Protein Science, 2020. **29**(12): p. 2398-2407.

110. Rius, M. and J. Chillarón, *Carrier subunit of plasma membrane transporter is required for oxidative folding of its helper subunit.* The Journal of biological chemistry, 2012. **287**(22): p. 18190-18200.
111. Quackenbush, E., et al., *Molecular cloning of complementary DNAs encoding the heavy chain of the human 4F2 cell-surface antigen: a type II membrane glycoprotein involved in normal and neoplastic cell growth.* Proceedings of the National Academy of Sciences, 1987. **84**(18): p. 6526-6530.
112. Verrey, F., et al., *Glycoprotein-associated amino acid exchangers: broadening the range of transport specificity.* Pflügers Archiv, 2000. **440**(4): p. 503-512.
113. Schroeder, N., et al., *The lipid raft-associated protein CD98 is required for vaccinia virus endocytosis.* J Virol, 2012. **86**(9): p. 4868-82.
114. Xiao, B., et al., *Nanoparticles with surface antibody against CD98 and carrying CD98 small interfering RNA reduce colitis in mice.* Gastroenterology, 2014. **146**(5): p. 1289-1300. e19.
115. Xiao, B., et al., *Glycoprotein CD98 as a receptor for colitis-targeted delivery of nanoparticle.* J Mater Chem B, 2014. **2**(11): p. 1499-1508.
116. Colavita, I., et al., *Membrane protein 4F2/CD98 is a cell surface receptor involved in the internalization and trafficking of human β-Defensin 3 in epithelial cells.* Chemistry & biology, 2015. **22**(2): p. 217-228.
117. Han, M.K., et al., *Overexpression of CD98 in intestinal epithelium dysregulates miRNAs and their targeted proteins along the ileal villus-crypt axis.* Scientific reports, 2018. **8**(1): p. 16220-16220.
118. Hayes, G.M., et al., *Antitumor activity of an anti-CD98 antibody.* Int J Cancer, 2015. **137**(3): p. 710-20.
119. Lee, Y., et al., *Cryo-EM structure of the human L-type amino acid transporter 1 in complex with glycoprotein CD98hc.* Nat Struct Mol Biol, 2019. **26**(6): p. 510-517.
120. Cai, S., et al., *CD98 modulates integrin β1 function in polarized epithelial cells.* Journal of Cell Science, 2005. **118**(5): p. 889-899.
121. Fleishman, S.J., et al., *An Automatic Method for Predicting Transmembrane Protein Structures Using Cryo-EM and Evolutionary Data.* Biophysical Journal, 2004. **87**(5): p. 3448-3459.
122. Yan, R., et al., *Structural insight into the substrate recognition and transport mechanism of the human LAT2-4F2hc complex.* Cell Discov, 2020. **6**(1): p. 82.
123. Bridges, R.J., N.R. Natale, and S.A. Patel, *System xc^- cystine/glutamate antiporter: an update on molecular pharmacology and roles within the CNS.* Br J Pharmacol, 2012. **165**(1): p. 20-34.
124. Armstrong, J.S., et al., *Role of glutathione depletion and reactive oxygen species generation in apoptotic signaling in a human B lymphoma cell line.* Cell Death & Differentiation, 2002. **9**(3): p. 252-263.
125. Liu, M.-r., W.-t. Zhu, and D.-s. Pei, *System Xc−: a key regulatory target of ferroptosis in cancer.* Investigational New Drugs, 2021.
126. Sato, M., et al., *The ferroptosis inducer erastin irreversibly inhibits system xc− and synergizes with cisplatin to increase cisplatin's cytotoxicity in cancer cells.* Scientific Reports, 2018. **8**(1): p. 968.
127. Verrey, F., et al., *New glycoprotein-associated amino acid transporters.* J Membr Biol, 1999. **172**(3): p. 181-92.
128. Nguyen, H.T.T., et al., *CD98 expression modulates intestinal homeostasis, inflammation, and colitis-associated cancer in mice.* The Journal of clinical investigation, 2011. **121**(5): p. 1733-1747.
129. Canup, B.S.B., H. Song, and H. Laroui, *Role of CD98 in liver disease.* Annals of Hepatology, 2020.
130. Kaira, K., et al., *CD98 is a promising prognostic biomarker in biliary tract cancer.* Hepatobiliary & Pancreatic Diseases International, 2014. **13**(6): p. 654-657.

131. Xiao, B., et al., *Silencing of Intestinal Glycoprotein CD98 by Orally Targeted Nanoparticles Enhances Chemosensitization of Colon Cancer.* ACS Nano, 2018. **12**(6): p. 5253-5265.
132. Laroui, H., et al., *Targeting intestinal inflammation with CD98 siRNA/PEI-loaded nanoparticles.* Molecular therapy : the journal of the American Society of Gene Therapy, 2014. **22**(1): p. 69-80.
133. Dutta, D. and J.G. Donaldson, *Sorting of Clathrin-Independent Cargo Proteins Depends on Rab35 Delivered by Clathrin-Mediated Endocytosis.* Traffic, 2015. **16**(9): p. 994-1009.
134. Jianrong, C., et al., *Nanotechnology and biosensors.* Biotechnology Advances, 2004. **22**(7): p. 505-518.
135. Malekzad, H., et al., *Noble metal nanoparticles in biosensors: recent studies and applications.* Nanotechnology reviews, 2017. **6**(3): p. 301-329.
136. Hashemi, S.A., et al., *Coupled graphene oxide with hybrid metallic nanoparticles as potential electrochemical biosensors for precise detection of ascorbic acid within blood.* Analytica Chimica Acta, 2020. **1107**: p. 183-192.
137. Wang, H.-X., et al., *N-acetylgalactosamine functionalized mixed micellar nanoparticles for targeted delivery of siRNA to liver.* Journal of Controlled Release, 2013. **166**(2): p. 106-114.
138. Wang, L., et al., *CD44 antibody-targeted liposomal nanoparticles for molecular imaging and therapy of hepatocellular carcinoma.* Biomaterials, 2012. **33**(20): p. 5107-14.
139. Xia, Y., et al., *Galactose-modified selenium nanoparticles for targeted delivery of doxorubicin to hepatocellular carcinoma.* Drug delivery, 2019. **26**(1): p. 1-11.
140. Zhao, R., et al., *Simultaneous inhibition of growth and metastasis of hepatocellular carcinoma by co-delivery of ursolic acid and sorafenib using lactobionic acid modified and pH-sensitive chitosan-conjugated mesoporous silica nanocomplex.* Biomaterials, 2017. **143**: p. 1-16.
141. Nune, S.K., et al., *Nanoparticles for biomedical imaging.* Expert opinion on drug delivery, 2009. **6**(11): p. 1175-1194.
142. Chapman, S., et al., *Nanoparticles for cancer imaging: The good, the bad, and the promise.* Nano today, 2013. **8**(5): p. 454-460.
143. Cormode, D.P., P.C. Naha, and Z.A. Fayad, *Nanoparticle contrast agents for computed tomography: a focus on micelles.* Contrast media & molecular imaging, 2014. **9**(1): p. 37-52.
144. Baetke, S.C., T. Lammers, and F. Kiessling, *Applications of nanoparticles for diagnosis and therapy of cancer.* Br J Radiol, 2015. **88**(1054): p. 20150207.
145. Zhang, X., et al., *Orally delivered targeted nanotherapeutics for the treatment of colorectal cancer.* Expert Opinion on Drug Delivery, 2020. **17**(6): p. 781-790.
146. Cho, C.S., et al., *Receptor-mediated delivery of all trans-retinoic acid to hepatocyte using poly(l-lactic acid) nanoparticles coated with galactose-carrying polystyrene.* Journal of Controlled Release, 2001. **77**(1): p. 7-15.
147. Dimov, N., et al., *Formation and purification of tailored liposomes for drug delivery using a module-based micro continuous-flow system.* Scientific Reports, 2017. **7**(1): p. 12045.
148. Kamruzzaman Selim, K.M., et al., *Surface modification of magnetite nanoparticles using lactobionic acid and their interaction with hepatocytes.* Biomaterials, 2007. **28**(4): p. 710-716.
149. Croissant, J.G., et al., *Synthetic amorphous silica nanoparticles: toxicity, biomedical and environmental implications.* Nature Reviews Materials, 2020. **5**(12): p. 886-909.
150. Saraswathy, M. and S. Gong, *Recent developments in the co-delivery of siRNA and small molecule anticancer drugs for cancer treatment.* Materials Today, 2014. **17**(6): p. 298-306.
151. Gelperina, S., et al., *The potential advantages of nanoparticle drug delivery systems in chemotherapy of tuberculosis.* American journal of respiratory and critical care medicine, 2005. **172**(12): p. 1487-1490.
152. Mishra, N., et al., *Efficient Hepatic Delivery of Drugs: Novel Strategies and Their Significance.* BioMed Research International, 2013. **2013**: p. 382184.

153. He, C., et al., *Effects of particle size and surface charge on cellular uptake and biodistribution of polymeric nanoparticles.* Biomaterials, 2010. **31**(13): p. 3657-3666.
154. Tavares, A.J., et al., *Effect of removing Kupffer cells on nanoparticle tumor delivery.* Proceedings of the National Academy of Sciences, 2017. **114**(51): p. E10871-E10880.
155. Rattan, R., et al., *Nanoparticle-macrophage interactions: A balance between clearance and cell-specific targeting.* Bioorganic & medicinal chemistry, 2017. **25**(16): p. 4487-4496.
156. Cheng, J., et al., *Formulation of functionalized PLGA–PEG nanoparticles for in vivo targeted drug delivery.* Biomaterials, 2007. **28**(5): p. 869-876.
157. Dhar, S., et al., *Targeted delivery of cisplatin to prostate cancer cells by aptamer functionalized Pt (IV) prodrug-PLGA–PEG nanoparticles.* Proceedings of the National Academy of Sciences, 2008. **105**(45): p. 17356-17361.
158. Baboci, L., et al., *The Dual Role of the Liver in Nanomedicine as an Actor in the Elimination of Nanostructures or a Therapeutic Target.* Journal of Oncology, 2020. **2020**: p. 4638192.
159. Jain, A., et al., *Recent advances in galactose-engineered nanocarriers for the site-specific delivery of siRNA and anticancer drugs.* Drug Discov Today, 2018. **23**(5): p. 960-973.
160. Medina, S.H., et al., *N-acetylgalactosamine-functionalized dendrimers as hepatic cancer cell-targeted carriers.* Biomaterials, 2011. **32**(17): p. 4118-29.
161. Li, H., et al., *Introduction of lactobionic acid ligand into mixed-charge nanoparticles to realize in situ triggered active targeting to hepatoma cells.* Materials Today Bio, 2019. **4**: p. 100034.
162. Tsend-Ayush, A., et al., *Lactobionic acid-conjugated TPGS nanoparticles for enhancing therapeutic efficacy of etoposide against hepatocellular carcinoma.* Nanotechnology, 2017. **28**(19): p. 195602.
163. Huang, L., et al., *Versatile redox-sensitive pullulan nanoparticles for enhanced liver targeting and efficient cancer therapy.* Nanomedicine, 2018. **14**(3): p. 1005-1017.
164. Ganeshkumar, M., et al., *Curcumin loaded on pullulan acetate nanoparticles protects the liver from damage induced by DEN.* RSC Advances, 2016. **6**(7): p. 5599-5610.
165. Zheng, X., et al., *Self-assembled dual fluorescence nanoparticles for CD44-targeted delivery of anti-miR-27a in liver cancer theranostics.* Theranostics, 2018. **8**(14): p. 3808-3823.
166. Kobyliak, N., et al., *Prevention of NAFLD development in rats with obesity via the improvement of pro/antioxidant state by cerium dioxide nanoparticles.* Clujul Medical, 2016. **89**(2): p. 229.
167. He, S., et al., *Targeted delivery of microRNA 146b mimic to hepatocytes by lactosylated PDMAEMA nanoparticles for the treatment of NAFLD.* Artificial cells, nanomedicine, and biotechnology, 2018. **46**(sup2): p. 217-228.
168. Wan, S., et al., *Resveratrol-loaded PLGA nanoparticles: enhanced stability, solubility and bioactivity of resveratrol for non-alcoholic fatty liver disease therapy.* Royal Society open science, 2018. **5**(11): p. 181457.
169. Zai, W., et al., *Targeted interleukin-22 gene delivery in the liver by polymetformin and penetratin-based hybrid nanoparticles to treat nonalcoholic fatty liver disease.* ACS applied materials & interfaces, 2019. **11**(5): p. 4842-4857.
170. Lü, J.-M., et al., *Current advances in research and clinical applications of PLGA-based nanotechnology.* Expert review of molecular diagnostics, 2009. **9**(4): p. 325-341.
171. Canup, B.S., et al., *CD98 siRNA-loaded nanoparticles decrease hepatic steatosis in mice.* Digestive and Liver Disease, 2017. **49**(2): p. 188-196.
172. Teng, W., et al., *The hepatic-targeted, resveratrol loaded nanoparticles for relief of high fat diet-induced nonalcoholic fatty liver disease.* Journal of Controlled Release, 2019. **307**: p. 139-149.
173. Maradana, M.R., et al., *Immunomodulatory liposomes targeting liver macrophages arrest progression of nonalcoholic steatohepatitis.* Metabolism, 2018. **78**: p. 80-94.

174. Liu, X., et al., *Deoxyschizandrin loaded liposomes on the suppression lipid accumulation in 3T3-L1 adipocytes.* Molecules, 2018. **23**(9): p. 2158.
175. Kobyliak, N.M., et al., *Antioxidative effects of cerium dioxide nanoparticles ameliorate age-related male infertility: optimistic results in rats and the review of clinical clues for integrative concept of men health and fertility.* EPMA Journal, 2015. **6**(1): p. 12.
176. Hirst, S.M., et al., *Bio-distribution and in vivo antioxidant effects of cerium oxide nanoparticles in mice.* Environ Toxicol, 2013. **28**(2): p. 107-18.
177. Carvajal, S., et al., *Cerium oxide nanoparticles display antilipogenic effect in rats with non-alcoholic fatty liver disease.* Scientific Reports, 2019. **9**(1): p. 12848.
178. Sutti, S. and E. Albano, *Adaptive immunity: an emerging player in the progression of NAFLD.* Nature Reviews Gastroenterology & Hepatology, 2020. **17**(2): p. 81-92.
179. Armstrong, L.E. and G.L. Guo, *Role of FXR in Liver Inflammation during Nonalcoholic Steatohepatitis.* Current pharmacology reports, 2017. **3**(2): p. 92-100.
180. Fiorucci, S., C. Di Giorgio, and E. Distrutti, *Obeticholic Acid: An Update of Its Pharmacological Activities in Liver Disorders.* Handb Exp Pharmacol, 2019. **256**: p. 283-295.
181. Thiagarajan, P. and G.P. Aithal, *Drug Development for Nonalcoholic Fatty Liver Disease: Landscape and Challenges.* Journal of clinical and experimental hepatology, 2019. **9**(4): p. 515-521.
182. Nguyen, H.T.T. and D. Merlin, *Homeostatic and innate immune responses: role of the transmembrane glycoprotein CD98.* Cellular and molecular life sciences : CMLS, 2012. **69**(18): p. 3015-3026.
183. Boulter, E., et al., *Cell metabolism regulates integrin mechanosensing via an SLC3A2-dependent sphingolipid biosynthesis pathway.* Nature Communications, 2018. **9**(1): p. 4862.
184. Bajaj, J., et al., *CD98-Mediated Adhesive Signaling Enables the Establishment and Propagation of Acute Myelogenous Leukemia.* Cancer cell, 2016. **30**(5): p. 792-805.
185. Kleiner, D.E., et al., *Design and validation of a histological scoring system for nonalcoholic fatty liver disease.* Hepatology, 2005. **41**(6): p. 1313-21.
186. Misra, R., et al., *In vitro control release, cytotoxicity assessment and cellular uptake of methotrexate loaded liquid-crystalline folate nanocarrier.* Biomed Pharmacother, 2015. **69**: p. 102-10.
187. Perala, S.R.K. and S. Kumar, *On the Mechanism of Metal Nanoparticle Synthesis in the Brust–Schiffrin Method.* Langmuir, 2013. **29**(31): p. 9863-9873.
188. Spengler, E.K. and R. Loomba, *Recommendations for Diagnosis, Referral for Liver Biopsy, and Treatment of Nonalcoholic Fatty Liver Disease and Nonalcoholic Steatohepatitis.* Mayo Clinic proceedings, 2015. **90**(9): p. 1233-1246.
189. Yan, Y., et al., *Characterization of the human intestinal CD98 promoter and its regulation by interferon-γ.* American Journal of Physiology-Gastrointestinal and Liver Physiology, 2007. **292**(2): p. G535-G545.
190. Nguyen, H.T.T., et al., *Intestinal epithelial cell-specific CD98 expression regulates tumorigenesis in ApcMin/+ mice.* Laboratory Investigation, 2012. **92**(8): p. 1203-1212.
191. Buzzetti, E., M. Pinzani, and E.A. Tsochatzis, *The multiple-hit pathogenesis of non-alcoholic fatty liver disease (NAFLD).* Metabolism, 2016. **65**(8): p. 1038-1048.
192. Tang, K.-T., et al., *Antitumour necrosis factor-α agents and development of new-onset cirrhosis or non-alcoholic fatty liver disease: a retrospective cohort.* BMJ open gastroenterology, 2020. **7**(1): p. e000349-e000349.
193. De Jong, W.H. and P.J.A. Borm, *Drug delivery and nanoparticles:applications and hazards.* International journal of nanomedicine, 2008. **3**(2): p. 133-149.

194. Liu, T., et al., *NF-κB signaling in inflammation.* Signal transduction and targeted therapy, 2017. **2**: p. 17023.
195. Svensson, K.J., et al., *Exosome uptake depends on ERK1/2-heat shock protein 27 signaling and lipid Raft-mediated endocytosis negatively regulated by caveolin-1.* Journal of Biological Chemistry, 2013. **288**(24): p. 17713-17724.
196. Powlesland, A.S., et al., *Targeted glycoproteomic identification of cancer cell glycosylation.* Glycobiology, 2009. **19**(8): p. 899-909.
197. Kudo, Y. and C. Boyd, *RNA interference‐induced reduction in CD98 expression suppresses cell fusion during syncytialization of human placental BeWo cells.* FEBS letters, 2004. **577**(3): p. 473-477.
198. Ohgimoto, S., et al., *Molecular characterization of fusion regulatory protein-1 (FRP-1) that induces multinucleated giant cell formation of monocytes and HIV gp160-mediated cell fusion. FRP-1 and 4F2/CD98 are identical molecules.* The Journal of Immunology, 1995. **155**(7): p. 3585-3592.
199. Watanabe, Y., et al., *Site-specific glycan analysis of the SARS-CoV-2 spike.* Science, 2020: p. eabb9983.
200. Chandrasekaran, G., et al., *Antibacterial and Antifungal Activities of Lectin Extracted from Fruiting Bodies of the Korean Cauliflower Medicinal Mushroom, Sparassis latifolia (Agaricomycetes).* Int J Med Mushrooms, 2016. **18**(4): p. 291-9.
201. Karasaki, Y., et al., *A garlic lectin exerted an antitumor activity and induced apoptosis in human tumor cells.* Food Research International, 2001. **34**(1): p. 7-13.
202. Mathew, B. and R. Biju, *Neuroprotective effects of garlic a review.* Libyan Journal of Medicine, 2008. **3**(1): p. 23-33.
203. Fleischauer, A.T. and L. Arab, *Garlic and cancer: a critical review of the epidemiologic literature.* J Nutr, 2001. **131**(3s): p. 1032s-40s.
204. Zhang, M., et al., *Edible ginger-derived nanoparticles: A novel therapeutic approach for the prevention and treatment of inflammatory bowel disease and colitis-associated cancer.* Biomaterials, 2016. **101**: p. 321-40.
205. Shevchenko, A., et al., *In-gel digestion for mass spectrometric characterization of proteins and proteomes.* Nature Protocols, 2006. **1**(6): p. 2856-2860.
206. Atwood, J.A., 3rd, et al., *Simple modification of a protein database for mass spectral identification of N-linked glycopeptides.* Rapid Commun Mass Spectrom, 2005. **19**(21): p. 3002-6.
207. Pérez-Gil, J., *Structure of pulmonary surfactant membranes and films: The role of proteins and lipid–protein interactions.* Biochimica et Biophysica Acta (BBA) - Biomembranes, 2008. **1778**(7): p. 1676-1695.
208. Shang, L., K. Nienhaus, and G.U. Nienhaus, *Engineered nanoparticles interacting with cells: size matters.* J Nanobiotechnology, 2014. **12**: p. 5.
209. dos Santos, T., et al., *Effects of Transport Inhibitors on the Cellular Uptake of Carboxylated Polystyrene Nanoparticles in Different Cell Lines.* PLOS ONE, 2011. **6**(9): p. e24438.
210. Younossi, Z., et al., *Global burden of NAFLD and NASH: trends, predictions, risk factors and prevention.* Nature Reviews Gastroenterology & Hepatology, 2018. **15**(1): p. 11-20.
211. Tannahill, G.M., et al., *Succinate is an inflammatory signal that induces IL-1β through HIF-1α.* Nature, 2013. **496**(7444): p. 238-242.
212. Gupta, A. and R.S. Sandhu, *Effect of garlic agglutinin and garlic extracts on the rat jejunum.* Nutrition Research, 1998. **18**(5): p. 841-850.
213. Henderson, N.C. and T. Sethi, *The regulation of inflammation by galectin-3.* Immunol Rev, 2009. **230**(1): p. 160-71.

214. Ke, C., et al., *A simple and accessible synthetic lectin for glucose recognition and sensing.* Nature Chemistry, 2012. **4**(9): p. 718-723.
215. Turner, M.W., *Mannose-binding lectin: the pluripotent molecule of the innate immune system.* Immunol Today, 1996. **17**(11): p. 532-40.
216. Evans, R.C., et al., *Diet and colorectal cancer: an investigation of the lectin/galactose hypothesis.* Gastroenterology, 2002. **122**(7): p. 1784-92.
217. Cheung, A.H.K., J.H. Wong, and T.B. Ng, *Musa acuminata (Del Monte banana) lectin is a fructose-binding lectin with cytokine-inducing activity.* Phytomedicine, 2009. **16**(6): p. 594-600.
218. Sakai, S., Y. Shigemasa, and T. Sasaki, *A self-adjusting carbohydrate ligand for GalNAc specific lectins.* Tetrahedron Letters, 1997. **38**(47): p. 8145-8148.
219. Regan, L.J., et al., *Selective expression of endogenous lactose-binding lectins and lactoseries glycoconjugates in subsets of rat sensory neurons.* Proc Natl Acad Sci U S A, 1986. **83**(7): p. 2248-52.
220. Delatorre, P., et al., *Crystal structure of a lectin from Canavalia maritima (ConM) in complex with trehalose and maltose reveals relevant mutation in ConA-like lectins.* J Struct Biol, 2006. **154**(3): p. 280-6.
221. Dam, T.K., et al., *Garlic (Allium sativum) lectins bind to high mannose oligosaccharide chains.* J Biol Chem, 1998. **273**(10): p. 5528-35.
222. Tagawa, Y.-i., K. Sekikawa, and Y. Iwakura, *Suppression of concanavalin A-induced hepatitis in IFN-gamma (-/-) mice, but not in TNF-alpha (-/-) mice: role for IFN-gamma in activating apoptosis of hepatocytes.* The Journal of Immunology, 1997. **159**(3): p. 1418-1428.
223. Park, E.J., et al., *Dietary and genetic obesity promote liver inflammation and tumorigenesis by enhancing IL-6 and TNF expression.* Cell, 2010. **140**(2): p. 197-208.
224. Hammerich, L. and F. Tacke, *Interleukins in chronic liver disease: lessons learned from experimental mouse models.* Clin Exp Gastroenterol, 2014. **7**: p. 297-306.
225. Fukunishi, S., et al., *Lipopolysaccharides accelerate hepatic steatosis in the development of nonalcoholic fatty liver disease in Zucker rats.* Journal of clinical biochemistry and nutrition, 2014. **54**(1): p. 39-44.
226. Kolodziejczyk, A.A., et al., *The role of the microbiome in NAFLD and NASH.* EMBO molecular medicine, 2019. **11**(2): p. e9302.
227. Stephens, M. and P.Y. von der Weid, *Lipopolysaccharides modulate intestinal epithelial permeability and inflammation in a species-specific manner.* Gut Microbes, 2020. **11**(3): p. 421-432.
228. Kiziltas, S., *Toll-like receptors in pathophysiology of liver diseases.* World journal of hepatology, 2016. **8**(32): p. 1354-1369.
229. Norris, C.A., et al., *Synthesis of IL-6 by hepatocytes is a normal response to common hepatic stimuli.* PloS one, 2014. **9**(4): p. e96053-e96053.
230. Sterling, S.R. and S.A. Bowen, *The Potential for Plant-Based Diets to Promote Health Among Blacks Living in the United States.* Nutrients, 2019. **11**(12).
231. Perumpail, B.J., et al., *Potential Therapeutic Benefits of Herbs and Supplements in Patients with NAFLD.* Diseases, 2018. **6**(3).
232. Soleimani, D., Z. Paknahad, and M.H. Rouhani, *Therapeutic Effects of Garlic on Hepatic Steatosis in Nonalcoholic Fatty Liver Disease Patients: A Randomized Clinical Trial.* Diabetes Metab Syndr Obes, 2020. **13**: p. 2389-2397.
233. Takaki, A., D. Kawai, and K. Yamamoto, *Multiple hits, including oxidative stress, as pathogenesis and treatment target in non-alcoholic steatohepatitis (NASH).* Int J Mol Sci, 2013. **14**(10): p. 20704-28.

234. Wang, Z., et al., *Proteomic analysis of urine exosomes by multidimensional protein identification technology (MudPIT).* Proteomics, 2012. **12**(2): p. 329-38.
235. Li, Y., et al., *Circular RNA is enriched and stable in exosomes: a promising biomarker for cancer diagnosis.* Cell Research, 2015. **25**(8): p. 981-984.
236. Escrevente, C., et al., *Interaction and uptake of exosomes by ovarian cancer cells.* BMC Cancer, 2011. **11**: p. 108.
237. Pegtel, D.M., et al., *Functional delivery of viral miRNAs via exosomes.* Proc Natl Acad Sci U S A, 2010. **107**(14): p. 6328-33.
238. Hood, J.L., R.S. San, and S.A. Wickline, *Exosomes released by melanoma cells prepare sentinel lymph nodes for tumor metastasis.* Cancer Res, 2011. **71**(11): p. 3792-801.
239. Barres, C., et al., *Galectin-5 is bound onto the surface of rat reticulocyte exosomes and modulates vesicle uptake by macrophages.* Blood, 2010. **115**(3): p. 696-705.
240. Kingwell, K., *New targets for drug delivery across the BBB.* Nature Reviews Drug Discovery, 2016. **15**(2): p. 84-85.
241. Hao, S., et al., *Mature dendritic cells pulsed with exosomes stimulate efficient cytotoxic T-lymphocyte responses and antitumour immunity.* Immunology, 2007. **120**(1): p. 90-102.
242. Jiang, Q.L., et al., *Plant lectins, from ancient sugar-binding proteins to emerging anti-cancer drugs in apoptosis and autophagy.* Cell Prolif, 2015. **48**(1): p. 17-28.
243. Wieckowska, A., et al., *Increased hepatic and circulating interleukin-6 levels in human nonalcoholic steatohepatitis.* Am J Gastroenterol, 2008. **103**(6): p. 1372-9.
244. Luo, X.Y., et al., *IFN-gamma deficiency attenuates hepatic inflammation and fibrosis in a steatohepatitis model induced by a methionine- and choline-deficient high-fat diet.* Am J Physiol Gastrointest Liver Physiol, 2013. **305**(12): p. G891-9.
245. Canup, B.S., *NON-ALCOHOLIC FATTY LIVER AND HEPATOCARCIMONA ATTENUATION BY SPECIFIC CD98 DOWN-REGULATION VIA NANOVECTORS*, in *Chemistry*. 2020, Georgia State University.
246. Song, H., et al., *Internalization of Garlic-Derived Nanovesicles on Liver Cells is Triggered by Interaction With CD98.* ACS Omega, 2020. **5**(36): p. 23118-23128.

APPENDIX

Appendix Table 1. Human Primers (h = human and m = mice)

Gene Name	Forward	Reverse
hGAPDH	5’-TTGGTATCGTGGAAGGACTCA -3’	5’-TGTCATCATATTTGGCAGGTTT-3’
hIFN-γ	5’-GCTTGAATCTAAATTATCAGTC-3’	5’-GAAGATTCAAATTGCATCTTTAT-3’
mIFN-γ	5’-TCAAGTGGCATAGATGTGGAAGAA-3’	5’-TGGCTCTGCAGGATTTTCATG-3’
hIL-6	5’-CAATCTGGATTCAATGAGGAGAC-3’	5’-CTCTGGCTTGTTCCTCACTACTC-3’
hCD98	5’-GCTTGCAGCCAAAACTCCAG-3’	5’-CCAACTACCGGGGTGAGAAC-3’
mCD98	5’-GAGGACAGGCTTTTGATTGC-3’	5’-ATTCAGTCGCTCCCCAGTG-3’
hCox-2	5’-GGTCTGGTGCCTGGTCTGATGATC-3’	5’-GTCCTTTCAAGGAGAAATGGTGC-3’
mCox-2	5’-TACCAGTCTCTCAATGAGTACC-3’	5’-TGGTAGGCTGTGGATCTT-GCACATTG-3’
hTNF-α	5'-ATCTACCTGGGAGGCGTCTT-3’	5'-GAGTGGCACAAGGAACTGGT-3'
mTNF-α	5’-AGGCTGCCCCGACTACGT-3’	5’-GACTTTCTCCTGGTATGAGA-TAGCAAA-3’
m36b4	5’-TCCAGGCTTTGGGCATCA-3’	5’-CTTTATCAGCTGCACATCACTCAGA-3’

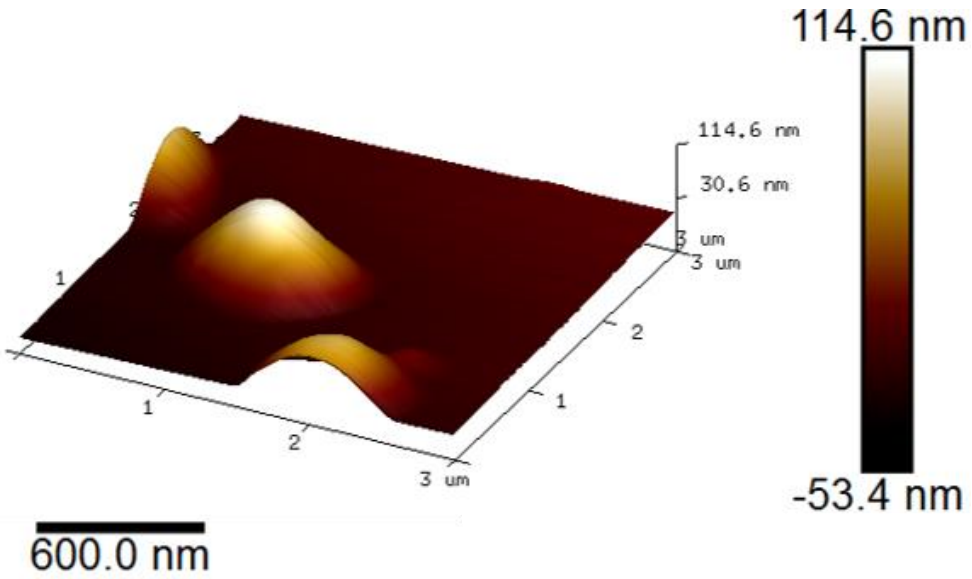

Appendix Figure 5-0.1: The shape of CD98 siRNA-loaded NPs was visualized by Atomic Force Microscopy (AFM).

Atomic force microscopy (AFM) image of CD98 siRNA-loaded NP. [171]

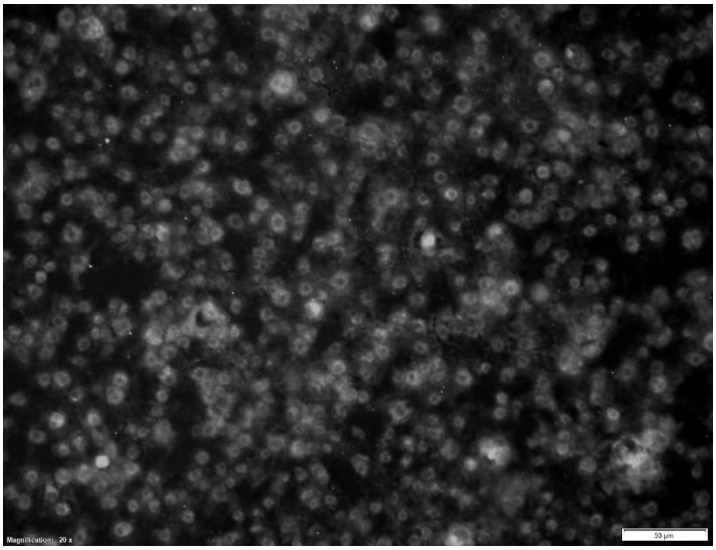

Appendix Figure 5-0.2: FITC-labeled siRNA-loaded NPs were uptake by the HepG2 cells.

Fluorescent microscopy (grayscale picture) of HepG2 cells after overnight incubation with FITC-labeled siRNA-loaded NPs (200µg/mL). The scale bar is 50 µm. **[171]**

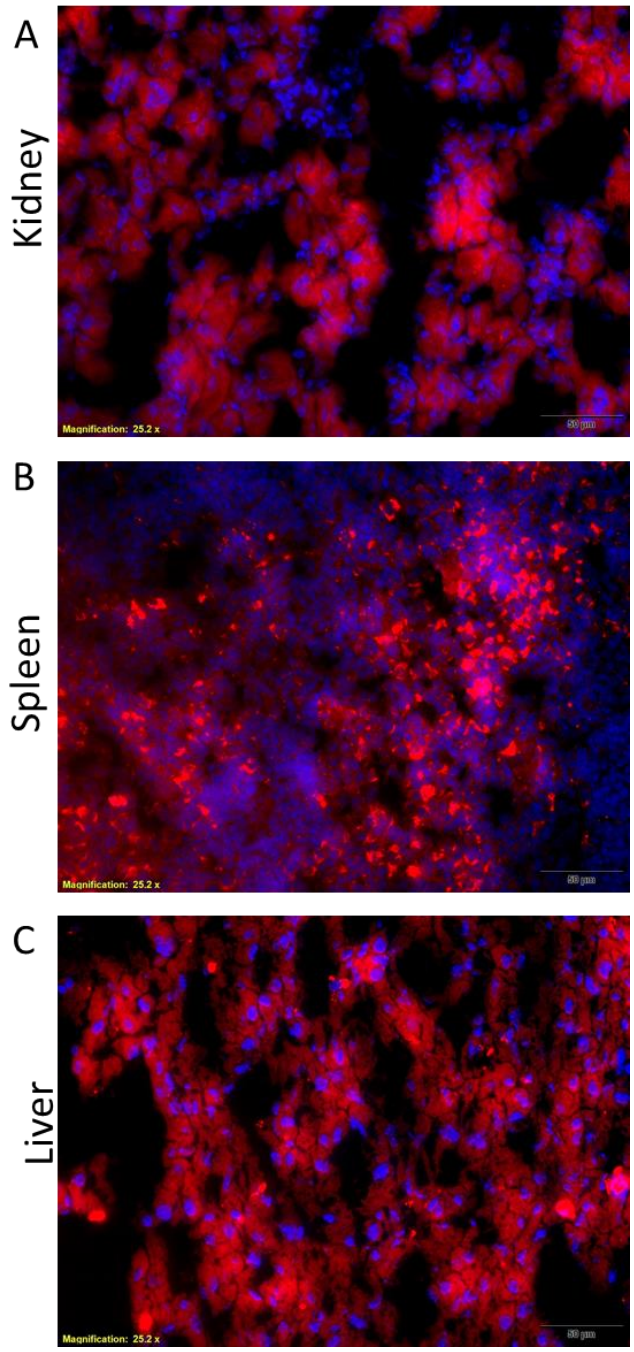

Appendix Figure 5-0.3: **The liver, spleen, and kidney from HFD mice without any FITC-labeled siRNA-loaded NPs treatments do not show the signal of FITC.**
The actin in kidney, spleen, and liver tissues was stained with the phalloidin (Alexa Fluor 568) and the nuclei were stained with DAPI. The scale bar is 50 μm.

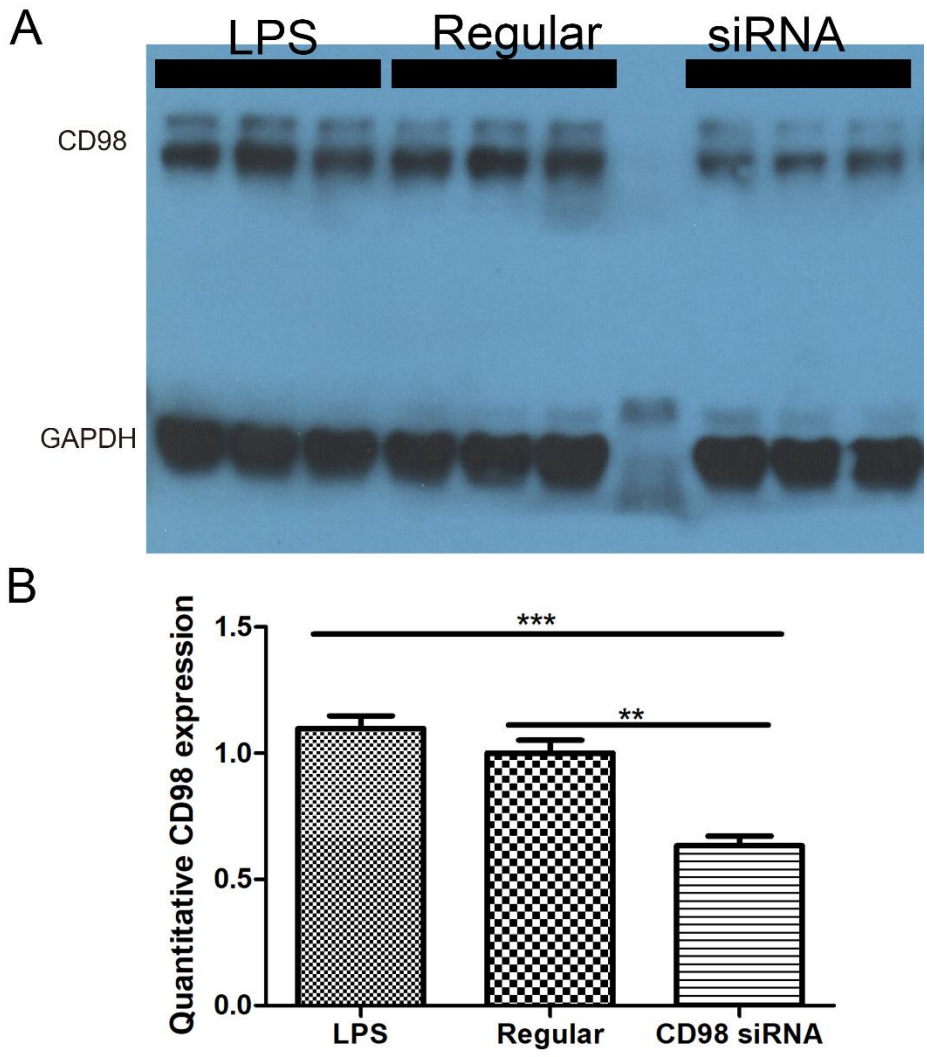

Appendix Figure 5-0.4: The CD98 expression level in HepG2 cells was decreased by using CD98 siRNA and increased by LPS-stimulation.

(A) the expression level of CD98 under three different treatments (LPS, control, CD98 siRNA).

(B) the expression amount was quantified. T-test was used to analyze the significance.

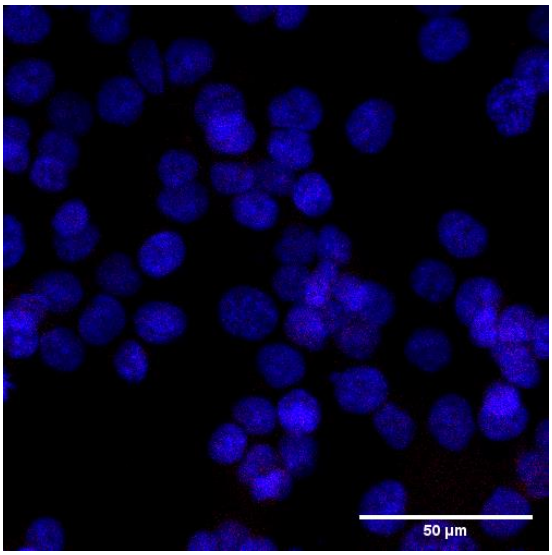

Appendix Figure 5-0.5: The secondary antibody (anti-Rabbit, tagged with Alexa Fluor 568) does not show the obvious signals in staining the HepG2 cells.

Same staining procedures with the CD98 staining except that CD98 primary antibody is not applied. The secondary antibody (anti-Rabbit) is tagged with Alexa Fluor 568 (if it is present, it is indicated as red) and the nuclear was stained in blue (DAPI). The scale bar is 50 µm.